Methods[1]

Expedition 337 Scientists[2]

Chapter contents

Introduction

This chapter documents the methods used for shipboard measurements and analyses during Integrated Ocean Drilling Program (IODP) Expedition 337. During Expedition 337, we conducted riser drilling from 646 to 2466 m drilling depth below seafloor (DSF) in IODP Hole C0020A, which had been suspended for six years since initial drilling during the D/V *Chikyu* shakedown cruise (Expedition CK06-06) in 2006. During riser drilling operations, a wide range of data and 32 sediment cores were retrieved from selected intervals of high interest. Circulating riser drilling mud was monitored routinely; gas from drilling mud was analyzed online in a newly constructed mud-gas monitoring laboratory. Cuttings were sampled for shipboard and shore-based analyses. Wireline logging and in situ fluid sampling and analysis were conducted to fill the noncored interval gaps.

Reference depths

Depths of each measurement or sample are reported relative to both the drilling vessel rig floor (rotary table) and the seafloor (see Table **T1**). These depths are determined by drill pipe and wireline length and are correlated with each other by use of distinct reference points. Drilling engineers refer to pipe length when reporting depth and report this as drilling depth below rig floor (DRF) in meters. Core depths are based on the drilling depth below rig floor to the top of the cored interval and curated length of the recovered core. Core depths are converted to core depth below seafloor, Method B (CSF-B), in which overlapping sections are compressed when recovery is >100% (IODP Depth Scales Terminology, **www.iodp.org/program-policies/**). Cuttings and mud depths are reported as mud depth below rig floor (MRF), based on DRF and the calculated lag depth of the cuttings (see below for further details).

In referring to wireline logging results, depths are initially reported as wireline log depth below rig floor (WRF). Wireline logging depths are corrected relative to DRF using a known reference datum, such as the seafloor ("mudline") or the base of the casing ("casing shoe"), and relative to each logging data set down the borehole, including tool speed corrections where appropriate. These corrected depths are then reported as wireline log matched depth below seafloor (WMSF) (see **"Downhole logging"** for further details).

[1] Expedition 337 Scientists, 2013. Methods. *In* Inagaki, F., Hinrichs, K.-U., Kubo, Y., and the Expedition 337 Scientists, *Proc. IODP,* 337: Tokyo (Integrated Ocean Drilling Program Management International, Inc.). doi:10.2204/iodp.proc.337.102.2013
[2] **Expedition 337 Scientists' addresses.**

doi:10.2204/iodp.proc.337.102.2013

The depths reported in depths below rig floor (DRF, MRF, and WRF) are converted to depths below seafloor (DSF or CSF-B, mud depth below seafloor [MSF], and WMSF, respectively) by subtracting water depth and the height of the rig floor from the sea surface, with corrections relative to DRF where appropriate (Fig. F1). These depths below seafloor (DSF, CSF-B, MSF, and WMSF) are therefore all equivalent. Seismic depths are reported in either time (s) or depth (m). For time sections, a two-way traveltime (s) scale is used below sea level. For depth sections, seismic depth below seafloor (SSF) or seismic depth below sea level (SSL) are expressed in meters.

Cuttings and mud depths

During riser drilling, drilling mud circulates within the riser pipe and the borehole between the drillship and the bottom of the hole. As the drill bit cuts through the formation, the fragments (i.e., cuttings) are suspended in the drilling mud and carried with the formation fluid and gas back to the ship. A cuttings sample is assumed to be a representative mixture of rock fragments and sediments from a given sample interval. The time between when the formation is cut by the drill bit and when these cuttings arrive at the ship is known as the "lag time," which is a function of drilling mud pumping rate and annular mud volume, and is used to calculate the "lag depth." At a constant pump rate, lag time and lag depth both increase as the hole is deepened and the volume of circulating mud increases. All of the depths recorded for cuttings and mud gas at Site C0020 have been corrected for this lag.

Numbering of sites, holes, cores, sections, and samples

Sites drilled by the *Chikyu* are numbered consecutively from the first site with a prefix "C." A site refers to one or more holes drilled while the ship is positioned within 300 m of the first hole. The first hole drilled at a given site is assigned the site number modified by the suffix "A," the second hole takes the site number and suffix "B," and so forth. These suffixes are assigned regardless of recovery, as long as penetration takes place. During Expedition 337, we drilled at Site C0020 and occupied Hole C0020A. The hole was drilled by reoccupying the cased Hole C9001D, which was drilled and cased during the *Chikyu* shakedown cruise in 2006.

Cored intervals are calculated based on an initial 9.5 m length, which is the standard core barrel length for each coring system. In addition, we specified the collection of shorter coring intervals in areas of poor recovery or slow rate of penetration (ROP) and longer coring intervals for large-diameter coring (LDC). Expansion of cores and gaps related to unrecovered material result in recovery percentages greater or less than 100%, respectively. Depth intervals are assigned starting from the depth below seafloor at which coring started (IODP coring depth scale calculated using Method A [CSF-A]; see IODP Depth Scales Terminology at www.iodp.org/program-policies/). Short cores (incomplete recovery) are all assumed to start from that initial depth by convention. Core expansion is corrected during final processing of core measurements by subtracting void spaces, subtracting exotic material, and accounting for expansion (CSF-B).

A recovered core is typically divided into 1.4 m long sections that are numbered sequentially from 1 beginning at the top. During Expedition 337, whole-round core (WRC) samples were removed for time-sensitive interstitial water sampling and assigned their own section number in order to allow for rapid X-ray computed tomography (CT) scanning of time-sensitive samples. Material recovered from the core catcher was assigned to a separate section, labeled core catcher (CC), and placed at the bottom of the lowermost section of the recovered core. The LDC core was cut into 1.0 m sections on the rig floor.

A full identification number for a sample from a core section consists of the following information: expedition, site, hole, core number, core type, section number, and top to bottom interval in centimeters measured from the top of the section. For example, a sample identification of "337-C0020A-2R-1, 80–85 cm," represents a sample removed from the interval between 80 and 85 cm below the top of Section 1 of the second rotary core barrel (RCB) core from Hole C0020A, during Expedition 337 (Fig. F1).

Sampling and classification of material transported by drilling mud

Solid (cuttings), fluid, and gas samples were collected during riser drilling of Expedition 337. Cuttings were taken at every 10 m depth interval (DRF) from the shale shakers. Drilling mud and mud gases were also sampled from the mud circulation line. Cuttings, fluid, and mud gas were classified by drill site and hole using a sequential material number followed by an abbreviation describing the type of material. The material type identifiers are as follows:

SMW = solid taken from drilling mud (cuttings).
LMW = liquid taken from drilling mud.
GMW = gas taken from drilling mud.

For example, "337-C0020A-123-SMW" represents the 123rd cuttings sample recovered from Hole C0020A during Expedition 337.

Identifiers of other sample material types include the following:

LMT = liquid taken from mud tank.
LWL = liquid taken by wireline sampling tool (Schlumberger Quicksilver probe).
SDB = solids from the retrieved drill bit.

Cuttings handling

Every 10 m, we routinely collected >2000 cm^3 of cuttings material from the shale shaker for shipboard analysis, long-term archiving, and personal samples for shore-based postexpedition research (Fig. F2). The unwashed cuttings samples were divided as follows:

- 70 cm^3 for photography and then micropaleontology,
- 5 cm^3 for headspace gas analysis,
- 50 cm^3 for microbiological study, and
- 400 cm^3 for archiving at the core repository.

The remainder of each cuttings sample was washed gently with seawater using a sieve (250 µm opening) at the core cutting area. During sieving, a hand magnet was used to remove iron contaminants originating from drilling tools and casing. The use of the hand magnet was cancelled after magnetic minerals were abundantly observed at 1256.6 m MSF. At this point, the following samples were taken:

- 70 cm^3 for photography and then lithology description,
- 35 cm^3 for bulk MAD, and
- 10 cm^3 for palynology.

Lithology samples were washed with freshwater in 1 and 4 mm mesh. Samples from the 1–4 mm fraction were used for lithology description and were then sent to vacuum drying and grinding for X-ray diffraction (XRD) and X-ray fluorescence (XRF). Moisture and density (MAD) measurements used sieved samples in addition to bulk samples. The remaining portion was rinsed with freshwater. At this point a 50 cm^3 sample was collected for biomarker analysis.

The remaining washed samples were rinsed again with Elix water and dried at 40°C. Approximately 400 cm^3 of samples, when available, was archived and sent to the core repository for future use. Sampling frequency for headspace gas analysis, community microbiology samples, and biomarker analysis was every 50 m. At each step of washing, personal samples were taken upon request.

Drilling mud handling

Drilling mud samples were collected at two locations: the mud tanks and the mud ditch. Sampling at the mud tanks was carried out once a day once drilling mud was ready for use. The addition of a chemical tracer (perfluorocarbon [PFC] tracer) was also conducted at the mud tank, typically at the active tank in use for mud circulation. Samples of drilling mud that returned from the borehole were taken at the mud ditch twice a day. Both samples were used to monitor PFC tracer and hydrocarbon concentration (see **"Microbiology"**).

Mud gas handling

Mud gas was extracted from drilling mud immediately after the mud returned from the borehole. A degasser with an agitator was installed on the bypass mud flow line, and the gas extracted in the degasser chamber was pumped to the mud-gas monitoring laboratory via a polyvinyl chloride (PVC) tube. Analysis in the unit is described in **"Organic geochemistry."**

In situ fluid sample handling

Formation fluid samples were collected by the Schlumberger Quicksilver probe and In Situ Fluid Analyzer (IFA) installed in the wireline downhole tool (see **"Downhole logging"**). The fluid samples were collected in a single-phase multisample chamber (SPMC) at depth and were then transferred shipboard to Single-Phase Sample Bottles (SSBs) using Schlumberger's sample transfer system. The SSBs were transferred to the laboratory, and the sample fluid was extracted to a glass vacuum bottle. Dissolved gas was collected in a separate sample bottle during the fluid transfer. Details of the Quicksilver probe are described in "**Downhole logging.**"

Core handling

Two types of coring tools were used: standard IODP (RCB) core with a plastic liner 6.6 cm in diameter and an industry-type (LDC) core with an aluminum liner 10 cm in diameter. In this report, the former is referred to as IODP core and the latter as LDC core. IODP and LDC cores were usually cut into 1.4 m sections at the core cutting area and 1.0 m sections at the drill floor, respectively.

Figure F3 shows the basic flow chart of core processing. A small volume (~5 cm^3) of sample was taken for micropaleontology from the core catcher section.

Some syringe samples were taken at freshly cut section ends for headspace gas analysis.

Considering the time, temperature, and redox sensitivity of analyses, the WRC samples were fast-tracked to the core cutting area and immediately transferred to the laboratory. These included

- Two 60 cm long sections for interstitial water squeezing and
- Two 15 cm long sections for community WRC samples.

The sections were examined by X-ray CT scan and processed as WRC samples. The community WRC sample was divided into subsamples for contamination tests using PFC tracer; cell count; DNA analysis; biomarker analysis; MAD; carbon, sulfur, and nitrogen content; inorganic carbon; and Rock-Eval analysis. A part of the community whole round was subsampled for shore-based microbiological and biogeochemical analyses.

All other sections were sealed with end caps with a slit and brought to the core processing deck. The sections were first placed in air-barrier ESCAL bags (Mitsubishi Gas Chemicals, Co., Japan) and vacuum-sealed with 3× N_2 flush. The anaerobically packed core sections were stored at room temperature (~23°C) prior to subsequent nondestructive measurement and WRC sampling. Based on the temperature gradient of 22.5°C/km in this area (Osawa et al., 2002), in situ temperature of coring depths is similar to or higher than that of the core processing deck. Flushing the samples with N_2 is very important for maintaining the activity of strictly anaerobic microbial components (e.g., methanogens). After the anaerobic packing of cored sections, the cored materials were examined by X-ray CT scan and whole-round multisensor core logger (MSCL-W). WRC samples were then cut out in the quality assurance/quality control (QA/QC) laboratory and stored under appropriate conditions or used for shipboard analyses. After WRC sampling, the core sections were split into working and archive halves. Digital images of archive-half sections were taken with the photo image logger (MSCL-I) before visual core description by sedimentologists and color reflectance measurement was carried out by the color spectroscopy logger (MSCL-C). Thermal conductivity measurements were performed on a sample from each core using the half-space method. Discrete cubes for *P*-wave velocity and impedance analysis were sampled from the working halves. Additional samples were taken for MAD, XRD, and XRF analyses. All half-round core sections were again vacuum-sealed in ESCAL bags with 3× N_2 flush and transferred to cold storage. After the expedition, all cores were transported under cool temperature for archiving at the Kochi Core Center (KCC) in Kochi, Japan.

LDC core sections were capped with rubber end caps and brought to the laboratory. In most sections, core material could be pushed out from the aluminum core liner and transferred to a plastic tray. The core material on the tray was immediately vacuum-wrapped in an ESCAL bag after N_2 flush. Core material of two sections, however, was stuck in the aluminum core liner. In those cases, two sides of aluminum liner were cut lengthwise using the rotary saw of the core splitter to transfer the core material. After wrapping in an ESCAL bag, LDC cores were handled in a work flow identical to the standard IODP cores.

Lithostratigraphy

Lithostratigraphic observations of cuttings and core samples from Site C0020 during Expedition 337 were performed using multiple approaches based on

- Macroscopic observations,
- Microscopic observations including smear slides or thin sections,
- Mineralogical and elemental analysis using XRD and XRF, and
- X-ray CT image observation.

The obtained lithostratigraphic data were correlated with data from downhole logging.

Cuttings and core description

Macroscopic observations

Cuttings

Cuttings are small fragments of rocks of various lithologies recovered during riser drilling. Cuttings were sampled for the first time in IODP operations during Expedition 319 (Saffer, McNeill, Byrne, Araki, Toczko, Eguchi, Takahashi, and the Expedition 319 Scientists, 2010) and for the second time during Expedition 337. These solid fragments are suspended in riser drilling mud that contains a considerable amount of clay minerals, such as bentonite, and the resulting contamination introduces uncertainty into the quantification of the true clay content. The separation procedure of cuttings from the drilling mud is described in **"Introduction."**

During Expedition 337, cuttings were the only solid samples collected from 635 to 1263 m DRF, whereas cuttings from 1263 to 2466 m DRF were collected together with spot cores. Sampling frequency was every 10 m through the drilled interval (184 samples in total). Using freshwater followed by deionized water, washed cutting samples were sieved into three different size fractions (>4 mm, 1–4 mm, and 0.25–1 mm)

and then used for sedimentological description. Based on macroscopic observations of the washed samples (i.e., semiconsolidated and/or consolidated sediments), we estimated the relative amount of coarse-grained (e.g., sand and gravel) and fine-grained (e.g., silt and clay) materials, the induration state of the bulk material, the occurrence of artificial mud/grain contamination, and the presence of wood or lignite fragments, as well as the appearance, softness, size, and relative degree of lithification of rock fragments. The legend we used for cuttings description is shown in Figure F4. Figure F5 shows an example of the macroscopic cuttings description. Sand and gravel were combined to one grain fraction in the macroscopic description. Wood/lignite fragments were the dominating fraction in the coal-bearing unit. Wood/lignite fragments were plotted separately because they are not clastic sediments with a defined grain size.

All macroscopic observations were recorded on visual cuttings description forms and summarized in C0020_T1.XLSX in LITH in "Supplementary material." In addition, Site C0020 macroscopic visual cuttings descriptions can be found in "Core descriptions."

Cores

Split cores were described by the shipboard sedimentologists. Visual core description was carried out on the archive half of each core using traditional Ocean Drilling Program (ODP) and IODP procedures (e.g., Mazzullo and Graham, 1988; Mazzullo et al., 1988). The terms "mudstone" and "shale" were used for the description of fine-grained sediments. To keep it simple, we did not differentiate between thin laminated shales and massive mudstones without laminae. Therefore, the terms "shale" and "mudstone" written in the text stand for the same lithotype. Information from the visual core description (VCD) was transferred to the J-CORES database before conversion to core-scale plots using Strater software (Golden Software, Inc., USA). The legend we used for VCDs is shown in Figure F6. An example of the VCD is presented in Figure F7. The content of the core-scale images is shown in Table T2. Scans of handwritten VCD forms entered into the J-CORES database are available in HANDWRITTEN VCD CORE 1-22.PDF and HANDWRITTEN VCD CORE 23-32.PDF in LITH in "Supplementary material." In addition, Site C0020 visual core descriptions can be found in "Core descriptions."

A short summary of the key features from each core section was also included in the J-CORES database.

Microscopic observations

Cuttings and cores

Smear slides were made from washed (for semiconsolidated and/or consolidated sediments) cuttings samples in order to identify major lithologic changes under the microscopes. Microscopic investigations of the washed 1–4 mm (coarse sand to granule size) fraction using binocular and/or polarizing microscopes allowed us to distinguish the relative abundances of different minerals, wood/lignite fragments, and fossils in the cuttings. Discrete samples were collected from cores for both smear slide and thin section to identify the main mineral groups and for estimating bulk sediment composition and grain size. These data are summarized in CUTTINGS_STRATER_MOD.XLSX and CORE_STRATER_MOD.XLSX in LITH in "Supplementary material." In addition, Site C0020 microscopic visual cuttings descriptions can be found in "Core descriptions."

Smear slides

Examination and description of cuttings and cores during Expedition 337 was undertaken using smear slides. This routine method was used for identifying and reporting basic sediment attributes (i.e., mineralogy, texture, form, and size) and for ascertaining the presence of biological debris in samples of both cuttings and cores. Smear slide samples were taken at regular intervals (i.e., 1 per 10 m in drilling depth for cutting samples and 1 per core section for core samples) or from any lithologically distinct layer. The method included taking a small amount (~0.1 cm) of sample using a toothpick, placing the sample on a clear microscope slide, dispersing with tap water, and then drying on a hot plate. Following drying, optical adhesive was added, covered with a cover glass, and then cured under ultraviolet (UV) radiation before microscope examination.

The estimation of biogenic, volcaniclastic, and siliciclastic abundance in the slide was conducted qualitatively using a visual comparison chart (Rothwell, 1989). In general, the constituents of abundance are reported based on relative percentage:

D = dominant (>50%).
A = abundant (>10%–50%).
C = common (>1%–10%).
F = few (0.1%–1%).
R = rare (<0.1%).

The relative abundance of major components was validated by XRD. The absolute weight of carbonate was verified by coulometric analysis. The sample location for each smear slide was entered into the J-

CORES database with a sample code of SS. Figure F8 shows an example of the microscopic cuttings description.

Thin sections

Most sediment samples observed in cores were semiconsolidated; therefore, we decided to take only a few thin sections per core from a few pieces of conglomerate components (e.g., volcanic rocks) and cemented sedimentary rocks observed in split cores. Thin sections were prepared for more intensive analysis of the mineralogy, structure, and fabric. A 30 µm × 2 cm × 3 cm section of sediment was used for each thin section. Thin sections were polished and observed in transmitted light using a Zeiss Axioskop AX10 polarizing microscope equipped with a Nikon DS-Fi1 digital camera.

Mineralogical analysis of cuttings and core

X-ray diffraction

During Expedition 337, XRD analysis was used in conjunction with smear slides to provide a comprehensive, integrated approach to petrologic evaluation. The primary goal of XRD analyses was to identify relative mineralogical changes with depth of total clay, quartz, feldspar, and calcite based on peak areas identified in the diffraction patterns. XRD analysis of cuttings was conducted on 1–4 mm size fractions of selected washed cuttings samples, whereas core samples for XRD analysis were selected at a resolution of one per core from the working half and in the areas of lithologic change. Cuttings samples from 636.5 to 1263 m MSF were taken every 10 m for XRD measurements, whereas cuttings samples from 1263 to 2466 m MSF were analyzed every 40–50 m at the same intervals as samples for XRF. In some cases, the position of XRD samples was the same as for organic carbon, Rock-Eval pyrolysis, biomarker analysis, and calcium carbonate analyses.

Sample preparation included drying the samples for 24–72 h using a vacuum dryer (Laboconco FZ-4.5 CL) followed by crushing with a planetary ball mill (Fritsch P-5/4 Fritsch) at 200 rpm for 2 min. Very hard granules remaining in the samples after milling were removed. Bulk powdered samples were then mounted on a glass holder 24 (large size) and analyzed using a PANanalytical CubiX PRO (PW3800) diffractometer with the X-ray generator set to 45 kV and 40 mA. Scanning was conducted from 2°2θ to 60°2θ with a step size of 0.01° and sampling time of 1 s per step.

Peak areas were measured using MacDiff software for peaks associated with total clay (2θ = 19.301°–20.369°), quartz (2θ = 26.260°–26.957°), plagioclase (2θ = 27.463°–28.275°), and calcite (2θ = 28.887°–29.975°). Relative abundances were calculated using linear regression of the measured peak areas to known abundances in mixed mineral standards. Standards used for calibration were the same as those from ODP Leg 190 and IODP Expeditions 315, 319, 322, and 333 (Underwood et al., 2003; Expedition 315 Scientists, 2009; Expedition 319 Scientists, 2010a; Expedition 322 Scientists, 2010; Expedition 333 Scientists, 2012). This set of 14 standards contains illite, smectite, and chlorite clay (14%–76%), quartz (6%–57%), plagioclase feldspar (5%–38%), and calcite (2%–70%). Previous expeditions that used these standard mixtures sampled sediments from the Nankai Trough accretionary complex. The dominant minerals are broadly similar between the southern (e.g., Steurer and Underwood, 2003; Guo and Underwood, 2012) and northern (Mann and Müller, 1980; Kurnosov et al., 1980) sections of the Japan margin. Therefore, the mineral types and weight percent ranges within the standards developed for the Nankai Trough sediments encompass those from offshore the Shimokita Peninsula. These standards were also used for the *Chikyu* shakedown cruise in 2006 (Aoike, 2007). Although the linear regression calibration method quantifies the relative abundance of standard mineral mixtures with little error, actual sample measurements should be considered semiquantitative estimates of a four-component mixture. The presence of other constituents in marine sediments such as biogenic silica, volcanic glass, and lithic fragments can introduce additional error to relative abundances calculated using the calibration method. Qualitative identification of the minerals present in the XRD pattern was conducted using the PANalytical X'pert program, and the d-spacings of each peak were annotated automatically or manually using the International Center of Diffraction Data (**www.icdd.com/**) database. XRD results are available in XRD-CORE.XLSX, XRD-CUTTINGS.XLSX, and XRD-QUALITATIVE.XLSX in LITH in **"Supplementary material."**

X-ray fluorescence

Core materials and cuttings were subjected to whole-rock quantitative XRF spectrometry for analysis of major elements (Na, Mg, Al, Si, Fe, P, K, Ca, Ti, and Mn). XRF analyses of all cuttings samples from Expedition 337 were conducted every 40–50 m at the same intervals as samples for XRD. In some cases, the position of XRF samples were the same as for total organic carbon (TOC), Rock-Eval pyrolysis, biomarker analysis, and calcium carbonate analysis using the 1–4 mm size fraction. On the other hand, XRF analyses of all core samples were done at a reso-

lution of one per core and in areas of lithologic change at the same interval as samples for XRD analyses. All samples were dried and crushed before analysis, together with samples for XRD.

Approximately 1 g of sample powder was pressed into a pellet before analysis. Analyses were performed using a Supermini XRF spectrometer (Rigaku) with a 200 W Pd anode X-ray tube operated at 50 kV and 4 mA. Rock standards from the National Institute of Advanced Industrial Science and Technology were used for calibration of the XRF spectrometer, using matrix corrections within the operation software. Results were reported as weight percent oxide (Na_2O, MgO, Al_2O_3, SiO_2, P_2O_5, K_2O, CaO, TiO_2, MnO, and Fe_2O_3). XRF results are available in XRF-CORE.XLSX and XRF-CUTTINGS.XLSX in LITH in **"Supplementary material."**

X-ray CT scan

During Expedition 337, the assessment of core quality and identification of unique structural and sedimentological features, as well as determination of sampling locations, were facilitated using X-ray CT scanned images. Scanning was done immediately after splitting the core into sections and headspace gas sampling in the core cutting area. WRC sections were screened to avoid destructive sample processing of critical structural features.

The X-ray CT scan of cores was useful for the identification of 3-D sedimentary features, such as bioturbation burrows or bedding planes, for the estimation of lithology differences in areas without VCDs, and for the lithologic description of coaly horizons. Coal has a very low density in comparison to sandstone. Depending on the macrolithotypes and the purity of coal, the density values change and it is possible to estimate the composition of the coal in more detail. Concretions, isolated grains, and veins, which are often filled with pyrite, show very high density values and are clearly visible in the X-ray CT scan.

The X-ray CT instrument on the *Chikyu* is a GE Yokogawa Medical Systems LightSpeed Ultra 16 (GE Healthcare, 2006) capable of generating sixteen 0.625 mm thick slice images every 0.5 s, the time for one revolution of the X-ray source around the sample (Table **T3**). Data generated for each core consist of core-axis-normal planes of X-ray attenuation values with dimensions of 512 × 512 pixels. Data were stored as Digital Imaging and Communication in Medicine (DICOM) formatted files. The DICOM files were restructured to create 3-D images for further investigation.

The theory behind X-ray CT has been well established through medical research and is very briefly outlined here. X-ray intensity varies as a function of X-ray path length and the linear attenuation coefficient (LAC) of the target material as

$$I = I_0 \times e^{-\eta L}, \quad (1)$$

where

I = transmitted X-ray intensity,
I_0 = initial X-ray intensity,
η = LAC of the target material, and
L = X-ray path length through the material.

LAC is a function of the chemical composition and density of the target material. The basic measure of attenuation, or radiodensity, is the CT number given in Hounsfield units (HU) and is defined as

$$\text{CT number} = [(\eta_t - \eta_w)/\eta_w] \times 1000, \quad (2)$$

where

η_t = LAC for the target material, and
η_w = LAC for water.

The distribution of attenuation values mapped to an individual slice comprises the raw data that are used for subsequent image processing. Successive 2-D slices yield a representation of attenuation values in 3-D pixels referred to as voxels.

Analytical standards used during Expedition 337 were air (CT number = –1000), water (CT number = 0), and aluminum (2477 < CT number < 2487) in an acrylic core mock-up. All three standards were run once daily after air calibration. For each standard analysis, the CT number was determined for a 24.85 mm^2 area at fixed coordinates near the center of the cylinder.

Scanning electron microscopy

Scanning electron microscopy and energy dispersive spectroscopy using a JEOL electron microscope were used for a detailed observation and detection of minerals of a few selected samples of interest, principally the coal and carbonate-rich layers.

Identification of lithology

Lithologic units and boundaries were identified with core and cuttings analyses (i.e., VCD, smear slides, XRD, and XRF), logging data, and physical properties measurements. Compositional and textural features were recorded mainly based on the archive halves of cores. As the size of cuttings was generally small, it was not possible to use cuttings for the determination of sedimentary structure attributes, whereas X-ray CT scan and multisensor core logger (MSCL) data were useful for lithostratigraphic description. WRC samples that were taken for microbi-

ology (MBIO), interstitial water (IW), or shore-based analyses were not available for core description or the MSCL-I. However, scraped sample portions and residues of MBIO and IW samples were described using the smear slide method.

Downhole log response is a good tool to support the identification of lithostratigraphic units, transitions, and boundaries. Especially in noncoring depth intervals, data from borehole logging and cuttings were extremely important for good interpretation of lithostratigraphic units. For this purpose, we used gamma ray, sonic, electrical borehole image, and resistivity logs (from 1263 meters below seafloor [mbsf] to the bottom of the hole; see **"Downhole logging"**).

The integration of all available data (e.g., cuttings, cores, X-ray CT scan, MSCL, logging data, and physical properties measurements) was used for the identification of the lithostratigraphic characterization, interpretation of geological features (e.g., transitions, sequences, and boundaries), and identification of the composition and physical properties within each unit.

Paleontology

Palynology

Samples were processed in different ways depending on organic and mineral content. For samples that were organic rich (e.g., coals), 2 g of sediment was crushed using a mortar and pestle and then placed directly into concentrated HNO_3 (~15 mL) for 20 min. The residue was then sieved through a 10 µm mesh sieve with at least 1 L of water. The residue was subsequently oxidized using 2 mL of sodium hypochlorite solution for 10 s in an ultrasonic bath and further sieved to remove all chemicals and to clean the residue of excess fine organic matter. For mineral-rich sediments such as clays and siltstones, treatment commenced on ~5 g of sediment using 35% HCl to dissolve carbonates. The next stage was to remove silicate minerals by heating the sediment in 49% hydrofluoric acid (HF) (15 mL) on a hot plate heated to 50°C for 1 h. The residue was sieved at 20 µm (or 10 µm for more organic-rich samples with potential for yields of pollen and spores) with at least 1 L of water and treated for 1 min in concentrated HCl before sieving to flush out remaining chemicals. Oxidation using 70% HNO_3 was necessary to remove amorphous organic matter, and clastic samples were washed in 2 mL of concentrated HNO_3 for 2 min. In all cases, samples were stained using safranin and then mounted onto two coverslips (24 mm × 24 mm), dried on a hot plate set to low temperature (50°C), and then mounted using a photocuring adhesive. Both coverslips were studied for palynomorphs, except where a count size of 300 grains or cysts was achieved from one coverslip. The remaining coverslip was scanned for the presence of important index taxa. Slides were analyzed for dinoflagellate cysts, spores, and pollen grains. Samples were analyzed on a Zeiss Axioplan 2 microscope in the paleontology laboratory on the *Chikyu* using mainly a 400× differential interference contrast and phase contrast lens.

Dinocyst nomenclature follows that of Williams et al. (1998) and studies from the northwestern Pacific by Matsuoka (1983), Bujak (1984), Kurita and Matsuoka (1994), Kurita and Obuse (2003), and Kurita (2004). The biostratigraphic schemes of Bujak (1984), Bujak and Matsuoka (1986), Matsuoka et al. (1987), Kurita and Obuse (2003), and Kurita (2004) were consulted to identify biostratigraphic index taxa and acme events. Nomenclature for fossil pollen and spores is not standardized, so the terms used here are based on regional standard names (Yamanoi, 1992; Sato, 1994; Wang et al., 2001; Wang, 2006), North American pollen and spore terminology, and similarly aged material in Europe and China (Kedves, 1969; Jingrong et al., 2000; Ruiqi et al., 2000; Wang, 2006).

Terms used in this report include first downhole occurrence and last downhole occurrence. In addition to first and last occurrence data, the abundance patterns of taxa were also noted because acmes have been indicated previously (Kurita and Obuse, 2003) and may have regional significance for biostratigraphy. Acmes are also important for assessing stratigraphic and environmental patterns in pollen and spore data (Yamanoi, 1992; Sato, 1994; Wang, 2006). Notes on palynomorph abundance within a sample or stratigraphic distribution were recorded as follows:

B = barren.
P = poor (1–75 specimens counted within a sample).
M = moderate (76–125 specimens counted within a sample).
G = good (>126 specimens counted within a sample).
X = reworked presence within a sample from an older stratigraphic interval.

Diatoms

Samples from RCB cuttings and cores were collected at 10 m intervals from Hole C0020A. Sample material of ~0.5 g was washed and soaked/softened in Milli-Q water then sieved using a 45 µm sieve. Strewn slides were prepared from the sieved sedi-

ment by first stirring/shaking the sediment into suspension, immediately removing part of the upper suspension with a disposable pipette, and injecting it into a droplet of Milli-Q water to cover a 24 mm × 36 mm coverslip. The strewn sample was dried on a hot plate (50°–60°C) then mounted to a glass slide using Norland Optical Adhesive 61 and cured in UV light. Samples were examined with a Zeiss Axioskop 40 polarizing light microscope at 400× magnification with identifications checked at 1000×.

Biostratigraphy is the primary objective of this study; therefore, only the occurrences of stratigraphically diagnostic diatoms were tabulated. Diatoms were counted when at least half of a valve was present and identifiable at the species level. Estimation of diatom abundance was qualitative and based on the following:

A = abundant (≥6 specimens per field of view [FOV] at 400× magnification).
C = common (1–5 specimens/FOV at 400×).
F = few (0.2–0.8 specimens/FOV at 400×).
R = rare (1–10 specimens/horizontal traverse at 400×).
B = barren.

Diatom preservation is recorded based on the degree of breakage and dissolution of diatom valves as described by Akiba (1986):

G = good.
M = moderate.
P = poor.

Strewn slides were also examined for calcareous nannofossils; however, restricted diversity and rare occurrence eliminate them as a useful biostratigraphic tool. Therefore, Neogene sediments were zoned using diatoms according to the Neogene North Pacific diatom zone code system of Yanagisawa and Akiba (1998).

Downhole logging

Logging data provide measurements of in situ properties in the borehole. Logging data at various depths of investigation into the formation are therefore complementary to centimeter-scale core studies and >10 m scale seismic images. The wireline logging tool is lowered into the open hole on a multiple-conductor contrahelically armored wireline, and measurements are usually taken from the bottom of the hole upward. For depth correlation purposes, we tried to maintain steady cable tension. Most wireline measurements are recorded continuously while the tool string is moving, except for stationary measurements including fluid sampling, pressure measuring tools, and a seismic array. The measurements are made shortly after the hole is opened with the drill bit and before continued drilling operations that adversely affect in situ properties and borehole stability.

During Expedition 337, open hole measurements in the 17½ inch hole from 511 (below the 20 inch casing shoe) to 1220 m DSF were planned but cancelled to overcome the delay in the operations schedule. Measurements in the 10⅝ inch open hole from 1220 to 2466 m DSF were conducted as planned during logging operations and included natural gamma radiation (NGR), spectral gamma ray, density, neutron porosity, photoelectric effect (PEF), resistivity borehole images from the Formation MicroImager (FMI), laterolog resistivity, spontaneous potential (SP), sonic velocity (*P*- and *S*-wave) from the Dipole Sonic Imager (DSI), zero-offset vertical seismic profile (VSP) using the Versatile Seismic Imager (VSI), six-arm calipers, mud resistivity, mud temperature, Nuclear Magnetic Resonance (NMR) logging, in situ fluid analysis and sampling by the Modular Formation Dynamics Tester (MDT), and the Quicksilver probe. NGR and VSI measurements were extended to the cased hole interval (511–1220 m WMSF), and DSI was also measured through the casing pipe from 1070 to 1220 m WMSF.

One of the most significant objectives of the geophysical logging operations was to determine the target depths of fluid sampling by Quicksilver probe. Because the time allowed for fluid sampling is limited for each sampling point, only layers with sufficient permeability and fluid mobility can be candidates and they need to be clearly identified before fluid sampling is attempted. The logging operations sequence was designed for this purpose. A total of five runs were conducted, and the tool strings used are shown in Figure **F9:**

- Logging Run 1 (Platform Express [PEX]-High-Resolution Laterolog Array [HRLA]-Hostile Environment Natural Gamma Ray Sonde [HNGS]-gamma ray) (Fig. **F9A**) was to identify the lithofacies.
- Logging Run 2 (FMI-DSI-Environmental Measurement Sonde [EMS]-gamma ray) (Fig. **F9B**) was to examine the detailed features of each layer.
- Logging Run 3 (combinable magnetic resonance [CMR]-gamma ray) (Fig. **F9C**) was to look for permeable layers.
- Logging Run 4 (MDT-gamma ray) (Fig. **F9D**) was the formation testing tool with fluid sampling.
- Logging Run 5 (VSI-gamma ray) (Fig. **F9E**) was to correlate the borehole to the seismic profile.

The gamma ray tool needed to be attached to all runs to adjust the depth of each tool to Run 1.

Wireline logging

Wireline logging system

In general, wireline depth is more precise than drilling depth, which is affected by the stretch of the borehole assembly, and is measured accurately during logging operations with an integrated depth wheel. This device uses tension measurement for the correction of cable stretch and provides calibrated absolute depth values.

Data from each wireline logging tool were recorded in the data logger within the tool and were available for real-time display on board the ship via Schlumberger's multitasking acquisition and imaging system (MAXIS). MAXIS receives and records an array of data from the downhole logging tools, and the real-time data were used for a quality check of data and processes. The MAXIS real-time log data were displayed remotely on a large monitor in the data integration center on the laboratory management deck via the local network.

During Expedition 337, a strong wireline cable (7-46ZVXXS) was used because of the heavy weight of the MDT module. The conventional passive heave compensator system was used with hydraulic lines to the auxiliary tank and for compensating the extra line, which was connected between the riser and the rig (Fig. **F10**).

Wireline logging tools

Natural gamma ray tools

The gamma ray tool measures natural radiation emitted by the formation in American Petroleum Institute gamma ray units (gAPI) and is a standard device for identifying lithologic units and data quality checks. Gamma ray tools were used in all runs, and the sensors were included in cartridge or combination tools. Gamma ray tools have a depth of investigation ranging from 24 to 61 cm.

Platform Express

The PEX has advantages in shorter total tool length and higher logging speed against a conventional triple combination (triple combo) tool string (resistivity, density, and porosity). The PEX consists of the Highly Integrated Gamma Ray Neutron Sonde (HGNS) and High-Resolution Mechanical Sonde (HRMS) (Fig. **F9A**).

The HGNS contains a radioactive source that radiates fast neutrons to the formation and detectors to count slowed neutrons deflected back to the tool. Because the neutrons are slowed primarily by hydrogen atoms in the formation, the measurements are scaled in porosity units in terms of formation water content. The porosity this tool measures includes the volume of intracrystalline water contained by clay minerals.

The HRMS houses the Three-Detector Lithology Density (TLD), which measures density and PEF, and Micro-Cylindrically Focused Log (MCFL) tools and also has a one-arm caliper function. The tool is provided with real-time speed correction and depth matching.

The TLD tool measures the attenuation of a gamma ray flux to determine the density of the formation. The gamma radiation interacts with the energy of the gamma ray photon. This energy decreases progressively, and gamma radiation is absorbed by matter by the PEF. The number of scattered gamma rays that reach the detectors is directly related to the number of electrons in the formation, which is related to bulk density. The TLD tool uses three detectors to obtain a high-resolution 8 inch density output. The TLD detector with 2 inch resolution is normally applied to correct for minor well bore changes resulting from the hole condition and mud cake. This logging environment allows the use of the 2 inch detector as a standalone porosity device to improve the visibility and reliability of the TLD curves.

The MCFL tool uses a cylinder electrode on which source electrodes emit a highly focused beam (diameter = 2.5 cm) that rapidly diverges and penetrates the formation as deep as 10 cm. The tool gives information on mud cake and flushed zone resistivity, which are useful for the lithology-density correction of the TLD tool.

High-Resolution Laterolog Array

The HRLA tool provides six resistivity measurements with different depths of investigation. They include mud resistivity and five measurements of formation resistivity with increasing penetration into the formation. The sonde sends a focused current into the formation and measures the intensity necessary to maintain a constant drop in voltage across a fixed interval, providing a direct resistivity measurement. The array has one central (source) electrode and six electrodes above and below it, which serve alternatively as focusing and returning current electrodes. By rapidly changing the role of these electrodes, a simultaneous resistivity measurement at six penetration depths is achieved. The tool is designed to ensure that all signals are measured at exactly the same time and tool position and to reduce the sensitivity to "shoulder bed" effects when crossing sharp beds thinner than the electrode spacing.

Hostile Environment Natural Gamma Ray Sonde

The HNGS tool uses spectroscopic analysis and two bismuth germanate scintillation detectors to determine the concentration of radioactive isotopes. The measurements focus on three common decay chain reactions of radioactive isotopes that are common in natural formation (potassium, thorium, and uranium), with each emitting photons at different energies. The HNGS measures gamma radiation from each decay that are converted to the concentrations of potassium, thorium, and uranium.

The radius of investigation depends on several factors: hole size, mud density, formation bulk density (denser formations display a slightly lower radioactivity), and the energy of the gamma rays (a higher energy gamma ray can reach the detector from deeper in the formation). This tool has a 24 cm depth of investigation and can also be used inside casing.

Formation MicroImager

The FMI provides an electrical borehole image and dip information generated from up to 192 microresistivity measurements. The four electrode flaps attached to the four pads are applied to the borehole wall by caliper arms (Fig. **F11**). The combination of measuring button diameter, pad design, and high-speed telemetry system produces a vertical and azimuthal resolution of 0.51 cm. This means that the dimensions of a feature larger than this resolution can be identified in the image. The size of features <0.51 cm is estimated by quantifying the current flow to the electrode. The azimuthal coverage of the borehole image is ~60% in the 10⅝ inch hole.

The General Purpose Inclinometry Tool, which integrates both a three-axis inclinometer and a three-axis magnetometer, is associated with the FMI to determine the orientation of its image. It can also provide the geometry of the borehole path. The Pad 1 orientation was recorded as P1AZ.

Dipole Sonic Imager

The DSI tool incorporates both monopole and crossed-dipole transmitters with a hydrophone array. The tool is made up of three sections (acquisition cartridge, receiver section, and transmitter section). An isolation joint is placed between the transmitter and receiver sections to prevent direct flexural wave transmission through the tool body. The transmitter section contains a piezoelectric monopole transmitter and two electrodynamic dipole transmitters perpendicular to each other. To the monopole transmitter, an electric pulse at sonic frequencies is applied to excite compressional and shear wave propagation in the formation. The two dipole transmitters obtain azimuthal shear wave anisotropy and are also driven at low frequency to excite the flexural wave around the borehole. The array of eight receiver stations spaced 15.24 cm apart, which confines the vertical resolution of this tool, provides spatial samples of the propagating wave field for full waveform analysis.

Environmental Measurement Sonde

The EMS measures mud resistivity and temperature along the tool axis to support borehole environmental corrections. Based on six independent caliper gauges, the ovality algorithm provides detailed information on the borehole geometry for more representative environmental correction of imaging tool measurements, improved borehole stress analysis, and more precise cement volume estimation.

Power Positioning Device and Caliper

The Power Positioning Device and Caliper (PPC) tool has a four-arm power caliper that delivers accurate (~1 mm) dual-axis borehole diameter measurements. The caliper log is essential for the processing of other logs and can be used in sedimentological and structural interpretation of the formation. With the powered arms, the PPC tool can centralize or decentralize other tools.

Versatile Seismic Imager

The VSI is a borehole seismic wireline tool optimized for VSPs. It can make multiple shuttles (each containing a three-axis geophone) separated by "hard wired" acoustically isolating spacers. During Expedition 337, we used the VSI with four shuttles with 15.12 m spacing. The acoustic waves were generated by a 750 in^3 generator-injector air gun positioned ~6 m below sea level and offset 48.2 m from the borehole (Figs. **F12, F13**). The VSI was clamped against the borehole wall at 15.12 m intervals, and the air gun was typically fired between 5 and 10 times at each station. The recorded waveforms were stacked, and one-way traveltime was determined from the median of the first breaks for each station, thus providing check shots for calibration of the integrated transit time calculated from sonic logs. Check shot calibrations were required for well-seismic correlation because *P*-wave velocities derived from the sonic log may differ significantly from the velocities determined by seismic data.

Combinable magnetic resonance

The basic technology behind the CMR tool (also known as an NMR tool) is based on measurement of the relaxation time of the magnetically induced pre-

cession of polarized protons. A combination of permanent magnets and directional antennas are used to focus a pulsed polarizing field into the formation (Fig. F14). Then the tool measures the relaxation time of polarized molecules in the formation. By exploiting the nature of the chemical bonds within pore fluids (for hydrogen in particular), the tool can provide estimates of the total porosity, permeability, and bound fluid volume. The vertical resolution was 22.86 cm for high-resolution mode acquisition, and the depth of investigation of the measurement was 3.81 cm into the formation.

Spontaneous potential

SP is the natural difference in electrical potential between an electrode in the borehole and a fixed reference electrode on the surface. A significant deflection in SP was observed at boundaries of permeable beds, and the magnitude of the deflection depended mainly on the salinity contrast between drilling mud and formation water and the clay content of the permeable bed. The SP log was useful for detecting permeable beds and estimating formation water salinity where formation clay content was low.

Shipboard data flow and data quality

The wireline logging data were stored in MAXIS, the Schlumberger data acquisition system, and then an initial data quality check was conducted by field engineers and the logging staff scientist. The data were then processed on board the ship for (1) depth-shifting all logs to the seafloor, (2) environmental corrections specific to individual tools and depth matching, and (3) logging data quality control comparing repeated sections. The FMI data processing steps included data format conversion, inclinometry quality check, speed correction equalization, resistivity calibration, and normalization. During Expedition 337, environmental corrections, depth matching, and image data processing were performed on board the ship by the Schlumberger Data Consulting Service. FMI image data needed to be processed on board the ship using Schlumberger's GeoFrame (version 4.4) software package and were imported into GMI Imager software for further analysis. After data processing and exchanging to a suitable format (digital log information standard [DLIS], log ASCII standard [LAS], or Society of Exploration Geophysicists format "Y" [SEGY]), the data were delivered to shipboard scientists (Fig. F15).

Logging data quality control

During processing, data quality control was mainly performed by cross-correlation of all logging data. Data quality was assessed in terms of realistic values for the lithology of the drilling interval, repeatability between different passes of the same tool, and correspondence between logs affected by the same formation property. For example, the resistivity log generally showed similar features to the acoustic log, and the conductivity log generally showed inverse response features to the gamma ray log. A short repeat session was acquired after or before the main log to check repeatability. The overall quality of the downhole logging data was evaluated in the context of borehole conditions with drilling parameters. This was because large and irregular borehole shapes reduced data quality for eccentralization/centralization tools, and rough surfaces degraded the contact condition for some tools.

Downhole fluid sampling and measurement

The MDT wireline logging tool allows customization for several downhole modules. During Expedition 337, for the first time in IODP we used the MDT tool (1) to measure pore fluid pressure and permeability, (2) to acquire in situ formation fluid and gas samples, and (3) to analyze geochemical parameters in the formation fluids. The tool configuration included the gamma ray sonde, electric power module, multisample module, IFA module (Composition Fluid Analyzer [CFA]), pumpout module, single-probe module (MRPS) for pressure and permeability tests, Quicksilver probe module (MRPS) for fluid sampling, and hydraulic power module (Fig. F9D).

Downhole pressure and permeability tests

Single-probe pore pressure measurements were made by attaching the probe to the borehole wall and extracting pore fluid (Fig. F16). Pressure inside the sealing zone was recorded with a sampling period of 300 ms during and after pore fluid extraction. For single-probe measurements during Expedition 337, a fluid volume of 5–10 cm^3 was extracted at a rate of 30–80 cm^3/min. The extracted volume was chosen based on anticipated formation permeability and was adjusted during multiple drawdown tests at a single measurement location. Three probe types are available for single-probe measurements: (1) conventional, (2) large-diameter probe, and (3) large-diameter packer.

For all Expedition 337 deployments, the large-diameter probe was used. We estimated in situ pore fluid pressure from the last pressure recorded during the pore pressure recovery in single-probe tests. During Expedition 337, we used Schlumberger's standard approach to estimate fluid mobility for single-probe measurements. Pore pressure was drawn down for a specified time (typically 15 s), and then the pressure was allowed to partially or fully recover. The mobil-

ity calculated by Equation 3 is dimensionally dependent:

$$k_D/\mu = Cq/(\Delta P/6894.8), \quad (3)$$

where

k_D = drawdown permeability (mD),
μ = viscosity (centipoise),
q = flow rate (volume of fluid extracted during the drawdown divided by time [cm^3/s]), and
ΔP = difference between drawdown pressure and in situ pressure (often approximated as the final build-up pressure) (Pa).

C is a constant that depends on the probe type (C = 5360, 2395, and 1107 for conventional, large-diameter probe, and large-diameter packer, respectively); C = 2395 for all Expedition 337 deployments.

Fluid sampling

The Quicksilver probe is a sophisticated probe used to sample pristine formation fluid with low contamination of the borehole fluid. The Quicksilver probe has a sample port at the center of the probe and an annular guard port outside the sample port (Fig. F17). The guard port is designed to extract contaminated fluid so that the sample probe can take clearer formation fluid. At the beginning, both probes were opened and sample and guard lines were drained. Once the level of contamination was deemed acceptable during monitoring of the sample and guard lines, the valves of the sample bottles were opened to extract fluid from the formation. The SPMC was used to keep downhole in situ pressure during retrieval of samples for analysis of fluids and dissolved gas (Fig. F18). On board the ship, high-pressure formation fluid was transferred to the SSB using a mechanism similar to the SPMC on the surface and delivered to the science party.

During Expedition 337, high permeability was not expected in the sediment formation. The single probe was used for pretest to avoid damage to the delicate Quicksilver probe pad. The "XX" high-pressure pumpout module was used in order to control the lower pump rate against low-permeability formation. Six Dursan-coated SPMC and six SSBs were used to minimize contamination of the fluid sample from the bottle material. The bottles were flushed with pure water before the operation.

In Situ Fluid Analyzer

During fluid sampling, the IFA and CFA were used to monitor the sampling line and guard line, respectively. Their purpose was to (1) analyze in situ formation fluid in the sample line and (2) know the timing to open/close valves by monitoring contamination. IFA monitoring of the sample line measured resistivity, temperature, pressure, hydrocarbon composition (C_1, C_2, C_{3-5}, C_{6+}), carbon dioxide, 16-channel grating spectrometer, 20-channel filter spectrometer, density, and viscosity. The monitoring properties, range, and accuracy of the IFA are shown in Table T4.

Physical properties

Physical properties measurements provide fundamental information required to characterize lithostratigraphic units. A suite of measurements taken during Expedition 337 allowed correlation of recovered sedimentary cores and cuttings samples with downhole logging data and complemented other data sets taken on board the ship. After X-ray CT scanning, core sections wrapped with ESCAL bags were applied to the MSCL-W for measurements of gamma ray attenuation (GRA) density, magnetic susceptibility (MS), natural gamma radiation (NGR), *P*-wave velocity, and noncontact electrical resistivity. For LDC sections, a wide-diameter sensor track on the split core multisensor core logger (MSCL-S) was used. Thermal conductivity was measured basically on working halves and partially on WRCs. Discrete samples were taken from working halves for MAD analyses, discrete *P*-wave velocity, and electric resistivity analyses. Samples were also available from community WRC samples. MAD analyses provide water content, bulk density, porosity, void ratio, and grain density. Discrete samples for MAD analyses were taken in cubic form. Riser drilling cuttings were also subjected to MAD analyses. Details and procedures for each physical properties measurement are described below.

MSCL-W

Gamma ray attenuation density

GRA density is based on detection of a gamma ray beam produced by a cesium source and directed through the WRC. The beam is produced by a ^{137}Cs gamma ray source at a radiation level of 370 MBq within a lead shield with a 5 mm collimator. The gamma ray detector includes a scintillator and an integral photomultiplier tube to record the gamma rays that pass through the WRC. GRA bulk density (ρ_b) is defined by

$$\rho_b = \ln (I_o/I)/\mu d, \quad (4)$$

where

I_o = gamma ray source intensity,

I = measured intensity of gamma rays passing through the sample,
μ = Compton attenuation coefficient, and
d = sample diameter.

The Compton attenuation coefficient and I_o are provided by the MSCL-W and are treated as constants, so ρ_b can be calculated from I.

The gamma ray detector is calibrated with a sealed calibration core (a standard core liner filled with distilled water and aluminum cylinders of various diameters). To establish the calibration curves, gamma ray counts are measured through a 7 cm diameter standard cylinder composed of aluminum with six different diameters (1–6 cm) (density = 2.7 g/cm^3) filled with surrounding water. The relationship between I and μd is

$$\ln (I) = A(\mu d)^2 + B(\mu d) + C, \quad (5)$$

where A, B, and C are coefficients determined during calibration. GRA density measurements were conducted on core samples every 4 cm for 4 s. GRA bulk density can be used to evaluate the sediment pore volume, which is used for evaluating the sediment consolidation state.

Magnetic susceptibility

MS is the degree to which a material can be magnetized by an external magnetic field. Therefore, MS provides fundamental information about sediment composition. A Bartington loop sensor (MS2C) with an 8 cm loop diameter was used to measure whole-round section MS. An oscillator circuit in the sensor produces a low-intensity (~80 A/m root mean square), nonsaturating, alternating magnetic field (0.565 kHz). Any material brought within the influence of this field will result in a change in the oscillating frequency. The frequency information (returned in pulse form to the susceptometer) was converted into MS. MS data were collected every 4 cm along the core. A reference piece with known MS was measured for condition calibration at least once a day.

Natural gamma radiation

NGR measurements provide insight into sediment composition and thus can be used to identify lithology. WRCs were monitored for NGR emissions to obtain spatial variability in radioactivity and to establish gamma ray logs of cores for correlation with downhole gamma ray logs. A lead-shielded counter, optically coupled to a photomultiplier tube and connected to a bias base that supplied the high-voltage power and a signal preamplifier, was used. Two horizontal and two vertical sensors were mounted in a lead cube-shaped housing. The NGR system records radioactive decay of long-lived radioisotopes ^{40}K, ^{232}Th, and ^{238}U. NGR has a resolution of 120–170 mm and was measured every 16 cm for 30 s. Background radiation noise was determined by making measurements on a water-filled calibration core. A granite reference material was measured for checking the calibration of the detector at least once a day.

P-wave velocity

P-wave data can be used to evaluate small strain moduli, to correlate between log and core data, and to evaluate pore structure and cementation. *P*-wave (compressional) velocity (V_P) is defined by the time required for a compressional wave to travel a set distance:

$$V_P = d/t_{core}, \quad (6)$$

where

d = path length of the wave across the core, and
t_{core} = traveltime through the core.

P-wave velocity transducers mounted on the MSCL-W system measure total traveltime of the compressional wave between transducers. The wave travels horizontally across the whole core and core liner. The total traveltime observed is composed of t_{core}, t_{delay}, and t_{liner}, where

t_{delay} = delay related to mechanical effects, and
t_{liner} = transit time through the core liner.

The system is calibrated using a core liner filled with distilled water, which provides control for t_{delay} and t_{liner}. With these calibrations, core velocity (V_P) can be calculated on whole-round specimens in core liners:

$$V_P = (d_{cl} - 2d_{liner})/(t_o - t_{delay} - 2t_{liner}), \quad (7)$$

where

d_{cl} = measured diameter of core and liner,
d_{liner} = liner wall thickness, and
t_o = measured total traveltime.

Electrical resistivity

Electrical resistivity measurements are useful for estimating other physical properties, such as porosity, tortuosity, permeability, and thermal conductivity. Bulk electrical resistivity is controlled by solid grain resistivity, pore fluid resistivity, and pore space distribution and connectivity. Electrical resistivity (R_e) is defined by the electrical resistance and geometry of the core measured:

$$R_e = R(A/L), \quad (8)$$

where

R = electrical resistance,
L = length of measurement, and
A = cross-sectional area of the core.

The noncontact resistivity sensor on the MSCL-W system induces a high-frequency magnetic field in the core with a transmitter coil. This generates an electrical current in the bulk sediment that is inversely proportional to its resistivity. A receiver coil measures the secondary magnetic field generated by this induced electrical current. To measure this smaller magnetic field accurately, a differencing technique has been developed that compares readings from the sample core to readings from an identical set of coils operating in air. Electrical resistivity data were obtained at 4 cm intervals on the MSCL-W. For the MSCL measurements including MSCL-S mentioned below, wrapping in an ESCAL bag may impede tight contact between the sensors and the core liner; therefore, *P*-wave velocity data quality were potentially compromised. However, test measurements of standard pieces wrapped in ESCAL bags showed that this issue is minimal for noncontact measurements of GRA, NGR, and MS. Cores were run on the MSCL-W without waiting for thermal equilibrium to room temperature. Hence, temperature-dependent electrical resistivity results on the MSCL-W were treated as supplementary data.

MSCL-S

The MSCL-S was used for LDC whole-round section measurements. Core material removed from the aluminum core liner was placed on a semicylindrical plastic tray with a diameter of 100 mm. The LDC WRC section and the tray were wrapped, flushed with N_2, and vacuum sealed in an ESCAL bag in the same manner as IODP cores. As the upper half was not covered with plastic, core thickness was not measurable because of unevenness due to a partially ragged surface along the sections. The MSCL-S was equipped with the same sensors as the MSCL-W, except for the NGR and MS sensors, which were equipped with wider loop sensors (125 mm loop diameter for NGR and 120 mm for MS).

Thermal conductivity

Thermal conductivity is the rate at which heat flows through a material and is dependent on mineral and fluid compositions, porosity, and structure. Most of the measurements were conducted on the working-half of WRC samples using a half-space line source (mini-HLQ) probe (Vacquier, 1985), and very partially a needle type (standard VLQ) probe was applied for WRCs of soft sediments (Von Herzen and Maxwell, 1959). This approach approximates the heating element as an infinite line source (Blum, 1997). The measurements were performed three times at each measurement point, and the intermediate thermal conductivity value among the three results was selected as a representative value. For HLQ probe measurements, samples must be smooth to ensure adequate contact with the probe. Visible saw marks were removed, when necessary, by grinding and polishing the split surface. The measurement produces a scalar value in a plane perpendicular to each orientation of the line source of the HLQ and the needle probe of the VLQ. All measurements were made after the sediment cores had equilibrated to ambient laboratory temperature. In order to eliminate the effect of rapid but small temperature changes, the sample and the sensor probes were equilibrated together in an insulated Styrofoam box for at least 10 min prior to measurement. The instrument internally measures drift and does not begin a heating run until sufficient thermal equilibrium is attained. Cores were measured at irregular intervals (aiming for one sample per section) depending on the availability of homogeneous and relatively vein/crack-free pieces that were also long enough to be measured without edge effects. At the beginning of each measurement, temperature in the sample was monitored to ensure that the background thermal drift was <0.04°C/min. After the background thermal drift was determined as stable, the heater circuit was closed and the increase in the probe temperature was recorded. The condition of the probes was checked at least once every 24 h. The condition check was performed on a Macor sample (glass ceramic) of known thermal conductivity.

Discrete sample measurements

For discrete samples, 8 cm^3 cubic samples were cut from the working halves of split cores at an average frequency of four samples per core. However, sampling frequency changed depending on lithology variation. Discrete samples were selected to best represent the general variation and lithologies of the core. These samples were measured for *P*-wave velocity, electrical resistivity, and MAD (discussed below). When a cubic sample could not be taken from the core, sediment blocks ~10 cm^3 in total were used for MAD measurements. In that case, *P*-wave velocity and electrical resistivity measurements were omitted. Samples for MAD measurements were also taken from community WRC samples.

Cuttings sample measurements

Cuttings samples used for physical properties measurements were washed using freshwater before sepa-

ration into four categories based on the size fraction (>>4 mm, >4 mm, 1–4 mm, and <1 mm) by sieving. Large-sized cuttings >10 mm on each side axis were collected and pressed into cubic shapes (5–10 cm^3 of bulk volume) for measuring *P*-wave velocity and electrical resistivity in addition to porosity. The methodology is identical to that of discrete samples, even though sample orientations were unknown.

MAD measurements

MAD data were obtained through mass and volume determinations on discrete samples. MAD data allow for calculation of several basic quantities: water content, bulk density, dry density, porosity, and void ratio. For the measurements, a dual-balance system and a pentapycnometer in the core laboratory were used. Each discrete sample taken from a working half, as well as cuttings from each depth, was treated in a beaker of known mass and volume during MAD measurements. Cuttings samples were separated into four categories: one represents the original bulk cuttings samples that were washed with seawater, and the other categories represent cuttings samples that were sieved into >4.0 mm, 1.0–4.0 mm, and 0.25–1.0 mm particle size fractions.

Dual-balance system

A motion-compensated shipboard balance system, a so-called dual-balance system, was used to measure both wet and dry masses. The two analytical balances were used to compensate for ship motion, one acting as a reference and the other for measurement of the unknown. A standard mass of similar value to the sample was placed on the reference balance to increase accuracy. The dual-balance system was calibrated at least once every 24 h. The calibration was performed with a standard mass of 40 g on both balances; an accuracy of ±0.005 g was required for calibration.

Pentapycnometer system

The pentapycnometer system (Quantachrome) measures dry sample volume at room temperature using pressurized, helium-filled chambers. A five-chamber Quantachrome pentapycnometer system allowed the measurement of four sample volumes and one calibration sphere. The medium volume sample chamber was selected during Expedition 337. Each measured volume is the average of five volume measurements. The stainless steel sphere (28.9583 cm^3 in volume) used for calibration was rotated between all measurement chambers to monitor for errors in each chamber. Spheres are assumed to be between 28.90 and 29.02 cm^3 in volume. Individual volume measurements were preceded by five helium purges of the sample chambers, followed by five data acquisition cycles. The pentapycnometer was calibrated with the stainless steel sphere at least once every 24 h.

Wet and dry mass measurements

Discrete samples taken from the working half and cuttings samples were measured for the determination of wet sediment mass (M_w). Cuttings and core samples were soaked in 35‰ NaCl solution for a few hours before measurement. After soaking, the wet cuttings samples were wiped to remove excess water. Dry sediment mass (M_d) and volume (V_d) were measured after drying the samples in a convection oven for >24 h at 105° ± 5°C. Dried samples were then cooled in a desiccator for >1 h before the dry mass was measured. Dry volume was measured using a helium-displacement pycnometer with a nominal precision of ±0.04 cm^3. Each reported value consists of an average of five measurements. A reference volume (calibrated sphere) was run with each group of four samples, and the sphere was rotated between cells to check for systematic error.

For calculation of sediment bulk density, dry density, grain density, porosity, and void ratio, conventional ODP methods were used (e.g., Shipboard Scientific Party, 1996). Water content, porosity, and void ratio were defined by the mass or volume of extracted water before and after the removal of interstitial water through the drying process. Standard seawater density (1.024 g/cm^3) was assumed as the pore water density.

Water content

Water content (W_c) was determined using the methods of the American Society for Testing and Materials (ASTM) designation D2216 (ASTM International, 1990). Corrections are required for salt when measuring the water content of marine samples. In addition to the recommended water content calculation in ASTM D2216 (i.e., the ratio of pore fluid mass to dry sediment mass [percent dry weight]), we also calculated the ratio of pore fluid mass to total sample mass (percent wet weight). The equations for water content were

$$W_c\ (\%\ \text{dry wt}) = (M_t - M_d)/(M_d - M_t) \quad (9)$$

and

$$W_c\ (\%\ \text{wet wt}) = (M_t - M_d) \times (1 + r)/M_t, \quad (10)$$

where

M_t = total mass of the saturated sample,

M_d = mass of the dried sample, and
r = salinity.

Bulk density

Bulk density (ρ) is the density of the saturated samples, with $\rho = M_t/V_t$ (V_t = total volume of the saturated sample). The mass (M_t) was measured using the balance, and V_t was determined from the pycnometer grain volume measurements and the calculated volumes of pore fluid (V_{pore}) and salt (V_s):

$$V_t = V_{pore} + V_d - V_s, \quad (11)$$

$$V_{pore} = M_w/\rho_w = (M_t - M_d)/[(1 - r)\rho_w], \quad (12)$$

and

$$V_s = M_s/\rho_{salt} = [(M_t - M_d)r/(1 - r)]/\rho_{salt}, \quad (13)$$

where

ρ_w = pore fluid density, and
ρ_{salt} = salt density (2.257 g/cm^3).

Porosity

Porosity (ϕ) was calculated using

$$\phi = (W_c \times \rho)/[(1 + W_c) \times \rho_w], \quad (14)$$

where

ρ = measured bulk density,
ρ_w = density of the pore fluid, and
W_c = water content expressed as a decimal ratio of percent dry weight.

Grain density

Grain density (ρ_{grain}) was determined from measurements of dry mass and dry volume made in the balance and in the pycnometer, respectively. Mass and volume were corrected for salt content using

$$\rho_{grain} = (M_d - s)/[V_d - (s/\rho_{salt})], \quad (15)$$

where

s = salt content (in grams), and
ρ_{salt} = salt density (2.257 g/cm^3).

P-wave velocity

Discrete *P*-wave velocity measurements were obtained on cubic discrete sediment samples using the *P*-wave logger for discrete samples (GeoTek). The cubic samples were soaked in 35‰ NaCl solution prior to *P*-wave measurement. The measurements used caliper-type contact probe transducers on the *P*-wave velocity gantry. Oriented samples were rotated manually to measure *x*-, *y*-, and *z*-axis velocities with the same instrument. The system uses delay line transducers, which transmit compressional wave at 230 kHz. To maximize contact with the transducers, deionized water was applied to sample surfaces. The signal received through the sample was recorded by the computer attached to the system, and the peak of the initial arrival was chosen. The distance between transducers was measured with a thickness sensor. Before measurements were made, calibration was performed every 24 h with acrylic and glass cylinders with known *P*-wave velocities of 2722 ± 33 m/s and 5507 ± 138 m/s, respectively. The determined system time delay from calibration was subtracted from the picked arrival time to yield a traveltime of the *P*-wave through the sample. The sample thickness was divided by the traveltime (in seconds) to calculate a *P*-wave velocity in meters per second.

Electrical impedance

Electrical impedance was measured on discrete cubic sediment samples using the Agilent 4294A Precision Impedance Analyzer. The cubic samples were soaked in 35‰ NaCl solution prior to the measurements. The samples are held between two stainless steel electrodes. For the measurements, paper filters soaked in NaCl solution allow better contact between the electrodes and the cubic sample on both top and bottom sides. Oriented samples were rotated manually to measure electrical impedance along *x*-, *y*-, and *z*-axes with the same instrument. The frequency of electric transmission is 25 kHz.

Electrical impedance is defined as the ratio of the voltage and the current in an alternating current circuit. By the measurements, magnitude of electrical impedance (|*Z*|) (in Ω), phase angle (θ) (in degrees), and sample length (*L*) are first given. Electrical resistivity on the x-axis (R_x) is described as

$$R_x = (|Z_x|\cos\theta - |Z_f|\cos\theta_f) \times (L_y \times L_z/L_x)/100, \quad (16)$$

where $|Z_f|\cos\theta_f$ is the resistance of the paper filters and L_x, L_y, and L_z are the lengths of the triaxial directions. Other resistivity values on the *y*- and *z*-axes (R_y and R_z) are described by the same equation.

Horizontal anisotropy of electrical resistivity (A_h) and vertical anisotropy of electrical resistivity (A_v) were calculated using the following equations:

$$A_h = 200(R_x - R_y)/(R_x + R_y) \quad (17)$$

and

$$A_v = 200[(R_x + R_y)/2 - R_z]/[(R_x + R_y)/2 + R_z], \quad (18)$$

where R_x, R_y, and R_z are electrical resistivity in each axial direction.

By assuming the anisotropy of resistivity, formation factor on the x-axis (F_x) is described as

$$F_x = R_x/R_f, \quad (19)$$

where R_f is the resistivity of pore fluid represented by standard seawater at room temperature (°C) as mentioned below. The relationship between R_f and temperature (T) is explained by (Shipley, Ogawa, Blum, et al., 1995):

$$R_f = 1/(2.8 + 0.1T). \quad (20)$$

Other formation factors on the y- and z-axes (F_y and F_z) are described by the same relation.

Formation factor of bulk rock (F_{bulk}) is defined as

$$F_{bulk} = R_{bulk}/R_{fluid}, \quad (21)$$

where R_{bulk} is the mean value of triaxial resistivity described as

$$R_{bulk} = (R_x^2 + R_y^2 + R_z^2)^{1/2} \quad (22)$$

and R_{fluid} is the resistivity of standard seawater (Shipley, Ogawa, Blum, et al., 1995).

Calibration was required prior to measurement and every 24 h when using the instrument continuously. For calibration, measurements on both open and short states were performed. A standard disk attachment was applied to the calibration with the nonconductive cap on in an open state and also without the cap at short state. Saturated filter papers were applied for better contact between the electrodes and the cubic sample, and a characterized tuff cubic sample with filter papers was measured for quality control.

Anelastic strain recovery analysis

The anelastic strain recovery (ASR) technique is a core-based stress measurement that can evaluate both orientation and magnitude of 3-D principal stress on rock at present. The ASR technique principally measures the anelastic strain change by releasing the stress soon after core recovery. The methodology used for the ASR measurement during Expedition 337 is based on Matsuki (1991), following the guideline described by Lin et al. (2007). After the X-ray CT scan and MSCL-W measurement, a 17 cm long fresh WRC was immediately taken to the QA/QC laboratory for ASR determination because the analysis is time-sensitive. First, the outer surface of the core was washed in seawater to remove drilling mud. Before starting the ASR measurement, an elliptical section of core sample was measured by a 2-D measurement sensor (Keyence Corporation, TM-065) on the rotary table (Fig. F19). Diameter measurement of the LDC core was not undertaken because the core diameter was out of range for the sensor. The anelastic strain of the specimen was measured in nine directions, including six independent directions, using 18-wire strain gauges. During the treatment of homogeneous shales and also alternating sandstone with silt, fractures developed parallel to the bedding plane, so glue was placed on the fractures to prevent splitting. The attachment of 14 strain gauges took 1–2 h to achieve, and the total elapsed time from the recovery of core on deck was 3–5 h until the time when strain data (core diameter) could be recorded. Strain data were collected every 10 min for up to a maximum of 21 days. The core samples were double-bagged (i.e., with plastic and aluminum) and submerged in a thermostatic chamber, where temperature changes were controlled to within less than ±0.1°C during measurement.

Deviation of stress is the most important parameter for understanding stress state at depth. Using the data obtained from 2-D measurement, the relationship between the maximum horizontal stress (S_{Hmax}) and the minimum horizontal stress (S_{Hmin}) is estimated by the following relationship:

$$S_{Hmax} - S_{Hmin} = (d_{max} - d_{min}) \times d_0 \times E/(1 - \nu), \quad (23)$$

where

d_{max} = maximum diameter,
d_{min} = minimum diameter,
d_0 = initial diameter before unloading of core samples,
E = Young's modulus, and
ν = Poisson's ratio.

By assuming that d_0 replaces the d_{min} and E and ν are the same among core samples, we can roughly expect $S_{Hmax} - S_{Hmin}$ to increase with depth. Generally, even though Young's modulus of sedimentary rocks increases with depth due to sediment consolidation, Young's modulus E as well as ν varies among lithologies.

Vitrinite reflectance analysis

Vitrinite reflectance (R_o) is a major indicator of the thermal maturity of organic sedimentary materials. During Expedition 337, R_o values of coal fragments were measured on board the ship using the vitrinite reflectance analyzer for small coal particles designed by Sakaguchi et al. (2011) (Fig. F20). Coal fragments were extracted by rough crushing with mortar and

separation in heavy liquid using a sodium polytungstate solution (density = 1.8 g/cm^3). The sediment fraction was sieved through 75 µm mesh, and large coal particles were collected. The coaly fragments were then polished using SiC abrasive papers (i.e., 800, 1200, and 2400 grit) and an alumina burnishing cloth with two alumina suspensions in 1 and 0.3 µm particle size. A random mean R_o value was obtained by measuring R_o for 100 randomly oriented fragments under an oil immersion microscope with a microspotlighting system. Five standard samples were used for R_o value calibration.

Inorganic geochemistry

Interstitial water collection

During Expedition 337, WRC samples were squeezed for interstitial water analyses. One or two WRC sections measuring 30–75 cm in length were sampled per core. The particular locations for interstitial water WRC sampling were selected after close inspection of the X-ray CT scan images of the cored sections. Core intervals characterized by high fracture density, disturbed lithologies, or cleat structures were disregarded, as such sediment material is more susceptible to contamination from drilling fluids. After examination for internal structures with X-ray CT scan, selected WRC samples were taken to the sample preparation laboratory and placed in nitrogen-flushed glove bags at room temperature (~23°C).

A portion of the sediment was immediately extruded from the core liner. Once extruded, ~1 cm on each end of the WRC was cut off, as these sediments had probably undergone significant degassing during WRC sample processing. Furthermore, ~0.5–1.0 cm of the exterior portion of WRCs was peeled off to remove portions of the section that were potentially contaminated by riser drilling mud or materials generated during liner splitting contamination. Peeling included internal portions of the cores adjacent to fractures. In the case of LDC, the time span between core recovery and arrival of interstitial water WRC samples in the Sample Preparation Laboratory amounted to as long as half a day because of the longer processing time involved with this type of coring method at the rig floor and core cutting area. This processing delay greatly enhanced the risk for sample contamination. Therefore, more sediment was peeled off from the LDC WRC sample surface and ends (i.e., up to 2–5 cm). Additionally, the integrity of the inner part of the sample was visually inspected and, where necessary, portions showing infiltrated drilling mud were removed. The peeled-off residue from WRC samples was saved for shipboard smear slides and core descriptions.

The cleaned sediment was placed into two 9 cm in diameter Manheim-type titanium squeezers (Manheim, 1966) on top of a stack of two pieces of filter paper rinsed with ultrapure deionized water (18.2 MΩ Milli-Q) and two titanium screens (40 mesh). Fluids released by squeezing were then passed through a sterile 0.22 µm disk filter connected to an acid-washed 20 mL plastic syringe. This process was repeated with the remaining sediment in each section. In cases of low yield, squeeze cakes were combined in one squeezer for further interstitial water recovery. Interstitial water was distributed into aliquots for both shipboard and shore-based geochemical analyses. Squeeze cakes were divided, placed in bags, and stored as requested for shore-based research. In the time between sampling and squeezing, the remaining interstitial water WRC samples were stored in a 4°C refrigerator in nitrogen-flushed, doubly sealed oxygen-impermeable ESCAL bags without applying a vacuum.

Because cores were not recovered during the drilling through Unit I (647–1256.5 m MSF), it was decided to sample and squeeze interstitial water from drilling cuttings across this interval. The unrinsed cuttings were placed on a tray and then transferred with a spatula to a Manheim squeezer. No further attempt was made to remove the drilling fluid that had soaked into the sediment cuttings. This procedure was continued at selected depths of Units II and III, in order to compare cuttings water with interstitial water from cores at the same corresponding depth.

Interstitial water analysis

The only other IODP riser drilling expedition to date encountered problems with limited interstitial water yields at elevated depths (Expedition 319 Scientists, 2010b). In anticipation of potentially the same problems during Expedition 337, several standard analytical shipboard procedures were modified. Interstitial fluid splits were not set aside for chlorinity titration; instead, a very small amount of interstitial water was diluted and used for chloride determination by ion chromatography (IC). Second, the IC analytical run for sulfate was also used to analyze for nitrate. Finally, in cases where the total interstitial water yield from the 60 cm WRC sample was <5 mL, the pH measurement was disregarded and alkalinity was determined by diluting a known volume of interstitial water dilution with 0.7 M KCl. In anticipation of potentially long squeezing times (Expedition 319 Scientists, 2010b) and the possibility that some of the

chemical and isotopic components of the interstitial water could be compromised by sediment degassing—in particular, the dissolved inorganic carbon (DIC) prepared for postcruise analysis and shipboard pH/alkalinity determinations—small aliquots of interstitial water for these time-sensitive analyses were prepared first, before the rest of the sediment was squeezed.

Interstitial water samples were analyzed using the standard IODP methods of shipboard geochemical measurements described previously (e.g., Expedition 319 Scientists, 2010a; Expedition 333 Scientists, 2012). A refractometer (Atago RX-5000) was used to determine salinity based on the refractive index. Immediately following interstitial water extraction, alkalinity and pmH were determined with a pH electrode and an autotitrator (Metrohm) with a 3 mL aliquot of interstitial water. The concentration of protons is reported as pmH rather than pH because the calibration was carried out with buffers in an artificial seawater solution of KCl, which approximates the ionic strength of the pore water samples themselves (Dickson, 1984). In cases where the total yield of interstitial water was <5 mL, we carried out a 1:10 dilution using 0.3 mL of interstitial water plus 2.7 mL of 0.7 M KCl solution in order to provide the minimum operational volume required by the alkalinity autotitrator. The 0.7 M KCl solution was used as a diluent both with the 0.3 mL sample and with the calibration standards, serving to maintain the ionic strength at values similar to seawater.

Sulfate, bromide, and nitrate concentrations were analyzed from an unacidified sample diluted with Milli-Q water to 1:100, whereas chloride was determined from a 1:1,000 dilution of the same sample using an IC (Dionex ICS-1500 ion chromatograph) with an anion column. A seawater standard (International Association for the Physical Sciences of the Oceans [IAPSO], Kanto Chemical Co., Inc., 07197-96) was analyzed for QC and to determine accuracy. The residue of the unacidified sample was analyzed with an UV-visible spectrophotometer (Shimadzu UV-2550) to determine dissolved ammonium and phosphate (Gieskes et al., 1991). A cation column was used on the Dionex IC to analyze major cations (Na, K, Mg, and Ca) on acidified (4% of 6 M HCl, trace metal grade) interstitial water samples diluted 1:200–1:800, depending on the concentration of the analyzed compound. The IAPSO standard was used for calibration, and dilutions of IAPSO were used for internal QC of the instrument. Inductively coupled plasma–atomic emission spectroscopy (Horiba Jobin Yvon Ultima2) was used to determine interstitial water minor element concentrations (B, Ba, Fe, Li, Mn, Si, and Sr). Samples were acidified and diluted 1:20 with Milli-Q water. Ultrapure primary standards (SPC Science PlasmaCAL) were prepared in a matrix solution of sulfate-free artificial seawater to fit the sample matrix, and yttrium was used as an internal standard (Shipboard Scientific Party, 2001).

Formation fluid analysis

Formation fluid samples were taken using an IFA coupled with a MDT, collected in a SPMC under in situ conditions, and then brought to the surface and transferred to SSBs for analysis (Dong et al., 2007; Mullins, 2008). Downhole Fluid Analysis (DFA) provides real-time data acquisition of resistivity and color data to identify target strata and to make a preliminary assessment of the potential to collect a water sample at depth (see **"Downhole logging"**). Once hydraulic communication was established with the sediment on the walls of the drill hole, 250 mL of formation water was pumped into the SPMC, where it was then pressurized and retrieved shipboard. This procedure was carried out at six selected depth horizons, providing a unique suite of samples to be divided between microbiologists, organic geochemists, and inorganic geochemists. After recovery, the sample fluids were transferred from the SPMC into a preevacuated glass SSB (see **"Organic geochemistry"**). After the gas extraction procedures were completed, the samples were placed in a glove box, where they were filtered and distributed into aliquots for both shipboard and shore-based geochemical analyses in much the same way as the interstitial water samples were handled (see above).

Analysis of drilling mud to correct for contamination

Sediment intervals that presented sulfate in the interstitial water bear the potential earmarks of contamination by seawater used in riser drilling mud and borehole fluids. As has been mentioned, an attempt to minimize this problem was carried out by peeling off the outer portion of the WRC sample prior to squeezing. However, sediment cores that have been fractured by the drilling process with the RCB and LDC, as well as those which present natural foliations or cleat structures, are susceptible to drilling fluid contamination that cannot be eliminated by simply removing the outer part of the WRC sample.

In order to assess and correct for possible contamination, mud from the circulation tanks was sampled twice before drilling, five times during the course of drilling, and once after drilling. Prior to analysis, dilution of drilling mud was necessary in order to facilitate separation of the water-soluble components of

drilling mud liquid (DML) from the colloidal components that include bentonite and a polymer viscosifier. A volume of 1 mL of drilling mud was diluted to a total volume of 10 mL with Milli-Q water, homogenized in an ultrasonic bath for 1 h, and then centrifuged for 1 h.

A small correction had to be made for the volume of drilling mud that was diluted, centrifuged, and analyzed because the volume of separated DML used to determine mud concentrations is not identical to the volume of drilling mud that was initially pipetted and diluted. For each mud sample, a separate ~20 mL aliquot of drilling mud was weighed and dried to find the proportion of salts and solids in a given volume of mud. Large-volume pipetting of the drilling mud proved inaccurate because of the highly viscous properties of the mud additives. In order to determine the volume of mud (V_{DM}), we relied on the density from the daily shipboard mud logging sheet form (ρ_{DM}) and the mass of the drilling mud before drying.

The major water-soluble constituents of drilling mud used in operations are generally 50 g KCl, 170 g NaCl, and 5 g soda ash (Na_2CO_3) dissolved in 1 L of seawater (assumed to contain 40 g/L salts) adjusted to a pH of 9.0–10.5 with KOH solution. These are combined with a number of commercial products, which act as colloidal lubricants and viscosifiers, including 5 g TelGel (bentonite), 8 g TelPolymerL (cellulose derivative), 10 g TelPolymerDX (starch derivative), 2.5 g Xanvis (xanthan gum derivative), 50 g CleanLubeL (lubricant and gas-hydrate inhibitor), 100 g RevDust (pseudocuttings), and 1 g TelniteGXL (antiseptic agent). Although actual concentrations may vary, we assume that the relative amounts of salts and nonwater-soluble components are roughly constant, such that the mass ratio of soluble salts to the net sum of soluble and insoluble and colloidal components (R_{wss}) is 0.600. The bulk dry density of water-soluble salts (ρ_{wss}) based on their relative weight abundance and respective densities is assumed to remain constant at 2.13 g/cm^3.

Using the initial mass of the wet mud and the mass of the residue (soluble and insoluble components) after freeze-drying, we can calculate the ratio of V_{DM} to the volume of DML (V_{DML}) as

$$V_{DM}/V_{DML} = V_{DM}/[(m_{H2O}/\rho_{H2O}) + R_{wss}(m_{sr}/\rho_{wss})], \quad (24)$$

where

V_{DM} = volume of drilling mud dried (calculated from the mass of the drilling mud and the density of the mud),
m_{H2O} = mass of water lost through freeze-drying (g),
ρ_{H2O} = density of pure water (1.000 g/cm^3),
m_{sr} = mass of solid residue (g),
R_{wss} = ratio of water-soluble solids to total solids in the mud (0.600 g/g), and
ρ_{wss} = bulk density of the water-soluble salts (2.13 g/cm^3).

Because $V_{DM} > V_{DML}$, the correction factor is a value >1. In cases where the mass correction is small ($m_{H2O}\rho_{H2O} >> m_{sr}R_{wss}\rho_{wss}$), the volume ratio approaches unity. DML concentrations were calculated from the diluted samples as follows:

$$[A]_{DML} = [A]_{dil}(V_{DM}/V_{DML})R_{dil}, \quad (25)$$

where

$[A]_{DML}$ = concentration of species A in the DML (expressed in mmol/L of DML),
$[A]_{dil}$ = diluted concentration measured in the laboratory, and
R_{dil} = dilution factor for the drilling mud that was centrifuged (10×).

Raw data for the freeze-drying procedure and volume correction results of the drilling mud are presented in MUD_VOL_CORR.XLSX in GEOCHEM in **"Supplementary material."** In all five mud samples, the volume correction is small, ranging from 1.035 to 1.078. The volume correction has been applied to all of the drilling mud results (see Table **T12** in the "Site C0020" chapter [Expedition 337 Scientists, 2013]).

Organic geochemistry

Expedition 337 was the first scientific initiative to drill and study a subseafloor hydrocarbon system with riser drilling technology. In this context, organic geochemists aimed to elucidate the cycling of carbon, including the conversion and transport of hydrocarbons, the flux of both thermogenically and biologically produced organic compounds, their utilization as carbon and energy sources by the deep biosphere, and the impact of deep hydrocarbon sources on the carbon budget of the shallower subsurface.

Methodologically, the shipboard organic geochemistry program of Expedition 337 was challenging in several ways. First of all, this expedition was only the second riser drilling operation in the history of scientific ocean drilling. Riser-specific scientific methods are still under development and require evaluation in terms of QA and QC. This is particularly true for the new types of samples that become available through riser technology (i.e., mud gas and cuttings

that arrive on board during the recycling of drilling mud). Second, riser drilling differs from riserless drilling with respect to the potential contamination of samples. Mud gas and cuttings are mixed with the drilling mud during their transport from the bottom of the hole to the rig, and the drilling mud used for riser drilling is more alkaline (pH = 9.3–11.9), more viscous, and has a higher density than seawater used for riserless drilling (see **"Drilling mud"** in the "Site C0020" chapter [Expedition 337 Scientists, 2013]). The potential contamination of sediment cores by drilling mud needs to be considered in the context of organic and inorganic geochemistry but is of the utmost importance for microbiological investigations and was comprehensively tested in the latter context (see **"Microbiology"**). Finally, DFA was performed for the first time in the framework of IODP (see **"Downhole logging"**). For the investigation of dissolved organic matter (DOM), dissolved hydrogen (H_2), and hydrocarbon gases, DFA provides large-volume fluid samples that are drawn directly from the formation and recovered at in situ pressure.

Organic geochemists investigated gas, solid-phase, and fluid samples. Where possible, established IODP protocols were used (e.g., Pimmel and Claypool, 2001; Underwood et al., 2009). The gas program included continuous online monitoring of mud gas that was extracted from the drilling mud in a separator unit, sampling of mud gas for shore-based analysis, shipboard analysis of gases in cuttings and sediment core samples (gas phase analysis of samples enclosed in gas-tight headspace vials), and sampling and preservation of solid-phase samples from cuttings and sediment cores for shore-based analysis of sorbed gases. Together with hydrocarbon gases and their stable carbon isotopic composition, H_2 and carbon monoxide (CO) were targets of high relevance to the expedition objectives. In addition, O_2, Ar, N_2, and noble gases were monitored in mud gas.

For solid-phase analyses, samples were collected from cuttings and sediment cores. The solid-phase program comprised the shipboard elemental analysis of sedimentary organic matter (C, N, and S), analysis of inorganic carbon content, and characterization of the kerogen type through Rock-Eval pyrolysis (Pimmel and Claypool; 2001). In addition, lipids, including fossil hydrocarbons, phospholipid fatty acids (PLFAs), and intact polar lipids (IPLs), were extracted from cuttings and sediment cores by accelerated solvent extraction (ASE) for both shipboard and shore-based analysis. These different types of biomarkers will help to characterize the deep coalbed biosphere and to constrain the thermal history of the borehole.

For fluid analyses, the interstitial water of sediment cores and fluids obtained by DFA were sampled, and shore-based analysis of DOM will yield information on concentrations and stable carbon isotopic compositions of organic metabolites and on the molecular composition of DOM.

Fresh sediment samples were taken from sediment cores for shipboard and shore-based incubation experiments to study microbial life. Shipboard ^{14}C-radiotracer experiments were employed to determine rates of microbial metabolic activities, such as methanogenesis, acetogenesis, acetate oxidation, and carboxidotrophic pathways. In addition, ^{13}C, ^{15}N, and deuterium (D) labeled compounds were used for stable isotope probing (SIP) experiments that will serve to track substrate utilization and uptake into cellular biomass (e.g., Morono et al., 2011; Kellermann et al., 2012; Wegener et al., 2012). SIP experiments were conducted in close collaboration with shipboard microbiologists, who on their part performed SIP on nucleic acids (see also see **"Microbiology"**). The analysis of gas, solid-phase, and fluid samples together with radiotracer and SIP experiments will allow us to track the carbon flow in the deep subseafloor biosphere within and above the Shimokita coalbed and will help us test the hypothesis that biogenic methane is formed in situ within the deeply buried subseafloor coalbeds.

In order to achieve our goals, additional equipment was brought on board the *Chikyu* and new methods were implemented. In particular, a mud-gas monitoring laboratory was set up in a container next to the rig floor, a radiotracer laboratory was installed in a van next to the core cutting area (see **"Microbiology"**), new protocols for shipboard lipid biomarker analysis were implemented, and additional third-party tools were employed (i.e., a reduced gas analyzer for the analysis of H_2 and CO was provided by the Japan Agency for Marine-Earth Science and Technology [JAMSTEC] Kochi Institute for Core Sample Research, and a radon analyzer came from the JAMSTEC Institute for Research on Earth Evolution [IFREE]).

Gases

Sampling and analysis of mud gas

Mud-gas monitoring laboratory

Continuous mud-gas monitoring during riser drilling is a standard procedure in oil and gas operations, where it is used to examine reservoir rocks for hydrocarbons and to fulfill safety regulations. In contrast, in scientific ocean drilling, real-time mud-gas monitoring of geochemical parameters is a new technique to investigate sediments that are drilled without coring. In the framework of IODP, continuous mud-gas monitoring was applied for the first time in 2009,

when riser drilling was conducted on the *Chikyu* during Expedition 319 (Saffer, McNeill, Byrne, Araki, Toczko, Eguchi, Takahashi, and the Expedition 319 Scientists, 2010). Our experimental setup builds on previous experience with scientific real-time mud-gas monitoring and sampling in the context of continental drilling (e.g., Erzinger et al., 2006; Wiersberg and Erzinger, 2007, 2011)+

Gas extraction system

Mud gas was extracted from the circulating drilling mud by a degasser. The degasser is composed of an explosion-proof electric motor on the top and a cylinder below (Fig. **F21A**). Inside the cylinder, a smaller degassing chamber, which connects to both the motor and the cylinder, is deployed in the place where gas is separated from the fluid. The gas is pumped online to the mud-gas monitoring laboratory, where the pumping rate that regulates the vacuum applied to the degassing chamber is set. A stirring impeller, which is operated by a motor, ensures the fluid circulation in the degassing chamber. An inlet and outlet on the cylinder allows drilling mud to flow through the whole system.

The degasser was installed right after the flow splitter, where the upcoming drilling mud is first exposed to the atmosphere (Fig. **F21B**). Some of the drilling mud flowed directly into a bypass line for the degasser. A safety valve outside the degassing chamber prevented overflow of drilling mud into the system (Fig. **F21C**). The safety valve is a 1 m long cylinder with a central tube that opens at both ends. Water is filled up to 40 cm in the cylinder and the tube. If the gas pressure from the degasser is not sufficient to sustain the preset pumping rate, air can be sucked in from outside and pushes water to flow from the central tube to the cylinder, where it compensates for the pressure difference. The reverse happens when gas pressure from the degasser exceeds the required level.

Gas extracted from the drilling mud traveled through a pipeline (3 mm inside diameter and ~50 m long) to the mud-gas monitoring laboratory, which was set up in a container next to the rig floor. It took ~3 min for gas to arrive at the mud-gas monitoring laboratory (Fig. **F21D**) (lag time was determined based on the time difference between the start of mud flow and the arrival of mud gas in the monitoring laboratory when drilling resumed after periods in which mud flow had been stopped). For such a short gas traveltime, diffusion loss during transportation is negligible (Wiersberg and Erzinger, 2007). In the mud-gas monitoring laboratory, particles and water vapor were removed from the incoming gas by a mist and moisture remover. Two sampling ports allowed sampling of mud gas either before or after passing the mist and moisture remover. All samples for shore-based analysis were taken from the mud gas before passing the mist and moisture remover. After passing the mist and moisture remover, the dry and clean gas was distributed online to different instruments.

Online analysis of hydrocarbon gases, CO_2, CO, Ar, and O_2 by gas chromatography

One part of the incoming mud gas was directed to a gas chromatograph (GC)-natural gas analyzer (NGA) (Agilent Wasson ECE 6890N). This instrument is designed to analyze hydrocarbon gases (C_1–C_5), Ar, O_2, N_2, CO, and carbon dioxide (CO_2). The main component of the GC-NGA system is a GC equipped with a gas sampling port with a multiposition valve. The carrier gas is helium (He). For analysis of hydrocarbon gases, the gas flow is first introduced into a 50 cm capillary column that retains hexane and heavier hydrocarbon components. C_1–C_5 hydrocarbon gases are then separated by another 49 m capillary column that connects to a flame ionization detector (FID). For analysis of nonhydrocarbon gases, Ar, O_2, and CO are separated from the rest of the components by an 8 inch micropack column (Wasson ECE Instrumentation, column Code 2378). CO_2 is separated by a 1.27 m capillary column (Wasson ECE Instrumentation, column Code S036). These two columns are connected to a thermal conductivity detector (TCD). The detection limit was 200 parts per million (ppm) for all nonhydrocarbon gases besides CO, which had a detection limit of 400 ppm. The detection limit was <1 ppm for all hydrocarbons. The GC-NGA provides a sensitive method for gas analysis, but the run time of each analysis is rather long (20–30 min), and consequently the temporal resolution and corresponding depth resolution of the mud-gas analysis are low. In addition, separation of Ar and O_2 can only be achieved with cryofocusing using liquid N_2. This procedure increases the analysis run time to 30–40 min and thus further decreases the depth resolution. Therefore, it was only applied sporadically.

The GC-NGA was calibrated on a daily basis in order to detect any sensitivity changes. Two standards were used. The standard mixture for the calibration of nonhydrocarbon gases contained 1% Ar, CO, Xe, O_2, H_2, CO_2, and He in a balance of N_2. The hydrocarbon standard mixture contained 1% C_1–C_5 in a balance of N_2.

GC-FID analysis informs us about the presence of C_1–C_5 hydrocarbon gases in the formation. However, the interpretation of concentration data is difficult because the gas yield from the drilling mud depends

not only on hydrocarbon concentrations in the drilled horizon but also on drilling conditions such as ROP and mud flow. Monitoring of drilling operations is crucial for the comparison and interpretation of quantitative data (see **"Recording of online gas analysis and monitoring of drilling operations, time, and depth"**). In contrast, the ratio of hydrocarbon gases varies only slightly when drilling parameters change and likely reflects in situ conditions. In particular, the C_1/C_{2+} ratio is a valuable parameter to distinguish between hydrocarbon gases from biogenic and thermogenic sources (Pimmel and Claypool, 2001; Ocean Drilling Program, 1992).

Ar and O_2 concentrations allow tracking the introduction of air into the mud-gas monitoring system during drilling operations. Air can be introduced into the borehole when the pipe is broken to recover core, when mud flow is stopped while new pipe connections are made (every 40 m), when pressure drops in the gas separator, and when mud gas is flowing from the bypass line into the flow splitter. Note that CO_2 can be analyzed by GC-NGA, but the resulting concentrations are not meaningful because the drilling mud is highly alkaline.

Online analysis of the stable carbon isotopic composition of methane

Another fraction of the incoming mud gas was transferred online to a methane carbon isotope analyzer (MCIA) (Los Gatos Research, Model 909-0008-0000), which detects the concentration and stable carbon isotopic composition of methane on the basis of cavity ring-down spectroscopy technology (cf. van Geldern et al., 2013). This instrument is composed of three parts: the main body of the MCIA, a gas dilution system (DCS-200), and an external pump. The stable carbon isotopic composition of methane is reported in the $\delta^{13}C$ notation relative to the Vienna Peedee belemnite (VPDB) standard and expressed in parts per thousand (per mil, ‰), with

$$\delta^{13}C = (R_{sample} - R_{VPDB})/R_{VPDB}, \quad (26)$$

$$R = {}^{13}C/{}^{12}C, \quad (27)$$

and

$$R_{VPDB} = 0.0112372 \pm 2.9 \times 10^{-6}. \quad (28)$$

The precision and analytical error of stable carbon isotope analysis by the MCIA was examined by serial dilution of gas standards (prepared manually). The error was <1‰ for CH_4 concentrations of >400 ppm but increased to 3‰ for concentrations ranging from 200 to 400 ppm. The gas dilution system can dilute sample gas 100× with zero-air (hydrocarbon-free compressed air). With such dilution ability, samples with methane concentrations from 200 ppm to 100% can be measured. However, the dilution system did not function because of technical problems and the concentration data from the MCIA were not utilized when they exceeded 1%. Although the quantification of methane by the MCIA is less sensitive than the GC-FID method and higher hydrocarbon gases cannot be analyzed simultaneously, MCIA analyses have the advantage of a short run time (a frequency of 1 measurement/s was chosen here), enabling continuous monitoring of CH_4 concentration. Typically, 100–200 measurements were conducted per meter of drilled sediments, depending on the ROP and mud flow rate. The sensitivity of this instrument was checked daily with a gas standard containing 2500 ppm CH_4 ($\delta^{13}C$ = –54.5‰ vs. VPDB) and balance air.

Together with C_1/C_{2+} ratios obtained by the GC-FID, the $\delta^{13}C$ of methane is an important parameter to distinguish biogenic and thermogenic sources of hydrocarbon gases during mud-gas monitoring (for details see Whiticar, 1999). The classical interpretation is based on the assumption that biological methanogenesis uses CO_2 with $\delta^{13}C$ values less than –10‰ vs. VPDB. If, however, the pool of dissolved inorganic carbon (DIC) in the sediment is enriched in ^{13}C, isotopic fractionation during methanogenesis will result in methane with similar $\delta^{13}C$ values as expected for thermogenic methane (Pohlman et al., 2009). The full interpretation of the stable carbon isotopic composition of methane will require shore-based analysis of the carbon isotopic composition of DIC in interstitial water samples retrieved from sediment cores and DFA.

In the MCIA, individual gas components are not separated prior to analysis and interferences could potentially impact the analysis. Because mud-gas monitoring with the MCIA was used for the first time in the history of scientific ocean drilling, the accuracy of the analysis needs to be confirmed. In order to further verify the analytical results obtained by the MCIA, we preserved samples of mud gas for shore-based stable carbon isotope analysis of methane by isotope ratio monitoring gas chromatography–mass spectrometry (Heuer et al., 2010; Ertefai et al., 2010). Shore-based investigations will also provide information on the stable hydrogen isotopic composition (δD) of methane and potentially on $\delta^{13}C$ and δD values of higher hydrocarbon gases, which will help to identify their sources.

Online analysis of gases by process gas mass spectrometer

The third fraction of the incoming mud gas was directed to a process gas mass spectrometer (PGMS) (Ametek ProLine process mass spectrometer) for continuous monitoring of H_2, He, O_2, Ar, Xe, N_2, CO, CO_2, methane, ethane, and propane contents. No carrier gas was added, as a vacuum was applied. The PGMS detects gases with a quadrupole mass filter based on the individual molecular masses of the target compounds. A Faraday cup detector provides an optimal scanning range of mass-to-charge ratio (*m/z*) 1–100 and an optional scanning range of *m/z* 1–200 with the mass resolution of 0.5 amu at 10% peak height. Input gas flow rate is set to 50 mL/min. For quantification of individual gas species, the PGMS was calibrated on a daily basis using the same standards as for GC-NGA. One standard contained 1% Ar, CO, Xe, O_2, H_2, CO_2, and He in a balance of N_2, and the other contained 1% C_1–C_5 in a balance of N_2. Pure N_2 and Ar were used for daily background checks. However, the regression line based on the standard could not be used because the concentration of major gas species (N_2, O_2, Ar, and CO_2) in the sample gas was significantly higher than the standard. Therefore, these gas species were calibrated by using the GC-NGA data of sample gas measurements at the same time point. The sensitivity of this instrument is 1 ppm. Although the PGMS is less sensitive than the GC-NGA, it allowed one measurement every 20 s for the selected scan (*m/z* 1–150) and resulted in better depth resolution.

O_2, Ar, and N_2 allow us to monitor the input of air during drilling operations (see **"Online analysis of hydrocarbon gases, CO_2, CO, Ar, and O_2 by gas chromatography"**), and O_2/Ar ratios provide information on corrosive processes at the drill bit and pipe, which might interfere with H_2 analysis.

Online analysis of radon

Radon analysis was carried out using a third-party laboratory instrument that was provided by JAMSTEC IFREE. The gas phase concentration of Rn that exsolved from the circulation mud was measured by a stand-alone radon monitor (AlphaGUARD PQ2000 PRO). The apparatus was attached to the auxiliary port of the scientific gas monitoring line parallel to other instruments. It has an ion-counting chamber 650 mL in volume (effective volume is ~500 mL), in which Rn decay is counted directly with a sensitivity of 100 Bq/m^3 in the concentration range of 2 to 2 × 10^6 Bq/m^3. Internal temperature, pressure, and relative humidity are recorded automatically. The time-sequential data can be exported to CSV format.

Sampling for shipboard and shore-based analysis

During mud-gas monitoring, discrete samples were taken by IsoTube samplers (Isotech Laboratories, Inc.) for shore-based analysis of $\delta^{13}C$ and δD values of hydrocarbon gases, δD values of H_2, and quantification of noble gases. In addition, 5 mL of gas was sampled occasionally from the sampling port of the gas flow line and transferred to 20 mL headspace vials for shipboard monitoring of the PFC tracer that was employed by the microbiologists to quantify core contamination with drilling mud (see **"Microbiology"**).

Recording of online gas analysis and monitoring of drilling operations, time, and depth

During riser drilling, the recovery of gases from drilling mud is affected by drilling operations. Drilling parameters were monitored and recorded in the SSX database. Lag depth was provided by the mud-gas logging contractor (Geoservices). The online data were available in the mud-gas monitoring laboratory and were used as a guide for sampling and data interpretation.

Ship time (UTC + 8) was the primary parameter against which all mud-gas monitoring operations, analyses, and sampling activities were recorded, except for Rn analysis, which used an internal clock set to the time zone UTC + 1. For the interpretation of raw data it is important to note that the internal MCIA clock could not be synchronized and was 90 s ahead of ship time. Because it takes time for mud to be recovered from the bottom of the hole, the depth of the arriving mud gas lags several meters behind the actual depth of the hole bottom at a given time. We used lag Depth A (as recorded in real time in the SSX database) to align data and samples from mud-gas monitoring to sediment depth. Lag Depth A was calculated by the mud-gas logging contractor (Geoservices, Schlumberger) based on mud flow, hole depth, and geometry and was recorded in drilling depth below rig floor (rotary table) (DRF). It can be converted to sediment depth in meters below seafloor (mbsf) by subtracting water depth (1180 m) and distance between water level and rotary table (28.5 m). The converted depth is treated as mud depth below seafloor (MSF).

Aside from drilling parameters, the SSX database also recorded online data that were generated during mud-gas monitoring by the GC-FID (see **"Online analysis of hydrocarbon gases, CO_2, CO, Ar, and O_2 by gas chromatography"**), MCIA (see **"Online analysis of the stable carbon isotopic composition of methane"**), and PGMS (see **"Online analysis of gases by process gas mass spectrometer"**). How-

ever, we noticed that the uploading of data from the instruments to the database suffered from technical problems, and it was not possible to correct for the faulty data. Therefore, we only used raw data as recorded by the individual instruments for further processing and interpretation.

Data were recorded nonstop during operations in Hole C0020A, including periods during which drilling did not advance into the formation and times without mud flow and/or mud-gas recovery. In the course of data processing, the time periods that did not yield meaningful information about the gas content of the geological formation were omitted from the raw data set. Subsequently, the high-resolution online records of the MCIA and PGMS, which yielded as many as 200 data points per drilled meter of sediment, were compiled into 1 m averages.

Background control, quality checks, and comparison of different sampling techniques

Several tests were conducted to account for various potential problems that might arise during geochemical mud-gas monitoring:

- Background control: the gases that are separated from the drilling mud in the degasser might result from the mixing of drilling mud with sediments, fluids, and gases in the formation, as well as from gases that are originally present in the drilling mud before being sent to the borehole. In order to account for background gases, drilling mud was regularly sampled from the tank and the hydrocarbon gas component was measured on board the ship. Samples were processed in the same way as samples from cuttings and sediment cores for headspace gas analysis with the GC-FID. The available instrumentation did not allow discrete sample analysis to determine background concentrations of other gases that were monitored online in the mud-gas monitoring laboratory.
- Mist and moisture remover: the mist and moisture remover is an essential unit in the online mud-gas monitoring system. However, it might cause fractionation both with respect to gas contents and their isotopic composition. In order to test the potential effect of the mist and moisture remover on gas contents and the carbon isotopic composition of methane, gas standards were measured with and without passing through the gas dryer. For methane, the effect of the mist and moisture remover was within the analytical uncertainty: compared to methane in the wet gas, the methane content of the dried gas was 3% lower and $\delta^{13}C$ values were 0.4‰ more positive (n = 13). For the PGMS, mist and moisture affected the analysis. When air was measured with and without passing through the gas dryer, H_2 and O_2 concentrations in the wet gas were both 2% higher than in the dried gas, whereas He and CO_2 concentrations in the dried gas were 67% and 84% higher than in the wet gas.
- Verification of results obtained from the MCIA: the MCIA for online mud-gas monitoring was used for the first time in scientific ocean drilling. In order to confirm its accuracy, samples of gas were taken for shore-based analysis by isotope ratio monitoring gas chromatography–mass spectrometry (Heuer et al., 2010; Ertefai et al., 2010).

Sampling and analysis of sediment cores

Hydrocarbon gases

Concentrations and distributions of light hydrocarbon gases, mainly methane (C_1), ethane (C_2), and propane (C_3), were monitored for each core following standard headspace sampling (Kvenvolden and McDonald, 1986). A 5 cm^3 sediment sample was collected with a cork borer from the freshly exposed end of the first section that was cut open in each core. In general, this was the section adjacent to the WRC cut for interstitial water sampling. The sample was extruded into a 24 mL glass vial and immediately sealed with a Teflon-coated septum and metal crimp cap. The exact bulk mass of the wet sample was determined after gas analysis was finished. For C_1–C_4 hydrocarbon gas analysis, the vial was placed in a headspace sampler (Agilent Technologies G1888 network headspace sampler), where it was heated at 70°C for 30 min before an aliquot of the headspace gas was automatically injected into an Agilent 6890N GC equipped with a packed column (GL HayeSep R) and FID. The carrier gas was He. In the GC temperature program, the initial temperature of 100°C was held for 5.5 min before the temperature was ramped up at a rate of 50°C/min to 140°C and maintained for 4 min. Chromatographic response of the GC was calibrated against five different authentic standards with variable quantities of low-molecular weight hydrocarbons and checked on a daily basis.

Methane concentration in interstitial water was derived from the headspace concentration using the following mass balance approach (Underwood et al., 2009):

$$CH_4 = [\chi_M \times P_{atm} \times V_H]/[R \times T \times V_{pw}], \qquad (29)$$

where

V_H = volume of headspace in the sample vial,
V_{pw} = volume of pore water in the sediment sample,

χ_M = molar fraction of methane in the headspace gas (obtained from GC analysis),
P_{atm} = pressure in the vial headspace (assumed to be the measured atmospheric pressure when the vials were sealed),
R = universal gas constant, and
T = temperature of the vial headspace in degrees Kelvin.

The volume of interstitial water in the sediment sample was determined based on the bulk mass of the wet sample (M_b), the sediment's porosity (ϕ, which was extrapolated from shipboard MAD measurements in adjacent samples), grain density (ρ_s), and the density of pore water (ρ_{pw}) as

$$V_{pw} = M_{pw}/\rho_{pw} = [\phi \times \rho_{pw}]/[(1 - \phi)\rho_s] \times M_b/\rho_{pw}, \quad (30)$$

where

M_{pw} = pore water mass,
ρ_{pw} = 1.000–1.024 g/cm^3 (adjusted to salinity based on shipboard data), and
ρ_s = 2.8 g/cm^3.

Hydrogen and CO

H_2 and CO analyses supplemented the routine shipboard analytical program and utilized a third-party laboratory instrument that was provided by the JAMSTEC Kochi Institute for Core Sample Research. The methodology described below focuses mainly on H_2. CO data were also generated during the H_2 analysis of the same sample set, but note should be taken that the underlying assumptions in the H_2 methodology do not necessarily apply to CO. A similar approach had previously been used on board the *Chikyu* during Expedition 322 (Underwood et al., 2009).

Dissolved H_2 concentrations were monitored using two different headspace equilibration techniques. For the first method, hereafter called the incubation method, ~5 cm^3 of sediment was collected from the freshly cut section ends. Samples were transferred into 20 mL headspace vials that were closed with thick blue butyl rubber stoppers (Chemglass Life Sciences, Vineland, New Jersey, USA), crimp capped, and thoroughly flushed with He in order to establish an O_2-free gas phase inside the vials. After analysis of the initial H_2 concentration, samples were incubated at estimated in situ temperatures and H_2 concentrations in the gas phase were monitored as a time series. At each time point, 1 mL of gas was sampled using a gas-tight syringe. In order to maintain a constant pressure inside the vials, the withdrawn amount of gas was substituted by injecting an equal volume of He after each analysis. In principle, the time series is supposed to continue until H_2 concentrations reach a constant level that represents a steady state between production and consumption. The incubation method allows the determination of dissolved H_2 concentration based on two fundamental assumptions: (1) H_2 in the headspace is in equilibrium with dissolved H_2 in the pore water, and (2) the incubation of samples in the laboratory allows the establishment of a biologically controlled steady state that is representative of in situ equilibrium (Hoehler et al., 1998).

The incubation method was initially developed for studies of freshwater sediments and microbial cultures (Lovely and Goodwin, 1988; Hoehler et al., 1998). In contrast to these metabolically active systems, deep-marine subsurface sediments host microorganisms that metabolize at very low rates (D'Hondt et al., 2002; Parkes et al., 2005). Therefore, it is unclear whether the required steady state can be reached within an acceptable time frame in the laboratory and whether such a steady state would be representative of in situ conditions. Alternative methods are needed for the determination of dissolved H_2 concentration in deeply buried sediments. However, the establishment of suitable methods is not a trivial task because of potentially low in situ H_2 concentrations and possible sampling artifacts. An alternative approach is the complete extraction of dissolved H_2 into a defined, H_2-free gas volume as previously used by Novelli et al. (1987) and D'Hondt et al. (2009), hereafter called the extraction method. In principle, this method is based on the assumption that the initially present H_2 exsolves from the liquid phase and can be captured in the defined headspace volume of a closed vial. Dissolved H_2 concentration can then be calculated using a mass balance (see below). The suitability of the extraction method for deep biosphere studies has recently been evaluated by Lin et al. (2012).

For the extraction method, ~3 cm^3 of sediment was sampled immediately after core recovery from the freshly exposed end of a core section. Typically, this was the same section that was used for hydrocarbon gas analysis. The sample was extruded into a 10 mL headspace vial, which was immediately completely filled with NaCl solution (3.5%), sealed with a butyl stopper (GL Science), and crimp capped. Excess water was allowed to escape through a hypodermic needle. Analysis was conducted as soon as possible after core recovery and sampling. A headspace was created by displacing 5–10 mL of the aqueous phase with an equal volume of H_2-free He. The gas-in needle was removed first, and the liquid-out needle connected to a syringe was allowed to equilibrate the pressure in

the vial headspace to atmospheric pressure. The volume offset in the liquid-out syringe was recorded. The vial was vortexed, and dissolved H_2 was allowed to diffuse out of the interstitial water and equilibrate with the headspace for 20 min before H_2 concentrations were analyzed in the headspace gas. Background controls are essential for accurate H_2 analysis by the extraction method. The reagent blank (analysis of vials filled with only NaCl solution) was 3.2 nM H_2. Samples of drilling mud were processed in the same way.

In both the incubation and extraction methods, dissolved H_2 concentration was determined based on the H_2 concentration in the headspace gas, which was analyzed by gas chromatography with a Reduced Gas Detector using a SRI 8610C (SRI Instruments). Samples are injected into a flow of carrier gas and separated on a packed column before they react with a heated bed of mercuric oxide and form mercury vapor that is subsequently detected in a photometer cell. For H_2, the reaction is $H_2 + HgO_{(solid)} \rightarrow H_2O + Hg_{(vapor)}$. The instrumental detection limit, evaluated statistically by a serial dilution of the primary standard with He, is ~300 parts per billion (ppb). The instrument was operated using a column temperature of 75°C and He as a carrier gas and was calibrated with a 3 ppm H_2 primary standard on a daily basis. Typically, 3 mL of gas sample was injected to thoroughly flush the 1 mL sample loop and the tubing between the injection port and the loop.

The incubation and extraction methods use different approaches to deduce the dissolved H_2 concentration from the analyzed headspace concentration, but for both methods, the first step is to convert H_2 concentration in the headspace from molar fractions to molar concentration ($[H_2]_g$):

$$[H_2]_g = \chi_{H2} \times P \times R^{-1} \times T^{-1}, \quad (31)$$

where

$[H_2]_g$ = expressed as nmol/L,
χ_{H2} = molar fraction of H_2 in the headspace gas (in ppb, obtained from GC analysis),
P = total gas pressure (in atm) in the headspace (1 atm),
R = universal gas constant, and
T = temperature of the gas phase in degrees Kelvin.

For the incubation method, the concentration of H_2 dissolved in the interstitial water ($[H_2]_{incub}$, expressed in nmol/L) is assumed to be in equilibrium with the gas phase and calculated as

$$[H_2]_{incub} = \beta \times [H_2]_g, \quad (32)$$

where β is an experimentally determined solubility constant corrected for temperature and salinity (Crozier and Yamamoto, 1974). The value of β is 0.01555 for seawater (salinity = 33.7 parts per thousand) at 19.3°C.

For the extraction method, the concentration of H_2 dissolved in the interstitial water ($[H_2]_{extract}$, expressed in nmol/L) is determined based on mass balance:

$$[H_2]_{extract} = ([H_2]_g \times V_g + [H_2]_{aq} \times V_{aq}) \times V_s^{-1} \times \phi^{-1}, \quad (33)$$

where

$[H_2]_g$ = calculated using Equation **31;**
$[H_2]_{aq}$ = H_2 concentration in the aqueous phase (obtained from Equation **32,** substituting $[H_2]_{aq}$ with $[H_2]_{incub}$ and β = 0.0061 for saturated NaCl solution [salinity = 264‰] based on the extrapolated value of Wiesenburg and Guinasso [1979]);
V_g = volume of the headspace;
V_{aq} = volume of the aqueous phase, including the pore water and the solution added;
V_s = volume of the sediment sample; and
ϕ = sediment porosity.

Lithification of sediments hampered the accurate measurement of sampled sediment volumes. Therefore, V_s was obtained based on the volume of NaCl solution that was added initially to completely fill the 14 mL headspace vial.

Gas analysis during downhole fluid analysis and sampling

In situ fluid analysis

DFA enables in situ fluid analysis as well as retrieval of fluid samples. In this manner, organic geochemistry was included in the downhole logging program. For more information see **"Downhole logging."**

Sampling and gas analysis in fluids retrieved by DFA

To determine the contents and isotopic compositions of dissolved volatile components in a fluid sample taken by DFA, we extracted the dissolved gases in the fluid under vacuum conditions (Saegusa et al., 2006). About 250 mL of sampled fluids was recovered in a gas-tight cylinder and transferred to a preevacuated glass extraction bottle (~350 mL), leaving ~100 mL headspace in the extraction bottle. In order to facilitate the extraction of the dissolved gases from the fluid into the headspace, the extraction bottle was ultrasonicated at 25°C for 5 min. To determine the total gas volume in the fluid, the pressure was measured by a pressure gauge. The extracted headspace gas was sampled into preevacuated stainless steel bottles and/or glass bottles and vacuum

glass vials. After extraction of dissolved gases, the fluid sample was further processed by inorganic geochemists (see **"Inorganic geochemistry"**) and microbiologists (see **"Microbiology"**).

Solid phase

Solid-phase sampling

Solid-phase sampling from cuttings

When drilling without coring, cuttings were sampled for both shipboard and shore-based investigations of the solid phase. For Unit I, in which there was no core retrieval, cuttings were sampled every 50 m for lipid biomarker work. The cuttings surfaces were contaminated by drilling mud or other organic materials used for drilling operations. To minimize signals from contaminants, volumes of 50 cm^3 cuttings were rinsed first with seawater obtained from the ship's seawater tap and then with freshwater. Subsequently, we ultrasonicated the cuttings three times, each time for 3 min, using organic solvents in the order of methanol, 1:1 v/v methanol/dichloromethane, and dichloromethane. The cleaned pellets were dried at 60°C and hand ground into powder for elemental, carbonate, Rock-Eval, and biomarker analyses. For Units II–IV, freshwater-washed cuttings were selected only from a few depths that are close to the coring intervals, vacuum-dried, and homogenized for subsequent analyses.

Solid-phase sampling from cores

In order to characterize the sedimentary organic matter and to analyze biomarkers in the solid phase of sediment cores (RCB and LDC), samples were taken from the WRCs dedicated for microbial community analysis ("community WRC") (see **"Microbiology"**). After the other small-volume samples were taken from the community WRCs, the remaining sediment was visually examined, the contaminated materials were removed, and the cleaned sediment was split into two aliquots. One aliquot (10–50 cm^3) was stored in a plastic bag and kept at –20°C for shipboard lipid biomarker analysis. The other aliquot (10–70 cm^3) was transferred into a high-density polyethylene can and kept at –20°C for shore-based supplementary lipid analyses and aqueous extraction of DOM. The shipboard sediment samples were vacuum-dried and ground into powder using either mortars or a SPEX CertiPrep 6850 freezer mill (SPEX CertiPrep Inc., Metuchen, New Jersey, USA), depending on the lithology of the sample. After homogenization, a small aliquot (3–5 g) of sediment was transferred into a glass vial and stored at room temperature for elemental, carbonate, and Rock-Eval analyses. The rest of the sediment powder was stored at –20°C before solvent extraction. In order to increase depth resolution, additional samples were taken in between community WRCs for elemental and Rock-Eval analysis.

For shipboard and shore-based experiments with live sediment, WRCs were first cut from undisturbed core sections after careful X-ray CT scanning; the sections of core liner containing the sediment were then closed with end caps, placed in air-tight bags, flushed with N_2, and finally stored at 4°C until further processing by the individual investigators.

Solid-phase analysis

Total carbon, nitrogen, and sulfur contents

Total carbon (TC), total nitrogen (TN), and total sulfur (TS) concentrations were determined using a Thermo Finnigan Flash EA 1112 carbon-hydrogen-nitrogen-sulfur (CHNS) analyzer. Calibration was based on the synthetic standard sulfanilamide, which contains 41.81 wt% C, 16.27 wt% N, and 18.62 wt% S. About 20–50 mg of sediment powder was placed in a tin container and weighed for TC and TN analyses. For TS analysis, the same amount of sediment powder was put into a tin container, weighed, and mixed with an equivalent mass of V_2O_5 catalyst. Sediment samples were combusted at 1000°C in a stream of O_2. Nitrogen oxides were reduced to N_2, and the mixture of CO_2, N_2, and SO_2 was separated by GC and detected by TCD on the CHNS analyzer. Standard deviations of TC, TN, and TS for the samples were less than ±0.1%. Accuracy of the analyses was confirmed using soil NCS reference material (Thermo Scientific, Milan, Italy), sulfanilamide standard (Thermo Scientific), and JMS-1 reference material.

Inorganic carbon, organic carbon, and carbonate content

With the same set of samples used for elemental analysis, we determined inorganic carbon concentrations using a Coulometrics 5012 CO_2 coulometer. About 10–20 mg of sediment powder was weighed and reacted with 2 M HCl. The liberated CO_2 was titrated, and the change in light transmittance was monitored with a photodetection cell. The weight percentage of calcium carbonate was calculated from the inorganic carbon content, assuming that all the evolved CO_2 was derived from dissolution of calcium carbonate, by the following equation:

$$CaCO_3\ (wt\%) = \text{inorganic carbon}\ (wt\%) \times 100/12. \quad (34)$$

No correction was made for the presence of other carbonate minerals. Standard deviations for repeated analyses on individual samples were less than ±0.1 wt%. NIST-SRM 88b and JSD-2 (standard reference materials) were used to confirm accuracy. Total organic carbon (TOC) contents were calculated by subtraction of inorganic carbon from TC contents as determined by elemental analysis.

Characterization of type and maturity of organic matter by Rock-Eval pyrolysis

Rock-Eval pyrolysis was used to characterize the type and maturity of the sedimentary organic matter and to identify its petroleum potential. In principle, Rock-Eval pyrolysis utilizes the sequential heating of a sample in the inert atmosphere (He) of a pyrolysis oven to quantitatively and selectively determine (1) the free hydrocarbons contained in the sample and (2) the hydrocarbon- and oxygen-containing compounds (CO_2) that are created during cracking of the kerogen in the sample. In addition, the shipboard instrument, a Rock-Eval6 Standard can also be used to oxidize and quantify the residual organic carbon (i.e., the organic matter remaining after pyrolysis).

Rock-Eval pyrolysis yields the following basic parameters (Espitalié et al., 1977; Peters, 1986):

- S1 = amount of free hydrocarbons (gas and oil) in the sample volatilized at temperatures <300°C (expressed in milligrams of hydrocarbon per gram of sediment).
- S2 = amount of hydrocarbons generated through volatilization of very heavy hydrocarbon compounds (>C_{40}) and the pyrolytic cracking of nonvolatile organic matter (in milligrams of hydrocarbon per gram of sediment). S2 is an indication of the quantity of hydrocarbons that the sediment can potentially produce should burial and maturation continue.
- S3 = amount of CO_2 (in milligrams CO_2 per gram of sediment) produced during combustion of the sample. S3 is an indication of the amount of oxygen in the kerogen.
- T_{max} = temperature at which the maximum release of hydrocarbons from cracking of kerogen occurs during pyrolysis. T_{max} is an indication of the stage of maturation of the organic matter.
- HI = hydrogen index (HI = [100 × S2]/TOC; in milligrams of hydrocarbon per gram of TOC). HI correlates with the H/C ratio, which is high for lipid- and protein-rich organic matter of marine algae.
- OI = oxygen index (OI = [100 × S3]/TOC; in milligrams CO_2 per gram of TOC). OI is a parameter that correlates with the O/C ratio, which is high for polysaccharide-rich remains of land plants and inert organic material (residual organic matter).
- PI = production index (PI = S1/[S1 + S2]). PI is used to characterize the evolution level of the organic matter by the proportion of free hydrocarbons present.
- PC = pyrolyzable carbon (PC = 0.083 × [S1 + S2]). PC corresponds to the carbon content of hydrocarbons volatilized and pyrolyzed during the analysis.
- RC = residual organic carbon.

Samples of ~60 mg of dry sediment were obtained from the same dried and homogenized bulk sample that had been used for elemental analysis. The temperature program of the pyrolysis oven used the following procedures. For 3 min, the oven was kept isothermally at 300°C and the volatilized free hydrocarbons were measured as the S1 peak (detected by the FID). The temperature was then increased from 300° to 550°C at 25°C/min. The hydrocarbons released from this thermal cracking were measured as the S2 peak (by the FID), and the temperature at which S2 reached its maximum was recorded as T_{max}. The CO_2 released from kerogen cracking was trapped in the 300°–390°C range. The trap was heated and the released CO_2 was detected as the S3 peak (by the TCD). The residual organic matter was oxidized in an oxidation oven kept at 600°C.

Lipid analysis

Analysis of hydrocarbon biomarkers in drilling cuttings is routine and has been demonstrated for commercial drilling (Peters et al., 2005), but this is not the case for PLFAs. Shipboard work focused on preparation of total lipid extracts (TLEs), which were split into two aliquots. One aliquot (20%) was used for shipboard analysis of fossil hydrocarbon molecular markers and free fatty acids. The other aliquot (80%) was stored at –20°C and shipped to the Center for Marine Environmental Sciences (MARUM; University of Bremen, Germany) where it will be used for shore-based analysis of PLFAs and IPLs. Shipboard analysis of fossil hydrocarbon markers aimed to characterize the sources of sedimentary organic matter and to construct a thermal history of Site C0020. Shore-based lipid analysis will be carried out to characterize the downcore distribution of PLFAs and IPLs. PLFAs are fatty acids derived from ester-linked phospholipids; IPLs include phospholipids and other types of membrane lipids with the polar head groups remaining attached to the core lipids. These polar

lipids are found to degrade rapidly after cell death or lysis (Harvey et al., 1986; Logemann et al., 2011) and have thus been used as proxies for extant prokaryotic biomass (e.g., Mills et al., 2006; Lipp et al., 2008). However, in deep subseafloor sediments, a fossil contribution of typical archaeal IPLs of >50% may complicate their use as quantitative proxies for live biomass (Xie et al., 2013). Results from the shore-based PLFA and IPL analyses will be compared with microbiological data to provide a complementary estimate of bacterial biomass. The analytical scheme for biomarker analysis is shown in Figure F22.

Solvent extraction of the solid phase and splitting of TLE. Both cuttings and samples taken from sediment cores were used for lipid analysis. The cuttings surfaces were contaminated by drilling mud or other organic materials used for drilling operations. To minimize signals from contaminants, we ultrasonicated the cuttings three times, for 3 min each time, using organic solvents in the order of methanol, 1:1 v/v methanol/dichloromethane, and dichloromethane. The cleaned pellets were dried at 60°C and hand ground into powder for lipid extraction.

The pulverized samples were subjected to ASE using an Accelerated Solvent Extractor 200 (Dionex, Osaka, Japan) and subsequently split into two aliquots as shown in Figure F22. Before extraction, known quantities of 1-alkyl-2-acetyl-*sn*-glycero-3-phosphocholine and 1,2-dihenarachidoyl-*sn*-glycero-3-phosphocholine were added for shore-based quantification of IPLs. The samples were loaded into 11 mL extraction cells and extracted twice under the following conditions:

Solvent = dichloromethane/methanol (9:1 v/v).
Temperature = 80°C.
Pressure = 1000 psi.
Preheat time = 1 min.
Heat-up time = 5 min.
Static extraction time = 5 min.
Cycles = 3.
Flush volume = 20%.
Purge time = 90 s.

To minimize and monitor the level of contamination during this procedure, all extraction cells were preprocessed using the same program before use, and an empty extraction cell was routinely processed along with the samples to make the procedural blank. The obtained TLE was evaporated under a stream of N_2 in a Zymark TurboVap LV (Sotax Corporation, Hopkinton, Massachusetts, USA) and transferred to preweighed glass vials. After determination of dry weight, the extracts were split into two aliquots for shipboard and shore-based analysis, respectively, and stored at –20°C until further processing.

Subsequently, the TLE split for the shipboard analysis of hydrocarbon molecular markers was subjected to silica gel column chromatography to separate saturated, aromatic, and polar fractions; a maltene-asphaltene separation was not performed. The saturated hydrocarbon fraction was eluted with hexane, the aromatic hydrocarbon fraction was subsequently eluted using 3:1 v/v hexane/dichloromethane, and the polar fraction was recovered using 1:1 v/v dichloromethane/methanol (on Fig. F22 these three fractions are denoted as F_1, F_2, and F_3, respectively). The polar fraction was dried under N_2 prior to the addition of a nonadecanoic acid standard and derivatization with BSTFA (*N*,*O*-bis[trimethylsilyl]trifluoroacetamide) to convert alcohols and carboxylic acids into their trimethylsilyl (TMS) ethers and esters. The standard 5β-cholane was added to fractions for quantification.

Instrumental analysis. Lipids were analyzed using an Agilent 5973 mass spectrometer linked to an Agilent 6890N GC (Agilent Technologies Inc., Santa Clara, California, USA). Separation of compounds was achieved using a HP-5MS column (30 m × 0.25 mm, 0.25 µm film thickness; Agilent Technologies Inc.) with He as the carrier gas. Samples were injected into a split/splitless injector at 300°C in splitless mode. Slightly different temperature programs were used to analyze different compound classes. For aliphatic and aromatic hydrocarbons, the oven temperature was set at 60°C upon sample injection and held for 1 min, increased to 150°C at 10°C/min, increased further to 310°C at 25°C/min, and held isothermal for 25 min. For fatty acids, the initial oven temperature was set to 80°C and the oven was kept at 310°C for 22.5 min. The mass spectrometer was operated in the selected ion monitoring (SIM) mode (ionization energy = 70 eV, operating in SIM mode, dwell time = 0.1 s/ion) for quantification. Compounds were identified by comparison of retention times to well-characterized samples, and selected samples were also analyzed in the scan mode to aid identification. The following standards were used to estimate the response factors of analytes in each compound class: anthracene for polycyclic aromatic hydrocarbons; C_{20}, C_{28}, and C_{31} *n*-alkane standards for *n*-alkanes; and C_{16}, C_{18}, and C_{20} *n*-alkanoic acids for alkanoic acids. Concentrations of sterenes, steranes, and hopanoids are reported relative to an internal 5β-cholane standard. The TMS ester of fatty acids was quantified in SIM mode with *m/z* 117 (O = $C^+OSi[CH_3]_3$) as the target ion.

Sample processing for shipboard and shore-based incubation experiments

Studies using ^{14}C radioisotope tracers

Shipboard incubations for the radiotracer experiments with ^{14}C labeled substrates were conducted by two methods: under in situ pressure using a pressurized incubation chamber and under atmospheric pressure.

Incubation under atmospheric pressure. WRCs were cut into 10 cm sections. Ten samples (2 mL) were taken from each WRC by open-cut 2.5 mL disposal plastic syringe or cork borer and transferred into 5 mL glass vials and capped with butyl rubber stoppers and aluminum caps in an anaerobic glove box. These samples were taken from the center of the WRC, avoiding sediment near the core liner to minimize the possibility of contamination. The vials were brought out of the glove box, and then 1 mL of anaerobic medium was added to make a slurry using a plastic disposable syringe via the butyl rubber stopper.

Radioisotope tracers were injected into slurries in the radioisotope container laboratory on the *Chikyu*. A total of 50 µL of dissolved radioisotope tracers (sodium [^{14}C]-bicarbonate, [1-^{14}C]-acetate, and [2-^{14}C]-acetate, 0.1 MBq in deoxygenated, deionized water) were separately injected into each vial using a glass microsyringe to determine hydrogenotrophic methanogenesis, acetoclastic methanogenesis, and syntrophic acetate oxidation. For carbon monoxide and methane turnover, 0.5 mL of gaseous radioisotope tracers ([^{14}C]-methane and [^{14}C]-carbon monoxide, 1 MBq) were injected by a plastic disposable syringe. The samples were incubated during the expedition at various temperatures (10°, 20°, and 40°C) depending on the estimated temperature at the drilled depth and sent to KCC for shore-based measurements.

Incubation in pressurized chamber. WRCs from selected lithologies were cut into 20 cm sections. From each 20 cm section, 10 samples (10 mL) were then taken by cork borer and transferred into a stainless steel chamber in an anaerobic glove box. The chamber consists of a Teflon-coated stainless steel tube (125 mm × 9.4 mm inside diameter) and two needle valves (Swagelok Tube Fitting, USA) attached at both sides of the tube. Pressurization and injection of radioisotope tracers were conducted in the radioisotope container laboratory. One side of the chamber was connected with a high-pressure liquid chromatograph (HPLC) pump (JUSCO Corporation, Japan) with a 1⅛6 inch HPLC line. The valve connected with the HPLC pump was opened, and the inner part of the chamber was pressurized by inflow of medium. The pressure was set to the estimated in situ pore water pressure (10–22 MPa). A total of 500 µL of dissolved radioisotope tracers and gaseous radioisotope tracers (sodium [^{14}C]-bicarbonate, [1-^{14}C]-acetate, and [2-^{14}C]-acetate, 0.5 MBq in deoxygenated, deionized water; [^{14}C]-methane and [^{14}C]-carbon monoxide, 0.5 MBq) were separately injected into each chamber via a sample loop. After pressurizing, the valve was closed and the chamber was disconnected and stored at different temperatures (10°, 20°, and 40°C) depending on the estimated in situ sediment temperature. The samples were sent to KCC for shore-based analysis.

Studies using stable isotope probing

Two types of SIP experiments were designed and carried out by organic geochemists during Expedition 337 to investigate biomass production and substrate degradation, respectively. SIP experiments conducted by microbiologists, involving nucleic acid-SIP, are discussed in "**Microbiology.**" The goal of the "biomass production" experiments was to assess the lipid production potential in the subseafloor sediment, whereas the "substrate degradation" experiments aimed at assessing the potential degradation rates of compounds that are relevant to the coalbed system. The WRC samples for the SIP experiments were chosen from the least disturbed core segments according to the images of X-ray CT scan. The WRCs were transferred into ESCAL bags, which were evacuated and flushed with N_2 for a total of three cycles before being heat-sealed and stored at 4°C before further processing. The experiments usually started on board the ship within 2 days after core retrieval and were designed to continue for several months postcruise at MARUM.

Biomass formation experiments. Two types of "biomass formation" experiments were started on board the ship:

- Type A: intact sediment chunks were incubated using the dual isotope labeling method introduced by Wegener et al. (2012) (i.e., D_2O and $NaH^{13}CO_3$ without addition of organic substrates). We assumed that such an incubation condition induces minimal disturbance to microorganisms and their habitats. Therefore, the lipid production rates derived from the labeling results can be considered as reasonable estimates of the in situ rates.
- Type B: sediment was homogenized and slurried with medium containing D_2O, $NaH^{13}CO_3$, and with/without unlabeled organic substrates. Microbial activity is intended to be stimulated because of increased contact with the aqueous phase and/or the presence of labile organic matter. The incubation condition is likely to stimulate microbes

that are dormant in situ, and the derived lipid production rates will be taken as indication of microbial vitality were the microbes given more water and/or more degradable carbon sources.

Shipboard salinity measurements did not indicate the presence of freshwater; therefore, we prepared an artificial seawater medium with the following salt ingredients and a salinity close to that of seawater for the experiments: 26.4 g NaCl, 11.3 g $MgCl_2 \cdot 6H_2O$, 1.5 g $CaCl_2 \cdot 2H_2O$, 0.68 g KCl, and 0.099 g KBr per liter. NH_4Cl and KH_2PO_4 were then added to a final concentration of 4.7 and 1.5 mM, respectively. To avoid dilution of the ^{13}C label, no $NaHCO_3$ was added to the medium. Resazurin was added as a redox indicator (final concentration = 1 mg/L). The medium was reduced with HCl-amended $Na_2S \cdot 9H_2O$ to a final concentration of 1 mM and neutralized with 1 M NaOH. The stock solutions of D_2O, $NaH^{13}CO_3$, glucose, and amino acid mixture were filter-sterilized (0.2 µm), and O_2 was removed by bubbling with N_2.

To start the experiments, the core segment was extruded from the core liner on a clean bench, visually inspected and contaminated material removed, and transferred immediately into a glove box before further processing. Two WRC samples containing coal were processed directly in the glove box to avoid extensive oxidation because of the highly fractured nature of the coal. Within the glove box, ~50 cm^3 of core sample, used as the time-zero sample for the Type A experiments, was transferred to a high-density polyethylene can and later stored at –20°C. Another 600 cm^3 of core sample was split into two 500 mL wide-neck Schott bottles for the Type A experiments, whereas the remaining sediment (~400–500 cm^3) was powdered over a sterilized tungsten mortar for the other experiments. Anoxic medium was added to fill ~80% of the headspace of the wide-neck bottles, which were then sealed with rubber stoppers and removed from the glove box. To make the sterilized control, one of the bottles was supplemented with zinc acetate to a final concentration of ~10% and pasteurized at 80°C for 8 h. D_2O and $NaH^{13}CO_3$ solution were then added.

About 50 cm^3 of the homogenized sediment was saved as the time-zero sample for the Type B experiments. The remaining sample powder was mixed with the anoxic medium to a volume ratio of 1:0.8. Slurry aliquots of 90 mL sediment slurry were distributed to 100 mL Schott bottles, which were sealed with rubber stoppers and removed from the glove box. Two of the bottles were incubated only with D_2O and $NaH^{13}CO_3$, whereas the others were amended with glucose or amino acid mixture (both to a final concentration of 1 mM) as separate substrates in addition to the labels.

For both experiments, the estimated labeling strengths were ~20% for D_2O and 50% for $NaH^{13}CO_3$, with the latter assuming an alkalinity of 10 mM in interstitial water (the highest alkalinity encountered in 337 was 14.2 mM). The actual values will be determined using samples taken from the aqueous phase of the incubation at the start of the experiments. The samples will be incubated at estimated in situ temperatures for up to 6 months and analyzed for lipid isotopic values at MARUM.

Substrate degradation experiments. The following three ^{13}C-labeled substrates were used in the "substrate degradation" experiments:

1. ^{13}C-labeled lignin purified from *Zea mays*,
2. Methoxy-^{13}C vanillin as the model monomer for plant-derived aromatic compounds, and
3. 1,2-^{13}C hexadecane as the model compound for aliphatic hydrocarbons.

Progress of biodegradation will be monitored by the $\delta^{13}C$ values of methane and DIC in the gaseous and aqueous samples taken from the sediment slurries. Once active biodegradation is confirmed, single-cell nanoscale secondary-ion mass spectrometry (NanoSIMS) analysis will be carried out using the solid phase in order to evaluate the extent of carbon assimilation from the labeled substrates into biomass (see **"Microbiology"**).

The anoxic medium described above (see **"Biomass formation experiments"**) was also used for the experiments. In a glove box, an aliquot of the homogenized sediment (~100 cm^3) was mixed with medium to a volume ratio of 1:1. Aliquots of 10 mL sediment slurries were transferred into 16 mL glass tubes, which were sealed with rubber stoppers and exported from the glove box. ^{13}C-labeled lignin was added as suspension to a final concentration of 0.06 mg/mL slurry for sediment and 1 mg/mL slurry for coal samples. The dosages of methoxy-^{13}C vanillin, amended as aqueous solution, were 0.06 mg/mL slurry for sediment and 0.7 mg/mL slurry for coal samples. The stock solution of 1,2-^{13}C hexadecane was prepared anoxically using 2,2,4,4,6,8,8-heptamethylnonane, an inert and nontoxic organic carrier, as the solvent. This labeled aliphatic hydrocarbon was added to a final concentration of 85 µg/mL slurry for both sediment and coal samples. After label addition, the time-zero tubes were immediately sampled for the gaseous and aqueous phase, whereas the remaining solid-phase slurry was fixed with 2% paraformaldehyde and preserved in phosphate-buffered saline (PBS)/ethanol (1:1 v/v) at –20°C until

analysis. The other sample tubes will be incubated at estimated in situ temperatures for as long as 6 months, with methane and DIC isotopic values monitored regularly at MARUM.

Microbiology

Expedition 337 was the first riser drilling IODP expedition to incorporate extensive shipboard microbiological and molecular biological analyses. These analyses included chemical and microbial contamination tests; molecular ecological studies based on DNA extracted from fresh, unfrozen subseafloor samples; cell detection and enumeration; metabolic activity measurements using various radioactive and stable isotopic tracers (see also **"Organic geochemistry"**); and a wide range of incubations that included cultivation, nucleic acid–, and whole cell–stable isotope probing (SIP) experiments (for lipid- and metabolic compound-SIP, see **"Organic geochemistry"**).

The shipboard molecular biological program included DNA extraction, quantitative polymerase chain reaction (qPCR) on bacterial and archaeal 16S rRNA genes, conventional polymerase chain reaction (PCR) assays of functional marker genes and eukaryotic 18S rRNA genes, and most-probable-number PCR (MPN-PCR) of contamination indicator organisms. Molecular fingerprinting assays were used to document changes in community composition with core depth and across changing lithologies and to evaluate the potential contribution of microbial contaminants. Cell enumerations were performed by manual microscopic observation, image-based discriminative cell enumeration (Morono et al., 2009), high-performance flow cytometry (Morono et al., in press), and fluorescence in situ hybridization (FISH). For measurements of potential activity, stable isotope-labeled carbon, nitrogen, oxygen, and hydrogen were added to fresh samples and incubations were initiated on board the ship under anaerobic conditions near in situ temperature. Radioactive tracers, such as ^{35}S-labeled sulfate and ^{14}C-labeled bicarbonate, were handled in the new radioisotope container laboratory on the *Chikyu*.

Complementary to core samples, a large number of samples were obtained from drilling mud and cuttings to evaluate the risk of background contamination during riser drilling. Analyses performed on these control samples included chemical contamination tests, cell counts, MPN-PCR targeting well-known contaminants, and shore-based incubation experiments. The sampling approaches and methods used are described in the following sections.

Sampling strategy

Cores

Cores were sampled for shipboard analyses and shore-based experiments (Table **T5**). All core sections underwent a nondestructive X-ray CT scan as soon as possible after arrival on deck and before further processing. A core section for a series of high-priority, mainly shipboard microbiological, geochemical, and geophysical investigations (referred to as community WRC hereafter) and a corresponding core section for interstitial water analysis (see **"Inorganic geochemistry"**) were processed immediately after the CT scan. Processing of community WRCs took place in the QA/QC laboratory on the core processing deck. All remaining core sections were packed into ESCAL bags, vacuum-sealed, and flushed with nitrogen. These core sections then underwent MSCL-W analyses at room temperature (see **"Introduction"**).

Community WRCs were typically 15 cm long and taken from 1 to 4 depths within each core. All handling of these community WRCs was carried out in a laminar flow hood to minimize sample contamination with cells from laboratory air. Because samples for PFC tracer contamination tests were taken from these community WRCs, rapid processing was necessary. This was to minimize PFC loss to volatilization and PFC diffusion from contaminated outer parts to cleaner inner parts of cores, both of which would lead to inaccurate quantification of core contamination (for more info on PFC method, see **"Contamination tests"**). In addition to PFC tracer analyses, samples for shipboard microbiological, geochemical, geophysical, and lithologic analyses, as well as shore-based fungal cultivation and solid-phase Fe and S analyses were taken from these community WRCs (Fig. **F23;** Table **T6** for overview).

All other WRC samples were cut by shipboard microbiologists in the QA/QC laboratory after MSCL-W scanning. Redox-sensitive samples used for radiotracer-based activity measurements, shore-based cultivation, and nucleic acid analyses were again packed into ESCAL bags, flushed with N_2, vacuum-sealed, and stored at 4°C until further processing; this anaerobic sample handling procedure was performed to prevent or minimize the potentially rapid growth of aerobic and mesophilic microbial contaminants from the riser drilling mud.

Drilling mud and cuttings

In addition to WRCs, samples of drilling mud from the active tanks, core liners, and mud ditch, as well as samples of core cuttings were obtained as follows:

active tanks were sampled on a daily basis, mud fluids from the core liner were taken from every core recovered, mud fluids from the mud ditch were taken around the time of core recovery, and cuttings samples were obtained at 50 m depth intervals throughout riser drilling operations. These samples were taken to monitor concentrations of chemical tracer, as well as changes in microbial cell abundance and community structure within drilling mud and cuttings over the course of the expedition. In addition, cuttings from six designated depths (796, 896, 996, 1096, 1996, and 2496 m MSF) were taken for shore-based cultivation experiments.

Formation fluid sampling

Formation fluid samples of ~250 mL volume were obtained from six different depths using the Schlumberger Quicksilver probe. All samples were processed for activity measurements (^{35}S and ^{14}C), shore-based cultivation, cell counts, FISH, and PFC tracer measurements. After separation of gas and liquid components from Quicksilver sampling bottles (see **"Sampling and gas analysis in fluids retrieved by DFA"**), fluids were immediately transferred into the glove box, where 100 mL was sampled for microbiological examinations. This 100 mL sample was used as follows:

1. 1 mL was transferred to a 20 mL headspace vial for PFC tracer measurement;
2. Four 15 mL samples were transferred to sterilized screw-cap glass bottles, flushed with nitrogen gas, and stored at 4°C for shore-based cultivation experiments;
3. A 5 mL aliquot was fixed with paraformaldehyde (PFA) for cell enumeration and FISH analysis and stored at –20°C;
4. A 10 mL aliquot of formation fluid was frozen using the alternating magnetic field freezer (Cell Alive System CAS-LAB1-M, ABI, Co., Ltd, Japan) for single-cell analysis;
5. Four 10 mL headspace vials containing 1 mL of fluid were used for measurement of sulfate reduction rates under N_2 and N_2/CH_4 (1:1), with two replicates for each headspace treatment; and
6. Ten 5 mL headspace vials were prepared for incubation experiments to determine rates of acetogenesis and methanogenesis in the formation fluid.

Sterile sampling and its tools

Samples for shipboard microbiological analyses were collected using devices that differed depending on sample lithology. Drilling mud was sampled by pipetting, where pipet tips had been cut off to enlarge the opening and facilitate drawing up this viscous fluid; cuttings and unconsolidated sand were sampled by spatulas or cut-off syringes; ceramic knives and cork borers were used for shales, coal, and consolidated sand; very hard samples, such as certain mud-, silt-, and sandstone, were sampled by core drill or handheld power drill; extremely hard samples, such as certain mud- and siltstones, could, however, only be sampled using a diamond-paste band saw system placed in a clean booth within the QA/QC laboratory (Masui et al., 2009). Sampling tools were sterilized by wiping with 70% ethanol followed by flaming and/or autoclaving. Additional cleaning was done periodically by spraying with RNAse AWAY surface decontaminants (Life Technologies).

Contamination tests

Contamination tests were carried out by chemical tracer quantification and by molecular monitoring of microbial communities.

Chemical tracer

Perfluoromethylcyclohexane (PMCH; C_7F_{14}), a PFC compound used as a chemical tracer during previous scientific ocean drilling expeditions on the riserless drill ship R/V *JOIDES Resolution* (Smith et al., 2000a, 2000b; House et al., 2003; Lever et al., 2006), was supplied directly to drilling mud in actively mixed mud tanks, and concentrations were monitored on a daily basis (Table **T7**). Additions were paused during logging operations and resumed 2 days prior to drilling. PFC tracer measurements followed the protocol outlined in Lever et al. (2006), except for the following modifications:

1. Headspace vials (20 mL) with silicone septa were used instead of Vacutainer tubes;
2. Prior to measurement, all samples were preincubated in an HB-80 hybridization incubator (TAITEC, Japan); and
3. Samples were analyzed by a gas chromatograph (GC) with an electron capture detector (ECD) (Network GC System 6890N, Agilent Technologies) connected to an autosampler (Network Headspace Sampler G1888, Agilent Technologies).

For preincubation, headspace vials were placed in a carousel within a hybridization oven and rotated in horizontal orientation at 20 revolutions per minute (rpm) for 2 h at 80°C. This change to the incubation protocol was performed after a 1 h preincubation step with gentle motion was found to drastically increase (≥36×) the release of PFC tracer from drilling mud into headspace compared to mere incubation without rotation for 5–10 min at 80°C in an incuba-

tion oven (as on previous riserless drilling expeditions) or for 30 min at 80°C in the GC-ECD autosampler (as in the *Chikyu* shipboard protocol; Fig. F24). Even after drilling mud had been incubated for 5 h without movement within the GC-ECD autosampler, headspace PFC tracer concentrations were drastically (≥15×) lower compared to vials that had been rotated for a 1 h period prior to insertion into the autosampler. Because of the anticipated even slower diffusion and volatilization of PFC tracer out of core samples compared to drilling mud, a preincubation time of 2 h with rotation was used in the final protocol, which was applied to all core samples. After this preincubation, headspace vials were rapidly transferred to the autosampler, where they were incubated for an additional 30 min at 80°C prior to measurement.

PFC tracer concentrations, which were calculated according to Smith et al. (2000b), were monitored in the exterior, halfway, and interior of cores (Fig. F23B; Table T6); in drilling mud from active tanks prior to and during drilling; in cuttings; and in mud fluid coming up with the cuttings (Table T7).

DNA-based contamination tracers

In community WRCs (Fig. F23; Table T6), as well as in several samples of drilling mud and cuttings, PFC tracer quantifications were complemented by DNA-based contamination tests. The latter were designed to quantify microbial contamination in cores and involved MPN-PCR assays with group-specific PCR primers (Table T8). Target groups were potential microbial indicators of

1. Drilling mud viscosifiers (*Xanthomonas* and *Halomonas*),
2. Anthropogenic wastewater (*Bifidobacterium*, *Blautia*, and *Methanobrevibacter*), and
3. Surface seawater (SAR11 and Marine Group I Archaea).

These were identified as target groups based on past evidence indicating viscosifiers, wastewater, and seawater as the main sources of microbial contamination in cores retrieved by scientific ocean drilling (Masui et al., 2008; Santelli et al., 2010). With the exception of *Methanobrevibacter*, 16S rRNA genes were targeted for PCR-based gene detection and quantification. In the case of *Methanobrevibacter*, the gene encoding the alpha subunit of methyl coenzyme M reductase (*mcrA*) was targeted. For details on DNA extraction method and PCR amplification, see **"DNA extraction and purification"** and **"PCR."**

Cell separation and enumeration

A 2 cm^3 core sample was transferred into a sterile 15 mL centrifuge tube containing 8 mL of 3× PBS (pH = 7.5; Invitrogen 70013), with 2% (v/v) neutralized PFA as a fixative, and then thoroughly mixed by vortexing to form a homogeneous suspension. After fixation for 6–12 h at 4°C, samples were washed twice with 10 mL of 3× PBS, resuspended in ethanol:3× PBS (1:1), and stored at –20°C. These suspensions were subjected to cell detachment and separation steps as follows:

1. Aliquots of 1000 µL of 1:5-diluted PFA-fixed core slurry were pipetted into 15 mL centrifuge tubes. Subsequently, 3000 µL of 2.5% NaCl, 500 µL of detergent mix (100 mM ethylenediaminetetraacetic acid [EDTA], 100 mM sodium pyrophosphate, and 1% [v/v] Tween-80), and 500 µL of pure methanol were added.
2. Samples were shaken using a Shake Master (Bio Medical Science, Japan) at 500 rpm for 60 min.
3. Slurry samples were sonicated at 160 W for 10 cycles, each 30 s long, and cooled in an ice-water bath for 30 s between cycles.
4. An aliquot of 500 µL of 10% hydrofluoric acid (HF) was then added, and samples were incubated at room temperature.
5. After 20 min, HF treatments were stopped by adding 500 µL of 1.5 M tris(hydroxymethyl)aminomethane.
6. Samples were transferred to 15 mL tubes, where they were placed on top of four density layers. These density layers consisted of a 30% Nycodenz (1.15 g/cm^3), a 50% Nycodenz (1.25 g/cm^3), an 80% Nycodenz (1.42 g/cm^3), and a 67% sodium polytungstate (2.08 g/cm^3) layer. These density layers had been prepared by sequentially overlaying 1 mL of each density solution, starting with the highest density at the bottom.
7. Cells and sediment particles were then separated by centrifugation with swinging rotors at 6000× *g* for 1 h at 20°C.
8. Starting from the top and using a 27G needle, density layers were collected down to where the first particles became visible. The latter often started to be visible in the 80% Nycodenz layer, of which only the particle-free upper part was then collected.
9. The density layers that contained particles (i.e., typically the polytungstate layer and in some cases part of the 80% Nycodenz layer) and pellets were then washed by resuspension with 5000 µL of 2.5% NaCl and followed by centrifugation at

5000× *g* for 15 min at 25°C. The recovered supernatant was combined with the one from Step 8.

10. Pellets were resuspended in 5000 µL of 2.5% NaCl, 500 µL detergent mix, and 500 µL of methanol and shaken at 500 rpm for 60 min at 25°C.
11. The resuspended sediment was again placed on top of density layers with 30% Nycodenz (1.15 g/cm^3), 50% Nycodenz (1.25 g/cm^3), 80% Nycodenz (1.42 g/cm^3), and 67% sodium polytungstate, and the cell extraction (Steps 6–9) was repeated. Particle-free layers and supernatants were combined with previously obtained ones.
12. A total of 50% of the resulting total cell extract was passed through a 0.22 µm polycarbonate membrane filter. Cells on the membrane filter were stained with SYBR Green I–staining solution (1/40 of SYBR Green I in Tris-EDTA [TE] buffer). The number of SYBR Green I–stained cells was enumerated by a fluorescent image-based cell counting system (Fig. **F25**) as described in Morono et al. (2009) and Morono and Inagaki (2010) with a careful check by visual observations.
13. Cells in the remaining 50% of the supernatant were trapped onto an Anopore inorganic membrane (Anodisc, Whatman) and stained with SYBR Green I. Membranes with stained cells were then put into 15 mL tubes with TE buffer and sonicated to detach the cells. Cell numbers in these suspensions were quantified using a Gallios flow cytometer (Beckman Coulter, CA) (Fig. **F26**) placed on an antivibration table.

All cell separation and filtration procedures were performed on clean benches, with great care to avoid contamination. Minimum quantification limit (MQL) of the cell count was estimated by blanks. Samples were processed in batches of ten plus two additional blank samples, in which sterile-filtered 2.5% NaCl solution replaced the sediment slurry. The blank was calculated as the average of all blanks processed during the expedition. The MQL was set as the blank value plus three times the standard deviation of the blank.

DNA extraction and purification

DNA extraction protocols are known to vary in total DNA yields and in efficiency of lysing different groups of organisms. Thus, we used three different DNA extraction methods: a hot alkaline lysis protocol, a chemical lysis protocol, and a modification of the chemical lysis protocol that included the separation of extracellular and intracellular DNA pools. All three protocols had been successfully tested across a wide range of subseafloor samples prior to the expedition.

Hot alkaline lysis protocol

This protocol was used for core samples only. To 2 g of core sample, 6 mL of 6.25 mM EDTA (pH = 8.0) was added and warmed to 70°C for 10 min. These suspensions were then amended and mixed with 800 µL of each 10% sodium dodecyl sulfate and 10 M NaOH and incubated for 20 min at 70°C. Suspensions were then centrifuged at 10,000× *g* for 1 min at 25°C and supernatants transferred to clean tubes. Pellets were washed with 4 mL of warmed (70°C) double-distilled water, centrifuged at 10,000× *g* for 1 min at 25°C, and supernatants combined with previously obtained ones. The supernatants were neutralized with 6 mL of a solution containing 1 M HCl and 0.3 M Tris-HCl (pH = 8.0), and 1 volume of phenol/chloroform/isoamylalcohol (24:24:1) was added. The resulting mixture was shaken manually and then centrifuged at 10,000× *g* for 10 min at 25°C. Aqueous supernatants were transferred to clean tubes, mixed by manual shaking with one volume of chloroform/isoamylalcohol (24:1), and centrifuged at 10,000× *g* for an additional 10 min at 25°C. Aqueous phases were collected and DNA was precipitated by adding 1/10 volume of 3 M sodium acetate, 3 µL of ethachinmate (Nippon Gene) as co-precipitant, and 2.5× volumes of 99.5% ethanol. The recovered DNA pellet was dissolved in 5 mL of a 1/1000× TE buffer containing 10 µM Tris-HCl and 1 µM EDTA (pH = 8.0) and purified using an Aurora DNA purification system (Boreal Genomics).

Chemical lysis protocol

This protocol was used to extract DNA from core samples, cuttings, and drilling mud. Amounts of 1 g, 0.2 g, and 100 µL were used per extraction from cores, cuttings, and drilling mud, respectively. Extractions from cuttings and drilling mud followed the same protocol, except in the initial steps, whereas extractions from cores followed the same protocol as for cuttings, except that all reagents were increased proportionally to the larger amount of sample used (i.e., by a factor of 5; more information below).

Cuttings samples were placed into 2 mL screw-cap tubes filled to ~20% with 0.1 mm diameter zirconia/silicate beads (Biospec Products, USA) and briefly mixed by tapping or vortexing with 100 µL of 100 mM deoxyribonucleotide triphosphate (dNTP) solution. A volume of 500 µL of lysis solution (30 mM Tris-HCl, 30 mM EDTA, 800 mM guanidium hydrochloride, pH raised to 10.0 with NaOH, and 2% Triton X-100) was then added and homogenized with tube contents by manual shaking or brief vortexing. Screw-cap tubes were then taped horizontally onto a

Vortex-Genie Pulse (Scientific Industries, Inc., USA) and shaken at the maximum speed setting (3000) for 10 min. Treatments of drilling mud samples differed as follows: only 10 µL of 100 mM dNTP solution was added; the lysis solution contained 0.5% Triton X-100; and the resulting mixture of drilling mud, dNTP solution, and lysis solution was vortexed for only 10 s at the maximum speed.

After these initial extraction steps, protocols for cuttings, cores, and drilling mud followed the exact same protocol. Samples were frozen at –80°C. After >20 min, the fully frozen samples were transferred to a shaker incubator (Iwashiya Bio Science, Japan) and shaken at 120 rpm for 1 h at 50°C. Samples underwent one more freeze cycle followed by incubation at 50°C, and were then centrifuged at 9500× *g* for 10 min at 4°C. Supernatants were transferred to clean vials and washed twice with 1 volume of chloroform/isoamylalcohol by vortexing for 10 s followed by centrifugation at 9500× *g* for 10 min at 4°C. The final supernatant was mixed with linear polyacrylamide (LPA) (final concentration 20 µg/mL) and 0.2 volumes of 5 M sodium chloride. After gentle mixing by tapping, 2.5 volumes of 99.5% ethanol were added, tubes were inverted five times for homogenization, and DNA was precipitated by incubation in the dark at room temperature for 2 h. After these 2 h, tubes were centrifuged at 14,000× *g* for 30 min, supernatants were poured and pipetted off, and pellets were redissolved in 100 µL molecular grade water after drying for 5 min in a laminar flow hood. The redissolved pellets were purified using a Norgen Clean-All DNA/RNA cleanup and concentration kit (Norgen Biotek Corp, Canada). All purified DNA extracts were stored at –80°C until PCR-based analysis.

Extracellular DNA extraction

Several studies over the past decades have reported a large fraction of DNA in marine sediment to be extracellular rather than intracellular, from living organisms (e.g., Ogram et al., 1987; Dell'Anno and Danovaro, 2005; Corinaldesi et al., 2011), and suggested that this extracellular pool might represent a genetic archive of past environmental change (e.g., Willerslev et al., 2003). To extract extracellular DNA, 5 cm^3 of sediment from designated 10 cm WRCs were homogenized with 5 cm^3 of carbonate dissolution/phosphate binding solution (0.47 M sodium acetate, 0.47 M glacial acetic acid, 10 mM EDTA, 100 mM sodium metaphosphate, and 3% NaCl) and rotated in a carousel at 1 rpm at room temperature. After 1 h, 40 mL of 10× TE buffer (pH = 10.0) (300 mM tris-HCl, 10 mM EDTA, and 3% NaCl, with pH raised with NaOH) were added, mixtures inverted five times or, if necessary, vortexed to ensure homogenization, and rotated for one additional hour. Samples were then centrifuged at 9500× *g* for 30 min at room temperature and supernatants containing extracellular DNA transferred to separate vials. Both vials (i.e., supernatants containing extracellular DNA and sediment pellets containing intracellular DNA) were then frozen at –80°C for comparative phylogenetic studies of extracellular and intracellular DNA pools at the on shore laboratory.

PCR

PCR-based quantifications

We quantified bacterial and archaeal 16S rRNA gene copies by qPCR using a StepOnePlus real-time PCR system (Life Technologies Japan, Tokyo, Japan) provided by the JAMSTEC Kochi Institute for Core Sample Research (Fig. **F27**) and SYBR Green I chemistry (Morrison et al., 1998). For amplification, the SYBR Premix DimerEraser kit (Takara Bio, Shiga, Japan) was used (5 µL SYBR Premix Dimer Eraser, 0.2 µL of ROX reference dye, 0.3 µL of 10 µM forward and reverse primer, 2 µL template, and 2.2 µL nuclease-free water). The standard consisted of plasmids containing full 16S rRNA gene inserts of uncultured bacterial clone N_194 (not deposited) and uncultured archaeal clone 1H3M_ARC08 (JN229535) for Bacteria and Archaea, respectively. The qPCR protocol consisted of

1. Initial denaturation for 30 s at 95°C;
2. 50 cycles of 5 s denaturation at 95°C, 30 s annealing (see Table **T8** for T_m), and 40 s elongation; and
3. A final elongation step of 3 min at 72°C. qPCR primers used are shown in Table **T8.**

MPN-PCR was performed to quantify drilling mud–derived microbial contaminants in cuttings and cores. All PCR amplifications were performed on Veriti Thermal Cyclers provided by the JAMSTEC Kochi Institute for Core Sample Research using Takara Ex Taq polymerase kits (Takara Bio, Shiga, Japan) following the manufacturer's suggestion, except that a bovine serum albumin (BSA) concentration of 1 mg/mL was included. All seven groups of contamination indicator organisms (see **"Contamination tests"** for more information) were amplified with group-specific PCR primers (Table **T8**). PCR protocols consisted of

1. Initial denaturation for 2 min at 98°C;
2. 50 cycles of 15 s denaturation at 95°C, 30 s annealing (see Table **T8** for T_m), and 30 s elongation at 72°C; and
3. A final elongation step of 5 min at 72°C.

A 10× dilution series of extracts was prepared, with the lowest dilution yielding correctly sized PCR am-

plicons used to estimate minimum target gene concentrations in samples.

Functional marker genes

Functional marker genes indicative of microbial energy metabolism were PCR-amplified via conventional PCR (Table T8). All PCR amplifications were performed on Veriti Thermal Cyclers provided by the JAMSTEC Kochi Institute for Core Sample Research using Takara Ex Taq polymerase kits (Takara Bio, Shiga, Japan) following the manufacturer's suggestion, except that a BSA concentration of 1 mg/mL was included. *mcrA* genes of in situ populations of methanogenic and anaerobic methane-oxidizing archaea were the primary target groups and amplified with two primer pairs. Additional targets were (1) formyl tetrahydrofolate synthetase (*fhs*) genes found in acetogens and other C1-compound metabolizing microbes and (2) dissimilatory sulfate reductase (*dsrB*) genes of sulfate-reducing microbes. PCR protocols consisted of

1. Initial denaturation for 2 min at 98°C;
2. 50 cycles of 15 s denaturation at 95°C, 30 s annealing (see Table T8 for T_m), and 60 s elongation at 72°C; and
3. A final elongation step of 5 min at 72°C.

PCR products were checked using 2% (w/v) low melting point agarose in a tris-acetic acid-EDTA (TAE) buffer and visualized with a SYBR Safe DNA gel stain (Invitrogen, USA) provided by the JAMSTEC Kochi Institute for Core Sample Research.

Molecular fingerprinting assays

Terminal restriction fragment length polymorphism (T-RFLP) analyses of PCR-amplified 16S rRNA genes were used to evaluate changes in bacterial and archaeal communities along environmental variables (e.g., depth, geochemistry, and lithology) and to evaluate whether amplified DNA derives from the indigenous microbial community or drilling mud. We followed a published general T-RFLP procedure (Singh et al., 2006; Suzuki et al., 1998). The detailed steps used during Expedition 337, which were modified from the original published protocols, are outlined below.

DNA was PCR-amplified using Veriti Thermal Cyclers with the 16S rRNA gene primer sets 27F-926R and 21F-958R to target the domains Bacteria and Archaea, respectively (Table T8). Both forward primers were 5′-end labeled with 6-carboxyfluoresce (6-FAM). PCR reaction mixtures consisted of 0.3 µM of each primer, 0.2 mM deoxyribonucleoside triphosphate, 1.6 µL of PrimeSTAR GXL polymerase, 1× PrimeSTAR GXL buffer (Takara Bio, Shiga, Japan), and 2 µL of extracted DNA. PCR amplification protocols consisted of 32 cycles for Bacteria and 40 cycles for Archaea, whereby each cycle consisted of 10 s denaturation at 98°C, 15 s annealing at 56°C, and 15 s elongation at 68°C.

PCR products were examined by gel electrophoresis on 2% (w/v) agarose gel followed by staining with SYBR Safe DNA dye. Gel-excised PCR products were purified with a NucleoSpin gel and PCR cleanup kit (Takara Bio, Shiga, Japan) according to the manufacturer's instructions. Purified PCR products were then digested by the restriction enzyme *Hha* I (cleavage site [GCG′C], where ′ shows the site of cleavage) in a hybridization oven for 6 h at 37°C. After DNA digestion, restriction enzymes were inactivated by 20 min of incubation at 65°C and digested PCR amplicons precipitated after adding ⅒ volume 3 M sodium acetate solution and 2 volumes of 99.5% ethanol. For the precipitation, mixtures were incubated for >1 h in a –20°C freezer followed by centrifugation at 12,000× *g* for 30 min. After decanting the supernatants, DNA precipitates were rinsed with 70% ethanol and air dried.

Air-dried DNA fragments were dissolved in 10 µL of deionized formamide supplemented with 0.3 µL of the internal GeneScan 1200 LIZ size standard (Applied Biosystems, Foster City, California, USA). After denaturing the fragments for 5 min at 94°C followed by immediate chilling on ice, the lengths of terminal restriction fragments (T-RFs) were analyzed by electrophoresis on an ABI 3130 XL Genetic Analyzer (Applied Biosystems) provided by the JAMSTEC Kochi Institute for Core Sample Research (Fig. F28). The injection time was 15 s and the run time was ~2 h. Microbial communities were compared in terms of genetic composition (size of peaks), richness (number of peaks), and evenness (height of peaks) based on the T-RFs.

Potential sulfate reduction rates

After the X-ray CT scan and MSCL-W measurements, a 5–10 cm long WRC sample was taken from each core to determine potential sulfate reduction rates (pSRR). The WRC was transferred to a glove box, the contaminated outer part (~1 cm) removed, and the cleaner innermost part homogenized or, if necessary, crushed. Approximately 5 mL of innermost sample was placed in a preweighed 20 mL crimp vial and flushed with N_2. Four replicate vials were prepared for each sample. After weighing the samples, slurries were prepared by adding 5 mL of sterile, anoxic salt medium (see Table T9 for composition) through the septa. Sulfate-depleted samples, as from the subseafloor at Site C0020, bear the risk that indigenous sulfate-reducing microorganisms immediately con-

sume all radioactive tracer, resulting in unrealistic turnover rates. To prevent this from happening, media were supplied with an additional background concentration of 1 mM Na_2SO_4. All vials were autoclaved, and solutions were filtered through sterile syringe filters (0.20 µm pore size) prior to use.

In the radioisotope laboratory on the *Chikyu*, a 15 mL volume of methane (99.9%, standard gas) was injected into the headspace of two vials to produce two duplicate incubation sets (i.e., two vials with N_2 headspace and two vials with N_2/CH_4 headspace [50/50]). The addition of CH_4 to N_2 in the headspace increased the pressure (to ~2 bar), which increased the dissolution of CH_4 into the medium. Subsequently, 30 µL of radiolabeled Na_2SO_4 (3.7 MBq) was injected and samples vigorously shaken. Samples were incubated for 10 days at temperatures within the in situ range. Samples from between 1200 and 1600 m CSF-B were incubated at room temperature (~25°C), samples from between 1600 and 2000 m CSF-B were incubated at 35°C, and samples from below 2000 m CSF-B were incubated at 45°C. After 10 days of incubation, 3 mL of 20% (w/v) zinc acetate solution was injected into each vial and vials were shaken before they were opened to trap produced H_2S gas. Slurries were then transferred to 50 mL centrifuge tubes containing 7 mL of 20% (w/v) zinc acetate solution. Tubes were shaken, frozen immediately at –20°C to stop microbial activity, and shipped to Aarhus University, Denmark, after the expedition for analysis of pSRR using the cold chromium distillation method published by Kallmeyer et al. (2004).

Onboard incubation for shore-based microbiological cultivation experiments

Anaerobic incubations of core, cuttings, and formation fluid samples with media targeting subseafloor microorganisms involved in the metabolism of C_1 and C_2 compounds (e.g., methanogenesis, homoacetogenesis, ferric iron reduction coupled to acetate oxidation, and syntrophic oxidization of volatile fatty acids; Table **T10**) were initiated on board the ship. Additional WRCs were stored under anaerobic conditions at 4°C for shore-based cultivations.

Inoculum and incubation media

Unwashed cuttings or formation fluids were mixed with anaerobic freshwater basal media (Table **T11**) or seawater basal media (Table **T12**). Various combinations of electron donors and acceptors were added to enrich for hydrogenotrophic and aceticlastic methanogens, homoacetogens, ferric iron reducers, and syntrophic volatile fatty acid oxidizers (Table **T8**). Reducing reagents (i.e., Na_2S [1.25 mM] and cysteine-HCl [1.7 mM]) and resazurin were added to ensure that media were completely anoxic. Enrichments of other hydrogenotrophic or chemolithoautotrophic microbes were performed with media containing 40 mM BES (2-bromoethanesulfonic acid), which is a methanogen-specific inhibitor (Smith, 1983). Anaerobic media (10 mL) were placed in glass test tubes sealed with butyl rubber septa and headspaces were flushed with N_2:CO_2 (80:20 [v/v]) and/or H_2:CO_2 (80:20 [v/v]). Samples were incubated at temperatures within the in situ temperature range. Unwashed cuttings samples from 696.5 to 1206.5 m MSF were incubated at 25°C. Formation fluid at 1279.5 m WMSF was incubated at 37°C, and the other fluid samples of 1844.0 and 1978.0 m WMSF were incubated at 50°C.

Incubation and microscopic observation of fungi

For shipboard enrichments of fungi, 1–3 mL of core sample was mixed with 5–13 mL of autoclaved seawater in 50 mL tubes and vortexed for 1–3 min. Each tube was then N_2-flushed, sealed with tape, and incubated at 28°C while shaking at 100 rpm for 5–15 days. After this incubation period, samples were vortexed again and allowed to settle for 30 min. Supernatants were then examined by light microscopy by placing one drop on a glass slide.

Sampling for shore-based investigations

Pooled master sample for multiple analyses

Eleven WRC samples from the coalbed and intercalated sandstone and clay layers from 1950 and 2000 m CSF-B were used to prepare a pooled master sample (Table **T13**). The pooled master sample was prepared after carefully removing the outer 1 cm of the WRC samples and powdering the inner, potentially uncontaminated part of the cores. Core from sand layers was excluded from this mixture because of the higher contamination risk, as determined by PFC tracer measurements. This pooled master sample was used to prepare slurries for shore-based microbial activity measurements, incubation and cultivation experiments, and shipboard radiotracer incubations.

Shore-based DNA extraction, functional gene characterization, and organic acid analyses

Remains of the 10 cm WRC for extracellular DNA extraction were transferred to sterile whirlpak bags and frozen at –80°C for further shore-based DNA extractions and functional gene assays, analyses of amino acid enantiomers, and measurement of amino acid, muramic acid, and dipicolinic acid concentrations (Lomstein et al., 2012).

Shore-based ^{35}S incubations

From each WRC sample used for shipboard ^{35}S incubations, a 50 cm^3 volume of clean inner core was packed in a gas-tight ESCAL bag, flushed with N_2, vacuum-sealed, and stored anoxically at 4°C.

Hydrogenase activity measurements

Samples for hydrogenase activity measurements were handled in an anoxic glove box and taken from the same WRCs used for pSRR measurements. A 50 cm^3 volume of clean inner core was packed in a gas-tight ESCAL bag, flushed with N_2, vacuum-sealed, and frozen at –80°C.

Cultivation experiments

WRC samples were taken for shore-based cultivation experiments. The heavily contaminated outermost parts were discarded and the clean inner portions were stored by placement either in glass bottles, where they were flushed with N_2 and sealed with butyl rubber stoppers, or gas-tight bags, which were flushed with N_2 and vacuum-sealed. All samples were stored at 4°C until shore-based cultivation studies targeting microbes (e.g., methanogens, homoacetogens, ferric iron reducers, dehalogenating bacteria, carboxidotorophs, syntrophs, and fungi) (see Table T10). For shore-based fungal cultivation, 20 cm^3 core samples obtained from each community WRC were sealed in a bag, flushed with N_2, and stored at 4°C.

Single-cell analyses of carbon and nitrogen assimilation rates of subseafloor microbes

We set up incubations for shore-based examinations of microbial physiologies and substrate-uptake ratios by NanoSIMS and other single-cell–based molecular ecological techniques. Contaminated surfaces of WRCs were peeled off with sterile ceramic knives, and less contaminated inner core parts were crushed with a sterile hammer under anaerobic conditions. Crushed samples were distributed to 50 cm^3 sterilized glass vials with rubber stoppers for incubation with a wide range of stable isotope-labeled substrates (Table T14). After flushing with argon gas, vials were sealed with screw caps and stored at 4°C. Substrates were added to achieve equimolar ^{13}C (mixture of 15 µM each of ^{13}C and natural abundance isotope ratio C-bearing substrates), ^{15}N (mixture of 1.5 µM of ^{15}N and natural abundance isotope ratio N-bearing substrates), and deuterium (20 vol% in water). For each vial, 19.8 mL anaerobic artificial seawater (1% PBS, 20% D_2O, 30 g/L NaCl, 12 g/L $MgCl_2$, and 3 g/L KCl) and 0.2 mL liquid and/or 5 mL gas substrate (50 vol% of ^{13}C or ^{15}N diluted with natural abundance isotope ratio C- or N-bearing substrates) were added. All reagents and gas components had been filtered through 0.2 µm polyvinyllidene fluoride membranes prior to use.

Additionally, a coal sample was prepared for shipboard stable isotope incubation. A WRC was dabbed with Kimwipes soaked in anaerobic Milli-Q water in a glove box and then gently broken into 1–2 cm thick fragments to create artificial fractured surfaces. UV-sterilized 47 mm polycarbonate and cellulose acetate membranes were soaked with substrate and placed between core-breaking points, and the whole thing was "sandwiched" and held together by wrapping the WRC fragments with parafilm. Additional pieces of coal were placed in 500 mL wide-neck glass bottles. Then 300 mL of 3× PBS amended with either 1 mM ^{13}C-bicarbonate and 0.1 mM of ^{15}N-ammonium or 1 mM ^{13}C-acetate and 0.1 mM of ^{15}N-ammonium was added to the bottles and incubated at 51.0°C.

Environmental tag-sequencing and metagenomics

Samples obtained during Expedition 337 provided an unprecedented opportunity to study genetic function and evolution in deeply buried microbial communities with state-of-the-art sequencing techniques. The contaminated outermost 0.5 cm of 20 cm long WRC samples, which had been taken from representative lithologies, were removed, and the less contaminated core interiors were placed into autoclaved perfluoroalcoxy alkane jars and quickly frozen at –100°C. These deep-frozen molecular samples were transferred to the JAMSTEC Kochi Institute for Core Sample Research, where they will be used for molecular ecological studies through 16S rRNA gene-tagged deep sequencing and whole-genome shotgun sequencing.

References

Akiba, F., 1986. Middle Miocene to Quaternary diatom biostratigraphy in the Nankai Trough and Japan Trench, and modified lower Miocene through Quaternary diatom zones for middle-to-high latitudes of the north Pacific. *In* Kagami, H., Karig, D.E., Coulbourn, W.T., et al., *Init. Repts. DSDP,* 87: Washington, DC (U.S. Govt. Printing Office), 393–481. **doi:10.2973/dsdp.proc.87.106.1986**

Aoike, K. (Ed.), 2007. *CDEX Laboratory Operation Report: CK06-06 D/V* Chikyu *shakedown cruise offshore Shimokita:* Yokohama (CDEX-JAMSTEC). **http://sio7.jamstec.go.jp/JAMSTEC-exp-report/902/CK06-06_CR.pdf**

ASTM International, 1990. Standard method for laboratory determination of water (moisture) content of soil and rock (Standard D2216–90). In *Annual Book of ASTM Standards for Soil and Rock* (Vol. 04.08): Philadelphia

(Am. Soc. Testing Mater.). [revision of D2216-63, D2216-80]

Blum, P., 1997. Physical properties handbook: a guide to the shipboard measurement of physical properties of deep-sea cores. *ODP Tech. Note,* 26. **doi:10.2973/odp.tn.26.1997**

Bujak, J.P., 1984. Cenozoic dinoflagellate cysts and acritarchs from the Bering Sea and northern North Pacific, DSDP Leg 19. *Micropaleontology,* 30(2):180–212. **doi:10.2307/1485717**

Bujak, J.P., and Matsuoka, K., 1986. Late Cenozoic dinoflagellate cyst zonation in the western and northern Pacific. *In* Wrenn, J.H., Duffield, S.L., and Stein, J.A. (Eds.), *Papers from the First Symposium on Neogene Dinoflagellate Cyst Biostratigraphy.* AASP Contrib. Ser., 17:7–26.

Corinaldesi, C., Barucca, M., Luna, G.M., and Dell'Anno, A., 2011. Preservation, origin and genetic imprint of extracellular DNA in permanently anoxic deep-sea sediments. *Mol. Ecol.,* 20(3):642–654. **doi:10.1111/j.1365-294X.2010.04958.x**

Crozier, T.E., and Yamamoto, S., 1974. Solubility of hydrogen in water, sea water, and sodium chloride solutions. *J. Chem. Eng. Data,* 19(3):242–244. **doi:10.1021/je60062a007**

Daims, H., Brühl, A., Amann, R., Schleifer, K.-H., and Wagner, M., 1999. The domain-specific Probe EUB338 is insufficient for the detection of all *Bacteria:* development and evaluation of a more comprehensive probe set. *Syst. Appl. Microbiol.,* 22(3):434–444. **doi:10.1016/S0723-2020(99)80053-8**

Dell'Anno, A., and Danovaro, R., 2005. Extracellular DNA plays a key role in deep-sea ecosystem functioning. *Science,* 309(5744):2179. **doi:10.1126/science.1117475**

DeLong, E.F., 1992. Archaea in coastal marine environments. *Proc. Natl. Acad. Sci. U. S. A.,* 89(12):5685–5689. **doi:10.1073/pnas.89.12.5685**

D'Hondt, S., Rutherford, S., and Spivack., A.J., 2002. Metabolic activity of the subsurface life in deep-sea sediments. *Science,* 295(5562):2067–2070. **doi:10.1126/science.1064878**

D'Hondt, S., Spivack, A.J., Pockalny, R., Ferdelman, T.G., Fischer, J.P., Kallmeyer, J., Abrams, L.J., Smith, D.C., Graham, D., Hasiuk, F., Schrum, H., and Stancine, A.M., 2009. Subseafloor sedimentary life in the South Pacific Gyre. *Proc. Natl. Acad. Sci. U. S. A.,* 106(28):11651–11656. **doi:10.1073/pnas.0811793106**

Dickson, A.G., 1984. pH scales and proton-transfer reactions in saline media such as sea water. *Geochim. Cosmochim. Acta,* 48(11):2299–2308. **doi:10.1016/0016-7037(84)90225-4**

Dong, C., O'Keefe, M., Elshahawi, H., Hashem, M., Williams, S., Stensland, D., Hegeman, P., Vasques, R., Terabayashi, T., Mullins, O., and Donzier, E., 2007. New downhole fluid analyzer tool for improved reservoir characterization. *Proc.—Offshore Eur. Oil Gas Conf.,* 7:231–241. **doi:10.2118/108566-MS**

Elwood, H.J., Olsen, G.J., and Sogin, M.L., 1985. The small-subunit ribosomal RNA gene sequences from the hypotrichous ciliates *Oxytricha nova* and *Stylonychia pustulata*. *Mol. Biol. Evol.,* 2(5):399–410. **http://www.ncbi.nlm.nih.gov/pubmed/3939705**

Ertefai, T.F., Heuer, V.B., Prieto-Mollar, X., Vogt, C., Sylva, S.P., Seewald, J., and Hinrichs, K.-U., 2010. The biogeochemistry of sorbed methane in marine sediments. *Geochem. Cosmochim. Acta,* 74(1):6033–6048. **doi: 10.1016/j.gca.2010.08.006**

Erzinger, J., Wiersberg, T., and Zimmer, M., 2006. Real-time mud gas logging and sampling during drilling. *Geofluids,* 6(3):225–233. **doi:10.1111/j.1468-8123.2006.00152.x**

Espitalié, J., Madec, M., Tissot, B., Mennig, J.J., and Leplat, P., 1977. Source rock characterization method for petroleum exploration. *Proc. 9th Annu. Offshore Technol. Conf.,* 3:439–448.**doi:10.4043/2935-MS**

Expedition 315 Scientists, 2009. Expedition 315 methods. *In* Kinoshita, M., Tobin, H., Ashi, J., Kimura, G., Lallemant, S., Screaton, E.J., Curewitz, D., Masago, H., Moe, K.T., and the Expedition 314/315/316 Scientists, *Proc. IODP,* 314/315/316: Washington, DC (Integrated Ocean Drilling Program Management International, Inc.). **doi:10.2204/iodp.proc.314315316.122.2009**

Expedition 319 Scientists, 2010a. Methods. *In* Saffer, D., McNeill, L., Byrne, T., Araki, E., Toczko, S., Eguchi, N., Takahashi, K., and the Expedition 319 Scientists, *Proc. IODP,* 319: Tokyo (Integrated Ocean Drilling Program Management International, Inc.). **doi:10.2204/iodp.proc.319.102.2010**

Expedition 319 Scientists, 2010b. Site C0009. *In* Saffer, D., McNeill, L., Byrne, T., Araki, E., Toczko, S., Eguchi, N., Takahashi, K., and the Expedition 319 Scientists, *Proc. IODP,* 319: Tokyo (Integrated Ocean Drilling Program Management International, Inc.). **doi:10.2204/iodp.proc.319.103.2010**

Expedition 322 Scientists, 2010. Methods. *In* Saito, S., Underwood, M.B., Kubo, Y., and the Expedition 322 Scientists, *Proc. IODP,* 322: Tokyo (Integrated Ocean Drilling Program Management International, Inc.). **doi:10.2204/iodp.proc.322.102.2010**

Expedition 333 Scientists, 2012. Methods. *In* Henry, P., Kanamatsu, T., Moe, K., and the Expedition 333 Scientists, *Proc. IODP,* 333: Tokyo (Integrated Ocean Drilling Program Management International, Inc.). **doi:10.2204/iodp.proc.333.102.2012**

Expedition 337 Scientists, 2013. Site C0020. *In* Inagaki, F., Hinrichs, K.-U., Kubo, Y., and the Expedition 337 Scientists, *Proc. IODP,* 337: Tokyo (Integrated Ocean Drilling Program Management International, Inc.). **doi:10.2204/iodp.proc.337.103.2013**

GE Healthcare, 2006. *LightSpeed Series Learning and Reference Guide-Multi Slice CT:* Waukesha, Wisconsin (GE Healthcare).

Gieskes, J.M., Gamo, T., and Brumsack, H., 1991. Chemical methods for interstitial water analysis aboard *JOIDES Resolution. ODP Tech. Note,* 15. **doi:10.2973/odp.tn.15.1991**

Guo, J., and Underwood, M.B., 2012. Data report: clay mineral assemblages from the Nankai Trough accretionary prism and the Kumano Basin, IODP Expeditions 315 and 316, NanTroSEIZE Stage 1. *In* Kinoshita, M., Tobin,

H., Ashi, J., Kimura, G., Lallemant, S., Screaton, E.J., Curewitz, D., Masago, H., Moe, K.T., and the Expedition 314/315/316 Scientists, *Proc. IODP,* 314/315/316: Washington, DC (Integrated Ocean Drilling Program Management International, Inc.). **doi:10.2204/iodp.proc.314315316.202.2012**

Harvey, H.R., Fallon, R.D., and Patton, J.S., 1986. The effect of organic matter and oxygen on the degradation of bacterial membrane lipids in marine sediments. *Geochim. Cosmochim. Acta,* 50(5):795–804. **doi:10.1016/0016-7037(86)90355-8**

Heuer, V.B., Krüger, M., Elvert, M., and Hinrichs, K.-U., 2010. Experimental studies on the stable carbon isotope biogeochemistry of acetate in lake sediments. *Org. Geochem.,* 41(1):22–30. **doi:10.1016/j.orggeochem.2009.07.004**

Hoehler, T.M., Alperin, M.J., Albert, D.B., and Martens, C.S., 1998. Thermodynamic control on hydrogen concentrations in anoxic sediments. *Geochim. Cosmochim. Acta,* 62(10):1745–1756. **doi:10.1016/S0016-7037(98)00106-9**

House, C.H., Cragg, B.A., Teske, A., and the Leg 201 Scientific Party, 2003. Drilling contamination tests during ODP Leg 201 using chemical and particulate tracers. *In* D'Hondt, S.L., Jørgensen, B.B., Miller, D.J., et al., *Proc. ODP, Init. Repts.,* 201: College Station, TX (Ocean Drilling Program), 1–19. **doi:10.2973/odp.proc.ir.201.102.2003**

Jingrong, L., Naimin, F., Zonghao, Z., and Zhenjian, H., 2000. Neogene palynology from north of Shandong. *In* Zonghao, Z., Guoguang, Z., and Chuanben, Z. (Eds.), *Symposium on Palynology of Petroliferous Basins in China:* Beijing (Petroleum Industry Press), 211–223.

Kallmeyer, J., Ferdelman, T.G., Weber, A., Fossing, H., and Jørgensen, B.B., 2004. A cold chromium distillation procedure for radiolabeled sulfide applied to sulfate reduction measurements. *Limnol. Oceanogr.: Methods,* 2:171–180. **http://www.aslo.org/lomethods/free/2004/0171.pdf**

Kedves, M., 1969. *Palynological Studies on Hungarian Early Tertiary Deposits:* Budapest (Akadémiai Kiadó Publ. House, Hungarian Acad. Sci.), 1–84.

Kellermann, M.Y., Wegener, G., Elvert, M., Yoshinaga, M.Y., Lin, Y.-S., Holler, T., Prieto Mollar, X., Knittel, K., and Hinrichs, K.-U., 2012. Autotrophy as a predominant mode of carbon fixation in anaerobic methane-oxidizing microbial communities. *Proc. Natl. Acad. Sci. U. S. A.,* 109(47):19321–19326. **doi:10.1073/pnas.1208795109**

Kurita, H., 2004. Paleogene dinoflagellate cyst biostratigraphy of northern Japan. *Micropaleontology,* 50(Suppl. 2):3–50. **doi:10.2113/50.Suppl_2.3**

Kurita, H., and Matsuoka, K., 1994. *Trinovantedinium boreale* Bujak-dominated dinoflagellate assemblages in Eocene–Oligocene stratified water in northern Japan. *Rev. Palaeobot. Palynol.,* 84(1–2):129–153. **doi:10.1016/0034-6667(94)90047-7**

Kurita, H., and Obuse, A., 2003. Middle Miocene–uppermost lower Pliocene dinoflagellate cyst biostratigraphy, ODP Leg 186 Hole 1151A, off Sanriku Coast of northern Japan, northwestern Pacific. *In* Suyehiro, K., Sacks, I.S., Acton, G.D., and Oda, M. (Eds.), *Proc. ODP, Sci. Results,* 186: College Station, TX (Ocean Drilling Program), 1–19. **doi:10.2973/odp.proc.sr.186.105.2003**

Kurnosov, V., Tseitlin, N., and Narnov, G., 1980. Clay minerals: paleogeographic and diagenetic aspects. *In* Scientific Party, *Init. Repts. DSDP,* 56/57: Washington, DC (U.S. Govt. Printing Office), 979–1003. **doi:10.2973/dsdp.proc.5657.134.1980**

Kvenvolden, K.A., and McDonald, T.J., 1986. Organic geochemistry on the *JOIDES Resolution*—an assay. *ODP Tech. Note,* 6: College Station, TX (Ocean Drilling Program). **doi:10.2973/odp.tn.6.1986**

Lane, D.J., 1991. 16S/23S rRNA sequencing. *In* Stackebrandt, E., and Goodfellow, M. (Eds.), *Nucleic Acid Techniques in Bacterial Systematics:* New York (Wiley), 115–148.

Lever, M.A., 2008. Anaerobic carbon cycling pathways in the subseafloor investigated via functional genes, chemical gradients, stable carbon isotopes, and thermodynamic calculations [Ph.D. thesis]. Univ. N. Carolina, Chapel Hill.

Lever, M.A., Alperin, M., Engelen, B., Inagaki, F., Nakagawa, S., Steinsbu, B.O., Teske, A., and IODP Expedition Scientists, 2006. Trends in basalt and sediment core contamination during IODP Expedition 301. *Geomicrobiol. J.,* 23(7):517–530. **doi:10.1080/01490450600897245**

Lever, M.A., Heuer, V.B., Morono, Y., Masui, N., Schmidt, F., Alperin, M.J., Inagaki, F., Hinrichs, K.-U., and Teske, A., 2010. Acetogenesis in deep subseafloor sediments of the Juan de Fuca Ridge flank: a synthesis of geochemical, thermodynamic, and gene-based evidence. *Geomicrobiol. J.,* 27(2):183–211. **doi:10.1080/01490450903456681**

Lever, M.A., Rouxel, O., Alt, J.C., Shimizu, N., Ono, S., Coggon, R.M., Shanks, W.C., III, Laphan, L., Elvert, M., Prieto-Mollar, X., Hinrichs, K.-U., Inagaki, F., and Teske, A., 2013. Evidence for microbial carbon and sulfur cycling in deeply buried ridge flank basalt. *Science,* 339(6125):1305–1308. **doi:10.1126/science.1229240**

Lin, W., Yeh, E.-C., Ito, H., Hirono, T., Soh, W., Wang, C.-Y., Ma, K.-F., Hung, J.-H., and Song, S.-R., 2007. Preliminary results of stress measurements using drill cores of TCDP Hole-A: an application of anelastic strain recovery method to three-dimensional in-situ stress determination. *Terr. Atmos. Oceanic Sci.,* 18(2):379. **doi:10.3319/TAO.2007.18.2.379(TCDP)**

Lin, Y.-S., Heuer, V.B., Goldhammer, T., Kellermann, M.Y., Zabel, M., and Hinrichs, K.-U., 2012. Toward constraining H_2 concentration in subseafloor sediment: a proposal for combined analysis by two distinct approaches. *Geochim. Cosmochim. Acta,* 77:186–201. **doi:10.1016/j.gca.2011.11.008**

Lipp, J.S., Morono, Y., Inagaki, F., and Hinrichs K.-U., 2008. Significant contribution of Archaea to extant biomass in marine subsurface sediments. *Nature (London, U. K.),* 454(7207):991–994. **doi:10.1038/nature07174**

Logemann, J., Graue, J., Köster, J., Engelen, B., Rullkötter, J., and Cypionka, H., 2011. A laboratory experiment of

intact polar lipid degradation in sandy sediments. *Biogeosciences,* 8(9):2547–2560. **doi:10.5194/bg-8-2547-2011**

Lomstein, B.A., Langerhuus, A.T., D'Hondt, S., Jørgensen, B.B., and Spivack, A., 2012. Endospore abundance, microbial growth and necromass turnover in deep subseafloor sediment. *Nature (London, U. K.),* 484(7392):101–104. **doi:10.1038/nature10905**

Lovley, D.R., and Goodwin, S., 1988. Hydrogen concentrations as an indicator of the predominant terminal electron-accepting reactions in aquatic sediments. *Geochim. Cosmochim. Acta,* 52(12):2993–3003. **doi:10.1016/0016-7037(88)90163-9**

Loy, A., Lehner, A., Lee, N., Adamczyk, J., Meier, H., Ernst, J., Schleifer, K.-H., and Wagner, M., 2002. Oligonucleotide microarray for 16S rRNA gene-based detection of all recognized lineages of sulfate-reducing prokaryotes in the environment. *Appl. Environ. Microbiol.,* 68(10):5064–5081. **doi:10.1128/AEM.68.10.5064-5081.2002**

Manheim, F.T., 1966. A hydraulic squeezer for obtaining interstitial waters from consolidated and unconsolidated sediments. *Geol. Surv. Prof. Pap. (U.S.),* 550-C:256–261.

Mann, U., and Müller, G., 1980. Composition of sediments of the Japan Trench transect, Legs 56 and 57, Deep Sea Drilling Project. *In* Scientific Party, *Init. Repts. DSDP,* 56/57: Washington, DC (U.S. Govt. Printing Office), 939–977. **doi:10.2973/dsdp.proc.5657.133.1980**

Masui, N., Morono, Y., and Inagaki, F., 2008. Microbiological assessment of circulation mud fluids during the first operation of riser drilling by the deep-earth research vessel *Chikyu. Geomicrobiol. J.,* 25(6):274–282. **doi:10.1080/01490450802258154**

Masui, N., Morono, Y., and Inagaki, F., 2009. Bio-archive core storage and subsampling procedure for subseafloor molecular biological research. *Sci. Drill.*, 8:35–37. **doi:10.2204/iodp.sd.8.05.2009**

Matsuki, K., 1991. Three-dimensional in situ stress measurement with anelastic strain recovery of a rock core. *Proc.—Int. Congr. Rock Mech.,* 4:557–560.

Matsuoka, K., 1983. Late Cenozoic dinoflagellates and acritarchs in the Niigata District, central Japan. *Palaeontogr., Abt. B,* 187(1–3):89–154.

Matsuoka, K., Bujak, J.P., and Shimazaki, T., 1987. Late Cenozoic dinoflagellate cyst biostratigraphy from the west coast of northern Japan. *Micropaleontology,* 33(3):214–229. **doi:10.2307/1485638**

Mazzullo, J., and Graham, A.G. (Eds.), 1988. Handbook for shipboard sedimentologists. *ODP Tech. Note,* 8. **doi:10.2973/odp.tn.8.1988**

Mazzullo, J.M., Meyer, A., and Kidd, R.B., 1988. New sediment classification scheme for the Ocean Drilling Program. *In* Mazzullo, J., and Graham, A.G. (Eds.), *Handbook for shipboard sedimentologists*. ODP Tech. Note, 8:45–67. **doi:10.2973/odp.tn.8.1988**

Medlin, L., Elwood, H.J., Stickel, S., and Sogin, M.L., 1988. The characterization of enzymatically amplified eukaryotic 16S-like rRNA-coding regions. *Gene,* 71(2):491–499. **doi:10.1016/0378-1119(88)90066-2**

Mills, C.T., Dias, R.F., Graham, D., and Mandernack, K.W., 2006. Determination of phospholipid fatty acid structures and stable carbon isotope compositions of deep-sea sediments of the northwest Pacific, ODP Site 1179. *Mar. Chem.,* 98(2–4):197–209. **doi:10.1016/j.marchem.2005.10.001**

Morono, Y., and Inagaki, F., 2010. Automatic slide-loader fluorescent microscope for discriminative enumeration of subseafloor life. *Sci. Drill.,* 9:32–36. **doi:10.2204/iodp.sd.9.06.2010**

Morono, Y., Terada, T., Kallmeyer, J., and Inagaki, F., in press. An improved cell separation technique for marine subsurface sediments: applications for high-throughput analysis using flow cytometry and cell sorting. *Environ. Microbiol.*

Morono, Y., Terada, T., Masui, N., and Inagaki, F., 2009. Discriminative detection and enumeration of microbial life in marine subsurface sediments. *ISME J.,* 3(5):503–511. **doi:10.1038/ismej.2009.1**

Morono, Y., Terada, T., Nishizawa, M., Ito, M., Hillion, F., Takahata, N., Sano, Y., and Inagaki, F., 2011. Carbon and nitrogen assimilation in deep subseafloor microbial cells. *Proc. Natl. Acad. Sci. U. S. A.,* 108(45):18295–18300. **doi:10.1073/pnas.1107763108**

Morrison, T.B., Weis, J.J., and Wittwer, C.T., 1998. Quantification of low-copy transcripts by continuous SYBR Green I monitoring during amplification. *Biotechniques,* 24(6):954–958.

Mullins, O.C., 2008. *The Physics of Reservoir Fluids: Discovery Through Downhole Fluid Analysis:* Houston (Schlumberger).

Muyzer, G., De Waal, E.C., and Uitterlinden, A.G., 1993. Profiling of complex microbial populations by denaturing gradient gel electrophoresis analysis of polymerase chain reaction–amplified genes coding for 16S rRNA. *Appl. Environ. Microbiol.,* 59(3):695–700. **http://aem.asm.org/content/59/3/695.full.pdf**

Nadkarni, M.A., Martin, F.E., Jacques, N.A., and Hunter, N., 2002. Determination of bacterial load by real-time PCR using a broad-range (universal) probe and primers set. *Microbiology,* 148:257–266. **http://mic.sgmjournals.org/content/148/1/257.full.pdf**

Novelli, P.C., Scranton, M.I., and Michener, R.H., 1987. Hydrogen distributions in marine sediments. *Limnol. Oceanogr.,* 32(3):565–576. **doi:10.4319/lo.1987.32.3.0565**

Ocean Drilling Program, 1992. Guidelines for pollution prevention and safety. *JOIDES J.,* 18 (Spec. Iss. 7). **http://odplegacy.org/PDF/Admin/JOIDES_Journal/JJ_1992_V18_No7.pdf**

Ogram, A., Sayler, G.S., and Barkay, T., 1987. The extraction and purification of microbial DNA from sediments. *J. Microbiol. Meth.,* 7(2–3):57–66. **doi:10.1016/0167-7012(87)90025-X**

Osawa, M., Nakanishi, S., Tanahashi, M., Oda, H., and Sasaki, A., 2002. Structure, tectonic evolution and gas exploration potential of offshore Sanriku and Hidaka provinces, Pacific Ocean, off northern Honshu and Hokkaido, Japan. *Sekiyu Gijutsu Kyokaishi,* 67(1):38–51. (in Japanese, with English abstract and figures)

Parkes, R.J., Webster, G., Cragg, B.A., Weightman, A.J., Newberry, C.J., Ferdelman, T.G., Kallmeyer, J., Jørgensen, B.B., Aiello, I.W., and Fry, J.C., 2005. Deep subseafloor prokaryotes stimulated at interfaces over geological time. *Nature (London, U. K.),* 436(7049):390–394. **doi:10.1038/nature03796**

Peters, K.E., 1986. Guidelines for evaluating petroleum source rock using programmed pyrolysis. *AAPG Bull.,* 70(3):318–329. **http://archives.datapages.com/data/bulletns/1986-87/data/pg/0070/0003/0300/0318.htm**

Peters, K.E., Walters, C.C., and Moldowan, J.M., 2005. Geochemical screening. In Peters, K.E., Walters, C.C., and Moldowan, J.M. (Eds.), *The Biomarker Guide* (Vol. 1): *Biomarkers and Isotopes in the Environment and Human History* (2nd ed.): Cambridge (Cambridge Univ. Press), 72–118. **doi:10.1017/CBO9780511524868.006**

Pimmel, A., and Claypool, G., 2001. Introduction to shipboard organic geochemistry on the *JOIDES Resolution*. *ODP Tech. Note,* 30. **doi:10.2973/odp.tn.30.2001**

Pohlman, J.W., Kaneko, M., Heuer, V.B., Coffin, R.B., and Whiticar, M., 2009. Methane sources and production in the northern Cascadia margin gas hydrate system. *Earth Planet. Sci. Lett.,* 287(3–4):504–512. **doi:10.1016/j.epsl.2009.08.037**

Rothwell, R.G., 1989. *Minerals and Mineraloids in Marine Sediments: An Optical Identification Guide:* London (Elsevier).

Ruiqi, G., Zonghao, Z., Guoguang, Z., and Chuanben, Z., 2000. Palynology of the eastern province. *In* Zonghao, Z., Guoguang, Z., and Chuanben, Z. (Eds.), *Palynology of Petroliferous Basins in China:* Beijing (Petroleum Industry Press), 83–112.

Saegusa, S., Tsunogai, U., Nakagawa, F., and Kaneko, S., 2006. Development of a multibottle gas-tight fluid sampler WHATS II for Japanese submersibles/ROVs. *Geofluids,* 6(3)234–240. **doi:10.1111/j.1468-8123.2006.00143.x**

Saffer, D., McNeill, L., Byrne, T., Araki, E., Toczko, S., Eguchi, N., Takahashi, K., and the Expedition 319 Scientists, 2010. *Proc. IODP,* 319: Tokyo (Integrated Ocean Drilling Program management International, Inc.). **doi:10.2204/iodp.proc.319.2010**

Sakaguchi, A., Chester, F., Curewitz, D., Fabbri, O., Goldsby, D., Kimura, G., Li, C.-F., Masaki, Y., Screaton, E.J., Tsutsumi, A., Ujiie, K., and Yamaguchi, A., 2011. Seismic slip propagation to the updip end of plate boundary subduction interface faults: vitrinite reflectance geothermometry on Integrated Ocean Drilling Program NanTroSEIZE cores. *Geology,* 39(4):395–398. **doi:10.1130/G31642.1**

Santelli, C.M., Banerjee, N., Bach, W., and Edwards, K.J., 2010. Tapping the subsurface ocean crust biosphere: low biomass and drilling-related contamination calls for improved quality controls. *Geomicrobiol. J.,* 27(2):158–169. **doi:10.1080/01490450903456780**

Sato, S., 1994. On the palynoflora in the Paleogene in the Ishikari coal field, Hokkaido, Japan. *J. Fac. Sci., Hokkaido Univ., Ser. 4,* 23(3):555–559. **http://hdl.handle.net/2115/36789**

Shipboard Scientific Party, 1996. Explanatory notes. *In* Mascle, J., Lohmann, G.P., Clift, P.D., et al., *Proc. ODP, Init. Repts.,* 159: College Station, TX (Ocean Drilling Program), 17–46. **doi:10.2973/odp.proc.ir.159.102.1996**

Shipboard Scientific Party, 2001. Site 1177. *In* Moore, G.F., Taira, A., Klaus, A., et al., *Proc. ODP, Init. Repts.,* 190: College Station, TX (Ocean Drilling Program), 1–91. **doi:10.2973/odp.proc.ir.190.108.2001**

Shipley, T.H., Ogawa, Y., Blum, P., et al., 1995. *Proc. ODP, Init. Repts.,* 156: College Station, TX (Ocean Drilling Program). **doi:10.2973/odp.proc.ir.156.1995**

Singh, B.K., Nazaries, L., Munro, S., Anderson, I.C., and Campbell, C.D., 2006. Use of multiplex terminal restriction fragment length polymorphism for rapid and simultaneous analysis of different components of the soil microbial community. *Appl. Environ. Microbiol.,* 72(11):7278–7285. **doi:10.1128/AEM.00510-06**

Smith, D.C., Spivack, A.J., Fisk, M.R., Haveman, S.A., and Staudigel, H., 2000a. Tracer-based estimates of drilling-induced microbial contamination of deep sea crust. *Geomicrobiol. J.,* 17(3):207–219. **doi:10.1080/01490450050121170**

Smith, D.C., Spivack, A.J., Fisk, M.R., Haveman, S.A., Staudigel, H., and the Leg 185 Shipboard Scientific Party, 2000b. Methods for quantifying potential microbial contamination during deep ocean coring. *ODP Tech. Note,* 28. **doi:10.2973/odp.tn.28.2000**

Smith, M.R., 1983. Reversal of 2-bromoethanesulfonate inhibition of methanogenesis in *Methanosarcina* sp. *J. Bacteriol.,* 156(2):516–523. **http://jb.asm.org/content/156/2/516**

Stahl, D.A., and Amman, R.A., 1991. Development and application of nucleic acid probes. *In* Stackebrandt, E., and Goodfellow, M. (Eds.), *Nucleic Acid Techniques in Bacterial Systematics:* New York (Wiley), 205–248.

Steurer, J.F., and Underwood, M.B., 2003. Clay mineralogy of mudstones from the Nankai Trough reference Sites 1173 and 1177 and frontal accretionary prism Site 1174. *In* Mikada, H., Moore, G.F., Taira, A., Becker, K., Moore, J.C., and Klaus, A. (Eds.), *Proc. ODP, Sci. Results,* 190/196: College Station, TX (Ocean Drilling Program), 1–37. **doi:10.2973/odp.proc.sr.190196.211.2003**

Suzuki, M., Rappé, M.S., and Giovannoni, S.J., 1998. Kinetic bias in estimates of coastal picoplankton community structure obtained by measurements of small-subunit rRNA gene PCR amplicon length heterogeneity. *Appl. Environ. Microbiol.,* 64(11):4522–4529. **http://aem.asm.org/content/64/11/4522**

Takai, K., and Horikoshi, K., 2000. Rapid detection and quantification of members of the archaeal community by quantitative PCR using fluorogenic probes. *Appl. Environ. Microbiol.,* 66(11):5066–5072. **doi:10.1128/AEM.66.11.5066-5072.2000**

Underwood, M.B., Basu, N., Steurer, J., and Udas, S., 2003. Data report: normalization factors for semiquantitative X-ray diffraction analysis, with application to DSDP Site 297, Shikoku Basin. *In* Mikada, H., Moore, G.F., Taira, A., Becker, K., Moore, J.C., and Klaus, A. (Eds.), *Proc. ODP, Sci. Results,* 190/196: College Station, TX (Ocean

Drilling Program), 1–28. doi:10.2973/odp.proc.sr.190196.203.2003

Underwood, M.B., Saito, S., Kubo, Y., and the Expedition 322 Scientists, 2009. NanTroSEIZE Stage 2: subduction inputs. *IODP Prel. Rept.,* 322. doi:10.2204/iodp.pr.322.2009

Vacquier, V., 1985. The measurement of thermal conductivity of solids with a transient linear heat source on the plane surface of a poorly conducting body. *Earth Planet. Sci. Lett.,* 74(2–3):275–279. doi:10.1016/0012-821X(85)90027-5

van Geldern, R., Hayashi, T., Böttcher, M.E., Mottl., M.J., Barth, J.A.C., and Stadler, S., 2013. Stable isotope geochemistry of pore waters and marine sediments from the New Jersey shelf: methane formation and fluid origin. *Geosphere,* 9(1):96–112. doi:10.1130/GES00859.1

Von Herzen, R., and Maxwell, A.E., 1959. The measurement of thermal conductivity of deep-sea sediments by a needle-probe method. *J. Geophys. Res.,* 64(10):1557–1563. doi:10.1029/JZ064i010p01557

Wang, W.-M., 2006. Correlation of pollen sequences in the Neogene palynofloristic regions of China. *Palaeoworld,* 15(1):77–99. doi:10.1016/j.palwor.2006.03.002

Wang, W.-M., Saito, T., and Nakagawa, T., 2001. Palynostratigraphy and climatic implications of Neogene deposits in the Himi area of Toyama Prefecture, Central Japan. *Rev. Palaeobot. Palynol.,* 117(4):281–295. doi:10.1016/S0034-6667(01)00097-5

Wegener, G., Bausch, M., Holler, T., Thang, N.M., Prieto Mollar, X., Kellermann, M.Y., Hinrichs, K.-U., and Boetius, A., 2012. Assessing sub-seafloor microbial activity by combined stable isotope probing with deuterated water and ^{13}C-bicarbonate. *Environ. Microbiol.,* 14(6):1517–1527. doi:10.1111/j.1462-2920.2012.02739.x

Whiticar, M.J., 1999. Carbon and hydrogen isotope systematics of bacterial formation and oxidation of methane. *Chem. Geol.,* 161(1–3):291–314. doi:10.1016/S0009-2541(99)00092-3

Wiersberg, T., and Erzinger, J., 2007. A helium isotope cross-section study through the San Andreas Fault at seismogenic depths. *Geochem., Geophys., Geosyst.,* 8(1):Q01002. doi:10.1029/2006GC001388

Wiersberg, T., and Erzinger, J., 2011. Chemical and isotope compositions of drilling mud gas from the San Andreas Fault Observatory at Depth (SAFOD) boreholes: implications on gas migration and the permeability structure of the San Andreas Fault. *Chem. Geol.,* 284(1–2):148–159. doi:10.1016/j.chemgeo.2011.02.016

Wiesenburg, D.A., and Guinasso, N.L., Jr., 1979. Equilibrium solubilities of methane, carbon monoxide, and hydrogen in water and sea water. *J. Chem. Eng. Data,* 24(4):356–360. doi:10.1021/je60083a006

Willerslev, E., Hansen, A.J., Binladen, J., Brand, T.B., Gilbert, M.T.P., Shapiro, B., Bunce, M., Wiuf, C., Gilichinsky, D.A., and Cooper, A., 2003. Diverse plant and animal genetic records from Holocene and Pleistocene sediments. *Science,* 300(5620):791–795. doi:10.1126/science.1084114

Williams, G.L., Lentin, J.K., and Fensome, R.A., 1998. *The Lentin and Williams Index of Fossil Dinoflagellate Cysts*. Am. Assoc. Stratigr. Palynol., Contrib. Ser., 34.

Xie, S., Lipp, J.S., Wegener, G., Ferdelman, T.G., and Hinrichs, K.-U., 2013. Turnover of microbial lipids in the deep biosphere and growth of benthic archaeal populations. *Proc. Natl. Acad. Sci. U. S. A.,* 110(15):6010–6014. doi:10.1073/pnas.1218569110

Yamanoi, T., 1992. Miocene pollen stratigraphy of Leg 127 in the Japan Sea and comparison with the standard Neogene pollen floras of northeast Japan. *In* Pisciotto, K.A., Ingle, J.C., Jr., von Breymann, M.T., Barron, J., et al., *Proc. ODP, Sci. Results,* 127/128 (Pt. 1): College Station, TX (Ocean Drilling Program), 471–491. doi:10.2973/odp.proc.sr.127128-1.150.1992

Yanagisawa, Y., and Akiba, F., 1998. Refined Neogene diatom biostratigraphy for the northwest Pacific around Japan, with an introduction of code numbers for selected diatom biohorizons. *Chishitsugaku Zasshi,* 104:395–414.

Yu, Y., Lee, C., Kim, J., and Hwang, S., 2005. Group-specific primer and probe sets to detect methanogenic communities using quantitative real-time polymerase chain reaction. *Biotechnol. Bioeng.,* 89(6):670–679. doi:10.1002/bit.20347

Publication: 30 September 2013
MS 337-102

Figure F1. IODP conventions for naming sites, holes, cores, and samples.

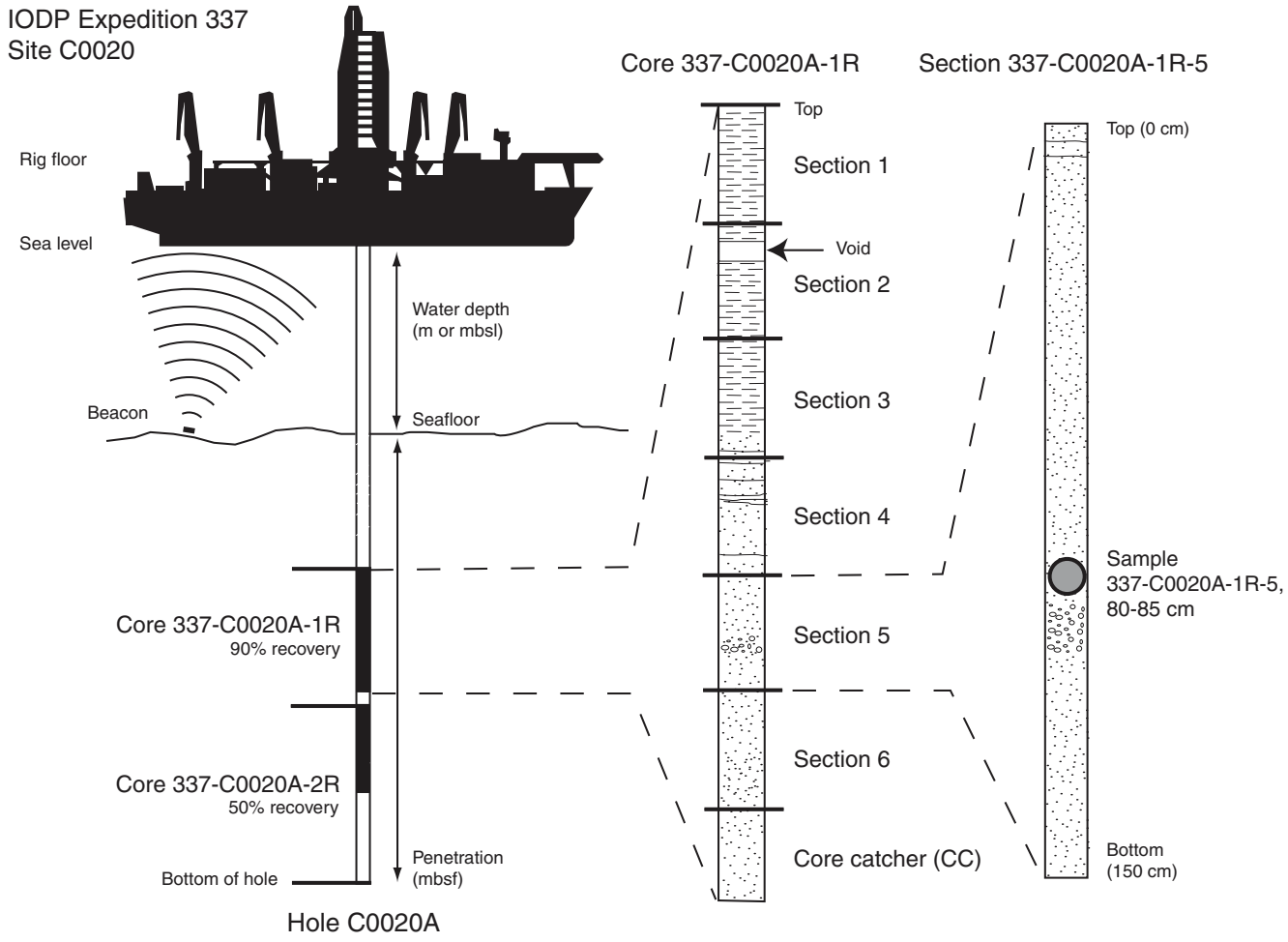

Figure F2. Cuttings analysis flow. HS = headspace, MBIO = microbiology, PAL = palynology, XRD = X-ray diffraction, XRF = X-ray fluorescence, EA = elemental analyzer, CA = carbonate analyzer, RE = Rock-Eval pyrolysis.

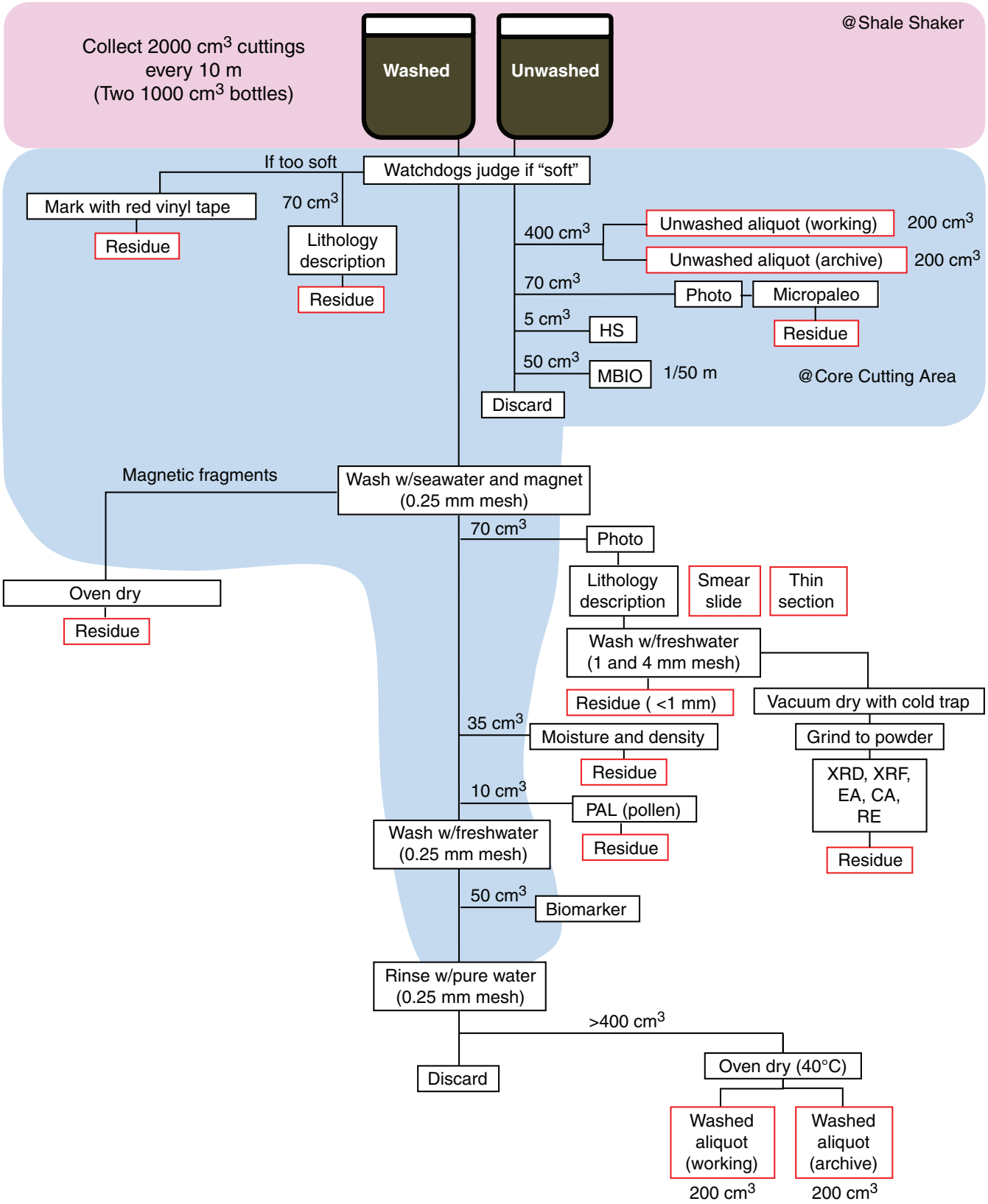

Figure F3. Core analysis flow. LDC = large-diameter coring, PVC = polyvinyl chloride, AL = aliquot. WRS = whole-round sample, WR = whole round. GC-FID = gas chromatograph–flame ionization detector, X-CT = X-ray computed tomography, MSCL-W = whole-round multisensor core logger, NGR = natural gamma radiation, MS = magnetic susceptibility, GRA = gamma ray attenuation, MAD = moisture and density, D-PWV = discrete sample *P*-wave velocity, FF = formation factor, MSCL-I = photo image logger, VCD = visual core description, MSCL-C = color spectroscopy logger, RMS = routine microbiological sample, XRD = X-ray diffraction, XRF = X-ray fluorescence, TCD = thermal conductivity detector, GC-ECD = gas chromatograph–electron capture detector, ICP-AES = inductively coupled plasma–atomic emission spectroscopy. IW = interstitial water. EA = elemental analyzer, CA = carbonate analyzer. RI = radioisotope.

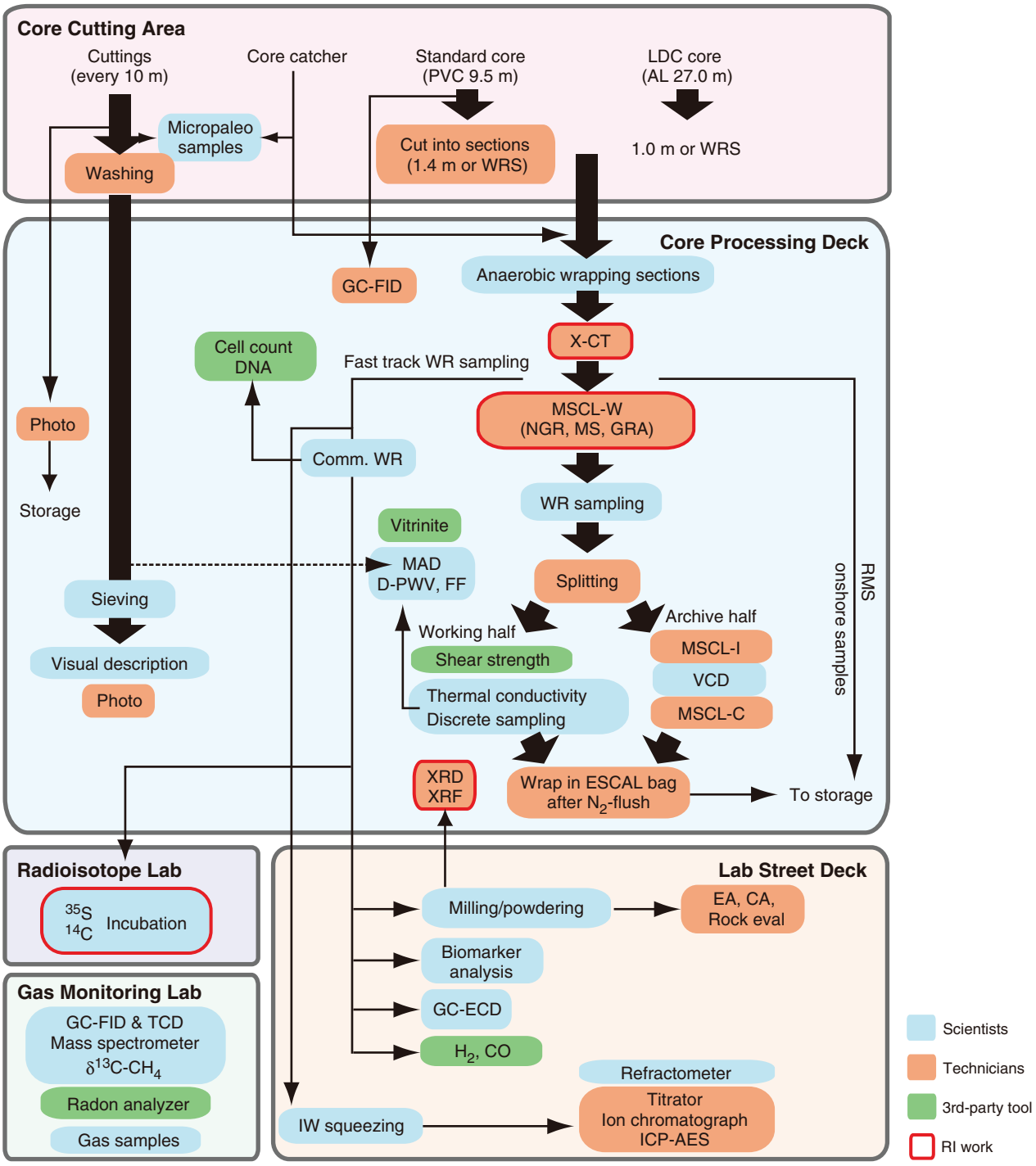

Figure F4. Graphic patterns and symbols used for macroscopic and microscopic descriptions of cuttings samples. The patterns and symbols for microscopic descriptions are also applicable for core samples.

Figure F5. Example of the macroscopic cuttings description.

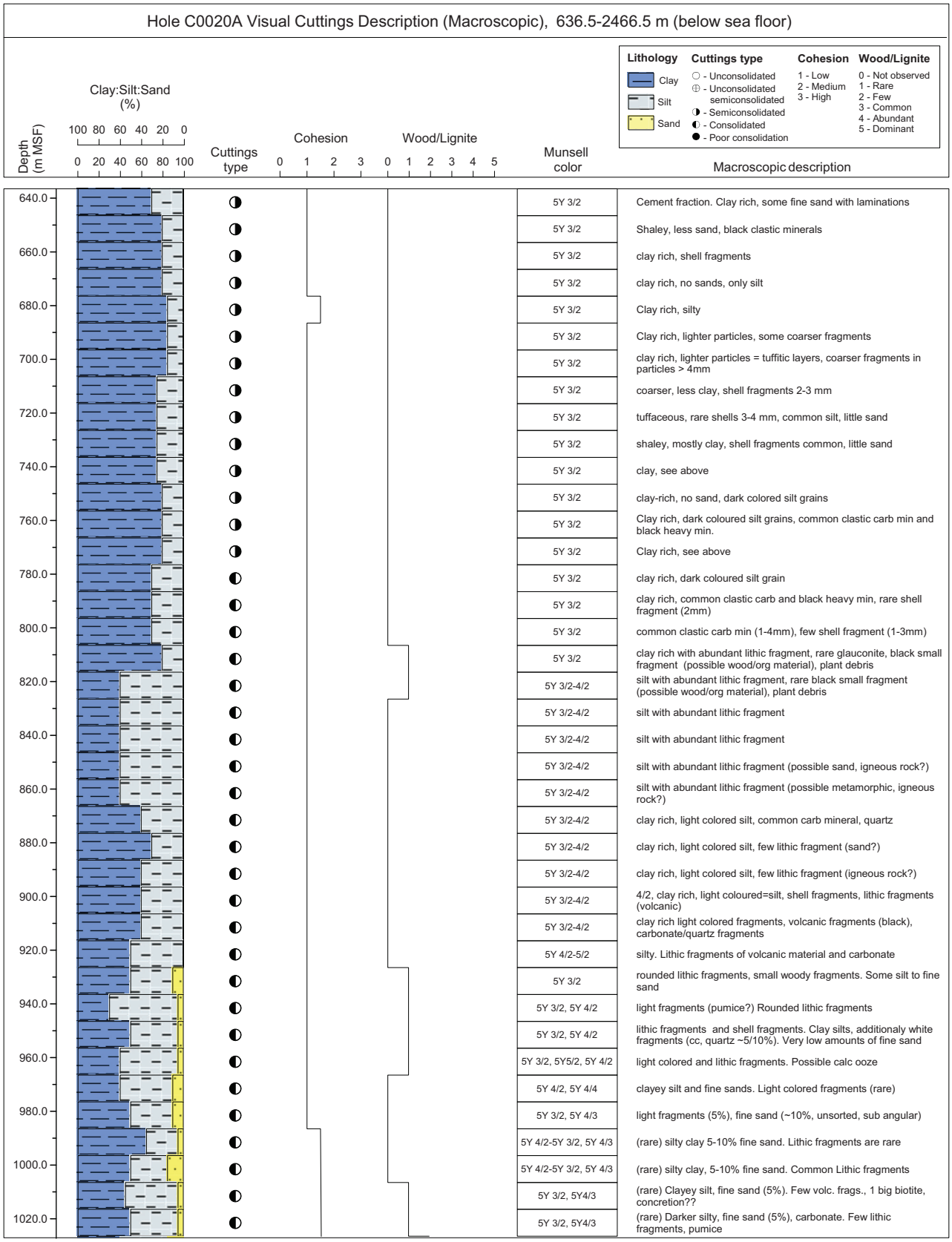

Figure F6. Graphic patterns and symbols used on visual core descriptions, Expedition 337. PFC = perfluorocarbon.

Llithology

- Shale/Mud/Mudstone
- Silt/Siltstone
- Sand/Sandstone
- Shale intercalated with sand
- Coaly shale
- Silty shale/Silty mudstone
- Sandy silt/Sandy siltstone
- Sand intercalated with silt/clay
- Gravel conglomerate
- Coal/Brown coal
- Clayey siltstone
- Silty sand/Silty sandstone
- Silt intercalated with shale/sand
- Breccia
- Whole-round sample

Shipboard samples

HS	Headspace gas	IMP	Resistivity	XRD	X-ray diffraction	MWIC	Mud water without acid
IW	Interstitial water	PWVD	*P*-wave velocity	XRF	X-ray fluorescence	MWP	Mud water/Plastic
PAL	Micropaleontology	SS	Smear slide	MBIO	Microbiology	MWICH	Mud water after alk
PP	Moisture and density	TSS	Thin section slide	HSECD	PFC contamination check	MWICP	Mud water with acid
BMK	Biomarker	RMS	Routine microbiology sample	HSECDM	PFC contamination check/Mud	VAC	Void gas sample
SEM	Scanning electron microscope					CARB	Inorganic carbon

Fossils

- Bivalve
- Radiolarian
- Shell fragments
- Organic materials
- Diatom
- Gastropod
- Spicule (sponge)
- Wood fragments/Plant remains

Bioturbation

- Slight bioturbation
- Moderate bioturbation
- Heavy bioturbation

Deformational structures

- Normal fault
- Vein
- Mineral lineation
- Joint/Extension fracture (tension fracture)
- Slickenside
- Fault breccia
- Deformation band

Lithologic accessories

- Pumice
- Oil-bearing
- Gravel
- Gl Glauconite
- Vein
- Isolated pebble
- Silt scattering
- Mud clast/Isolated mud clast
- Carbonate nodule/Concretion
- Isolated granule
- Py Pyrite/Pyrite nodule
- Mineral-filled fracture
- C Carbonate cement

Sedimentary structures

- F Fining upward
- Planar bedding (lamination)
- Wave ripple cross-lamination
- Tabular cross-bedding (lamination)
- C Coarsening upward
- Wavy bedding (lamination)
- Lenticular bedding
- Load structure
- Sand lamina
- Cross bedding (lamination)
- Flaser bedding/Flaserlike bedding
- Flute cast
- Silt lamina
- Ripple cross-lamination
- Hummocky cross-stratification
- Dish structure/Dish and pillar structure
- Chaotic bedding
- Current ripple cross-lamination
- Trough cross-bedding (lamination)

Drilling disturbance

- Slightly fractured by drilling or splitting
- Slightly disturbed
- Soupy
- Moderately fractured by drilling or splitting
- Moderately disturbed
- Biscuit
- Heavily fractured by drilling or splitting
- Heavily disturbed
- Drilling breccia

Figure F7. Example of the visual core description. See Figure F6 for explanation of sample type symbols. CT = computed tomography, GRA = gamma ray attenuation.

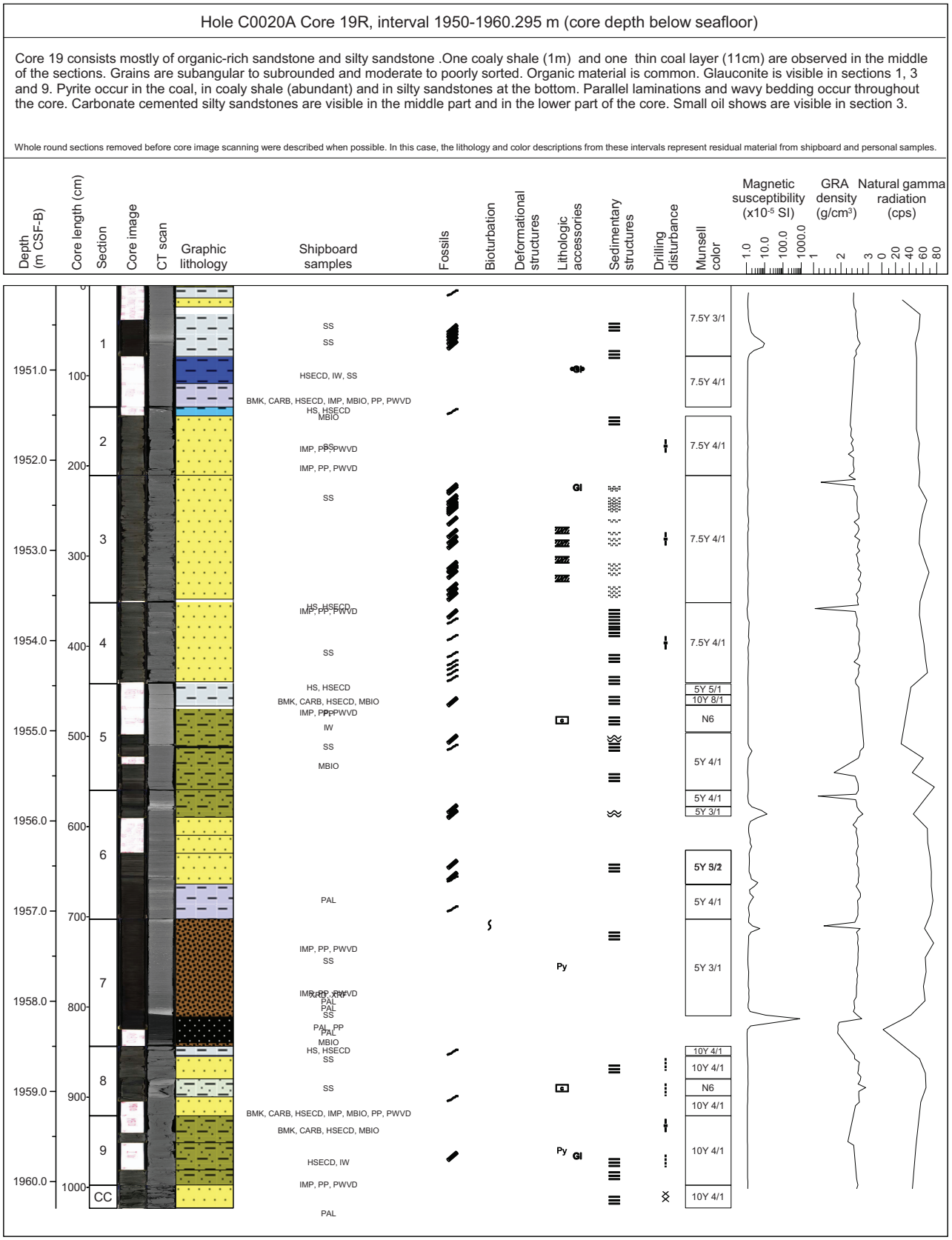

Figure F8. Example of the microscopic cuttings description.

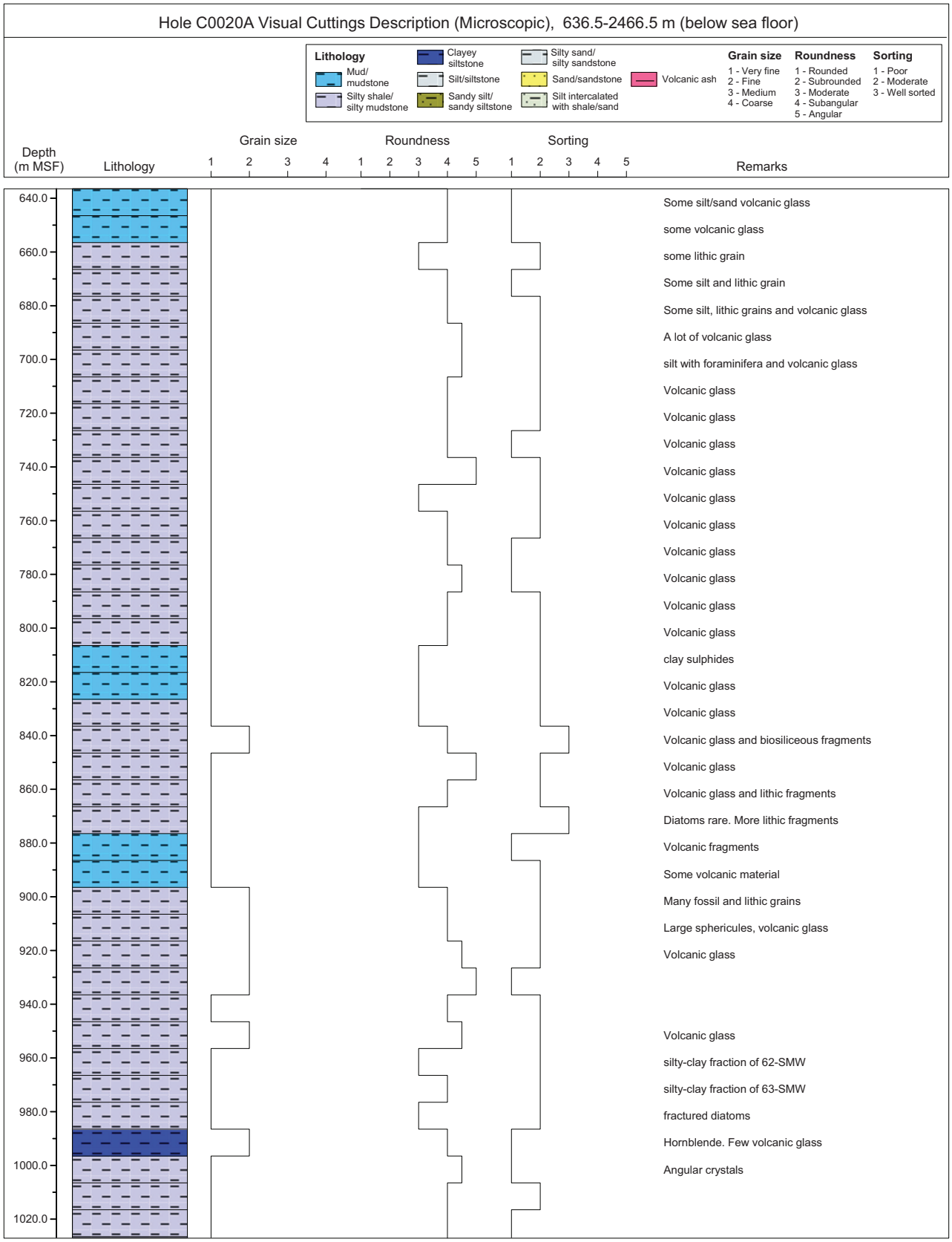

Figure F9. A–E. Tool string sketches for logging Runs 1, 2, 3, 4, and 5, respectively, Expedition 337. SP = spontaneous potential, HNGS = Hostile Environment Natural Gamma Ray Sonde, HRLA = High-Resolution Laterolog Array, PEX = Platform Express, HGNS = Highly Integrated Gamma Ray Neutron Sonde, HRMS = High-Resolution Mechanical Sonde, MCFL = Micro-Cylindrically Focused Log, TLD = Three-Detector Lithology Density, PEF = photoelectric effect, PPC = Power Positioning Device and Caliper, EMS = Environmental Measurement Sonde, DSI = Dipole Sonic Imager, GPIT = General Purpose Inclinometry Tool, FMI = Formation MicroImager, CMR = combinable magnetic resonance, NMR = Nuclear Magnetic Resonance, MRPC = electric power module, MRMS = multisample module, IFA = In Situ Fluid Analyzer, MRPO = pumpout module, MRHY = hydraulic power module, MRPS = single-probe module for pressure test, CFA = Composition Fluid Analyzer, VSI = Versatile Seismic Imager. (Continued on next page.)

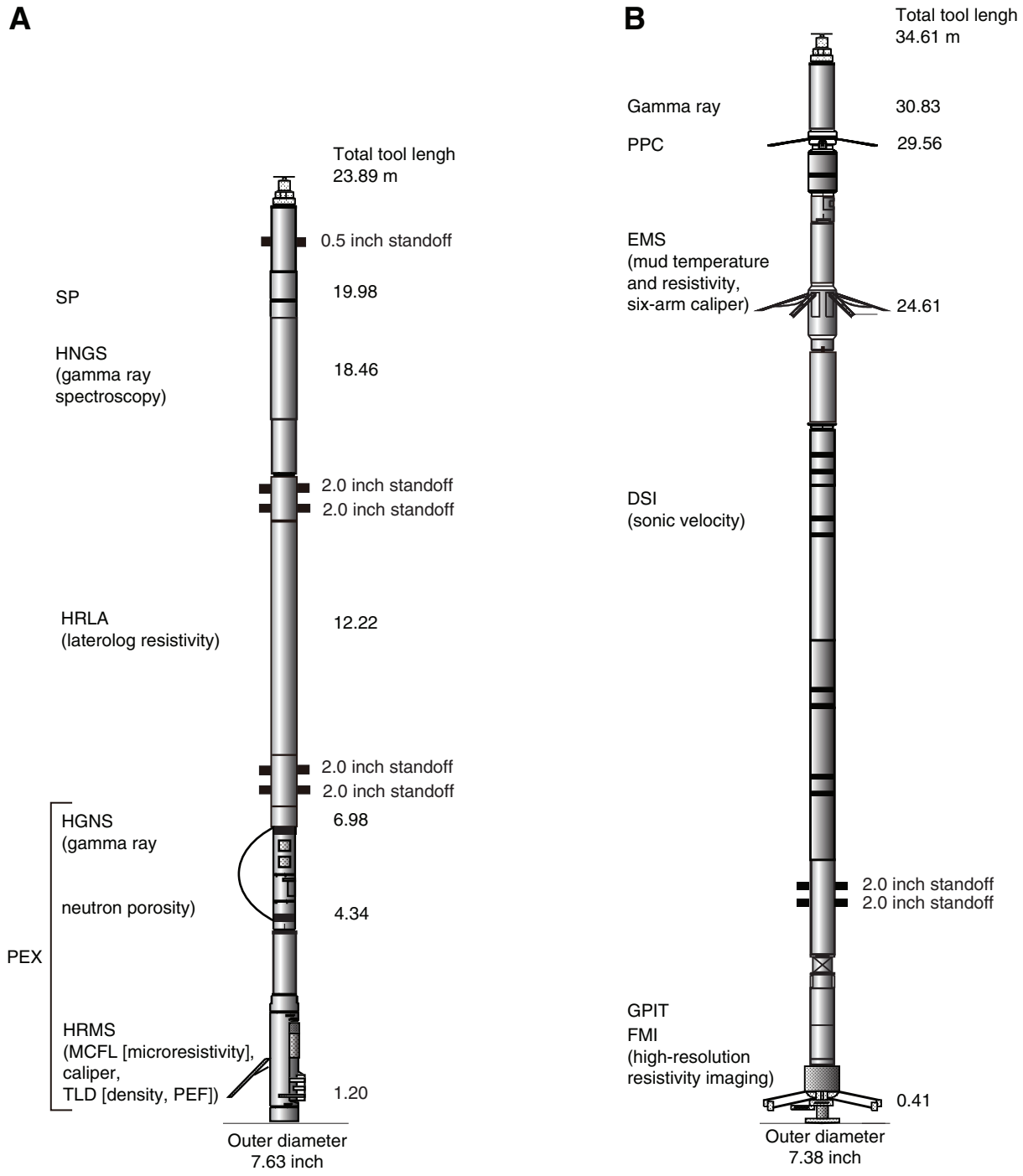

Figure F9 (continued).

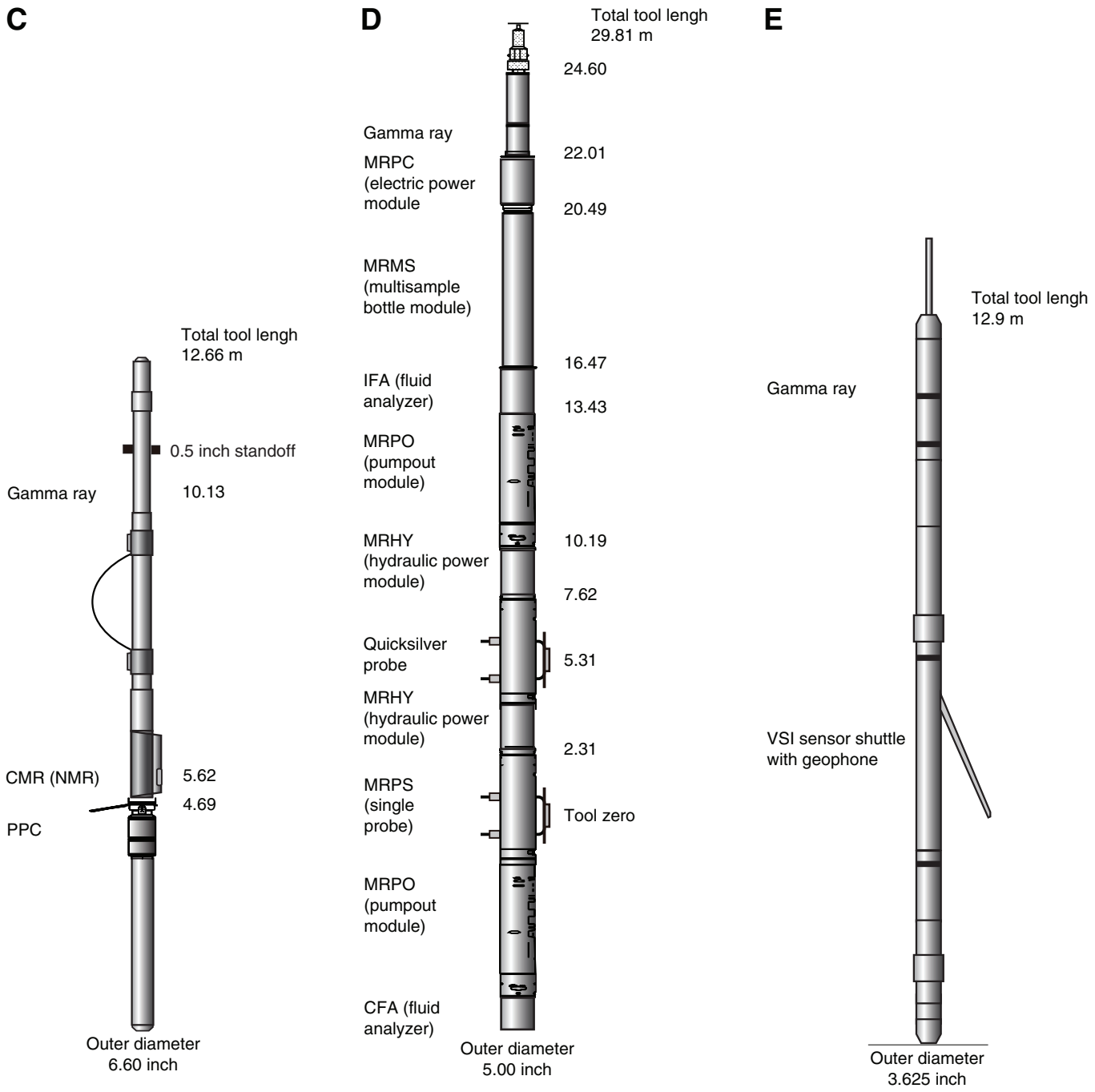

Figure F10. Schematic of passive heave compensator, Expedition 337.

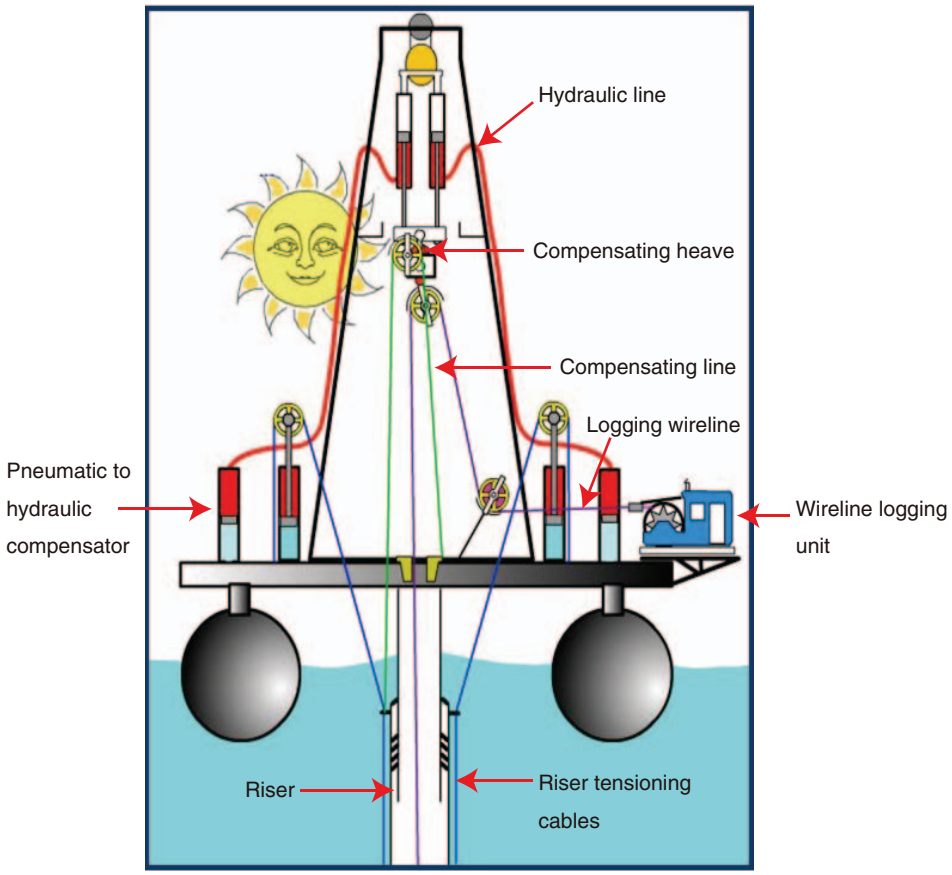

Figure F11. Fullbore Formation MicroImager (FMI), Expedition 337. **A.** FMI has four pads and four flaps on a total of four arms. **B.** Two lines of 12-row electrodes are placed on each pad and flap.

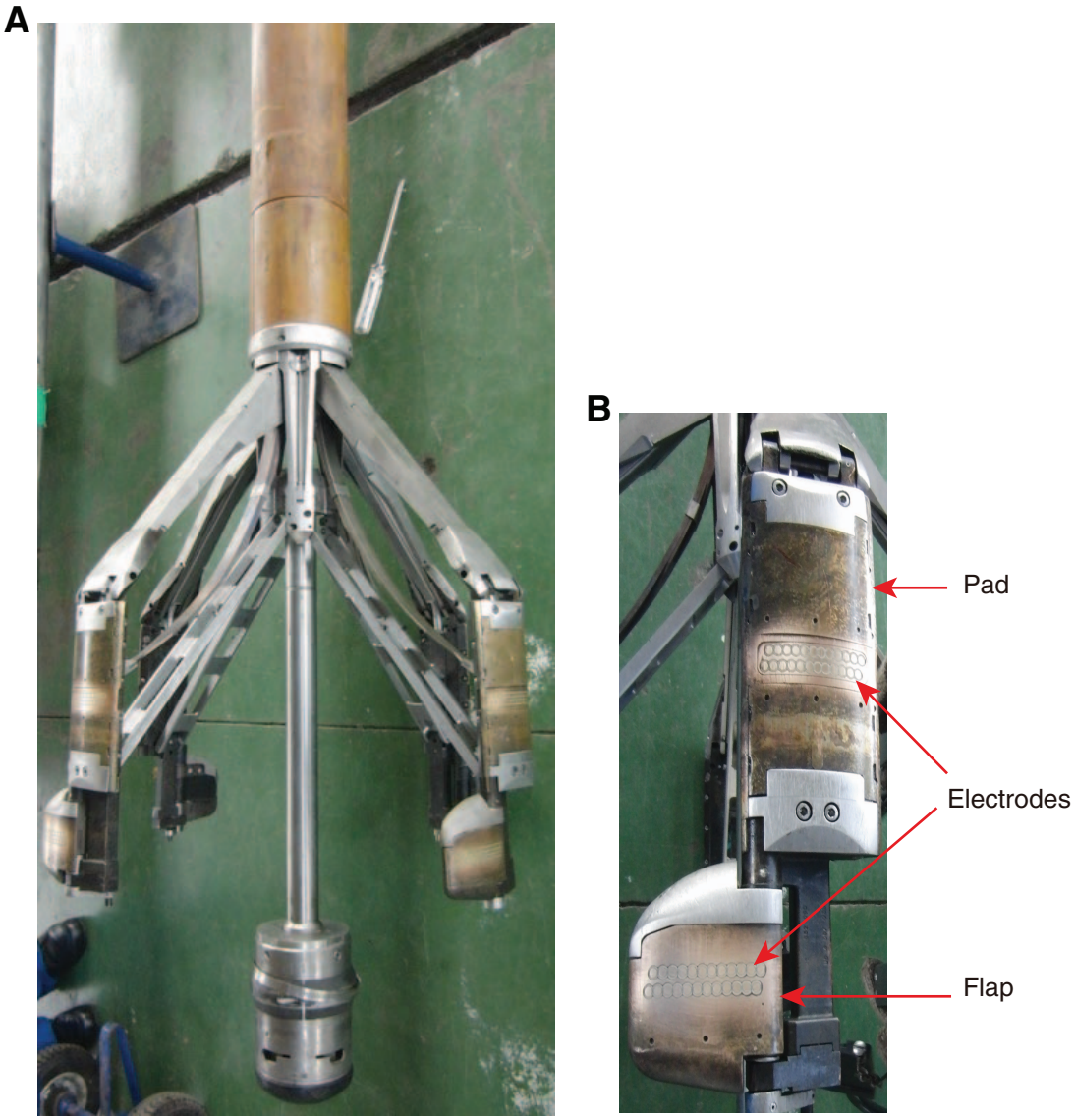

Figure F12. Photographs of VSP air gun system, Expedition 337. **A.** Air gun array. **B.** Deployment of air gun. **C.** Air gun shooting.

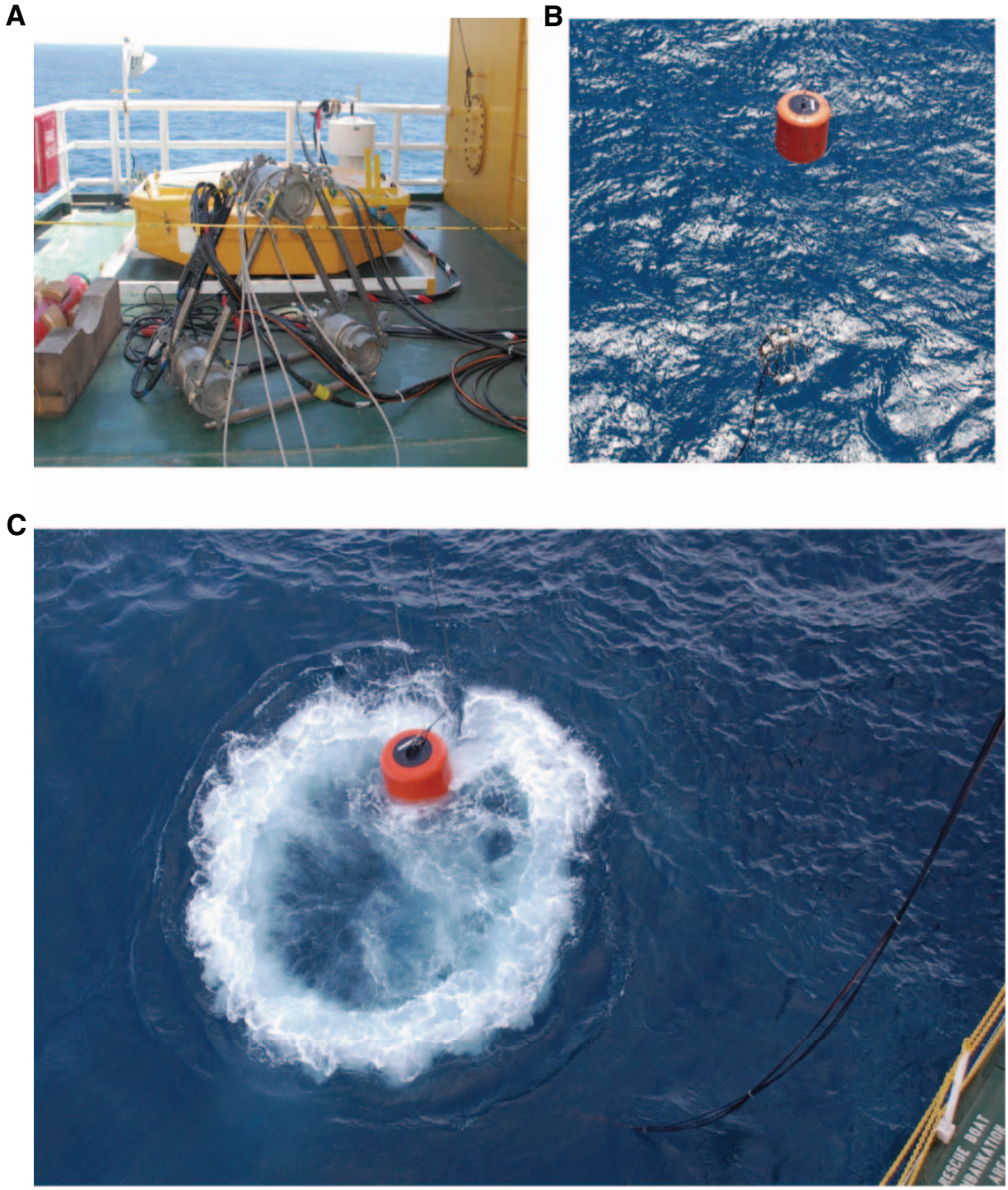

Figure F13. Acquisition geometry of zero-offset VSP on the D/V *Chikyu*, Expedition 337.

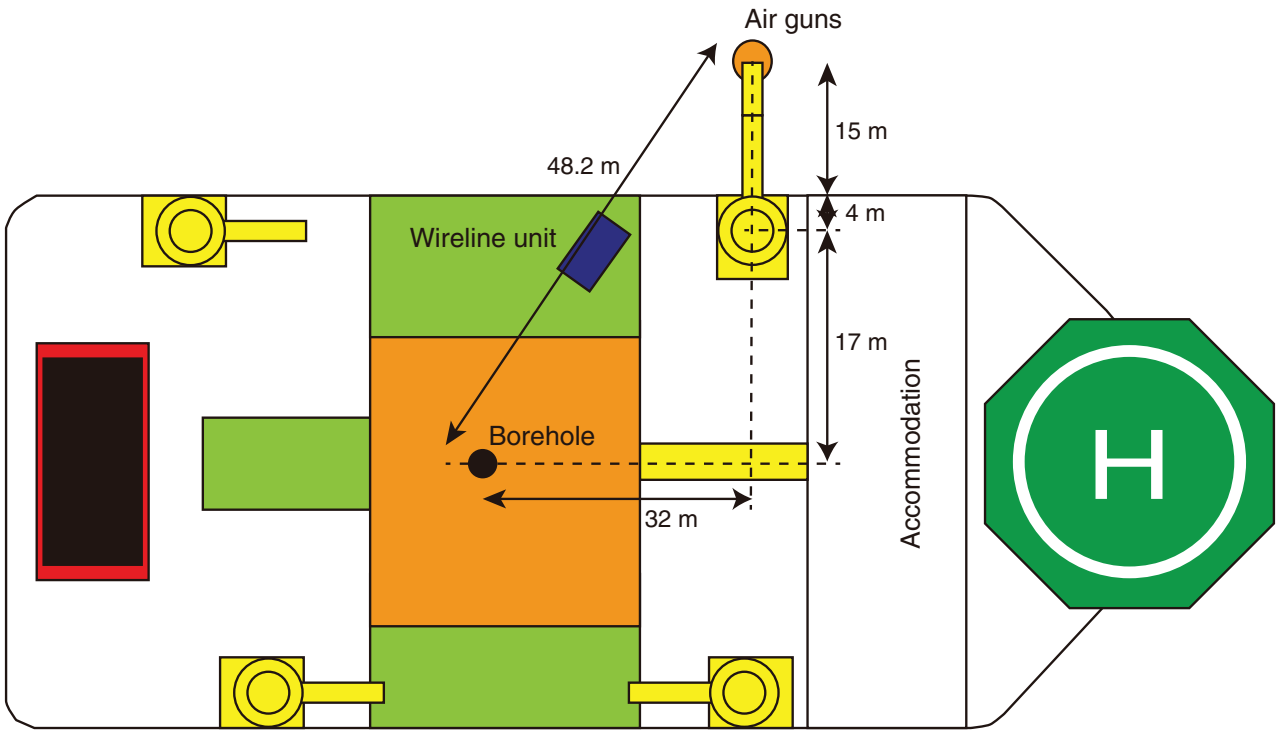

Figure F14. Diagram of combinable magnetic resonance (CMR) Plus tool and section of CMR skid, Expedition 337.

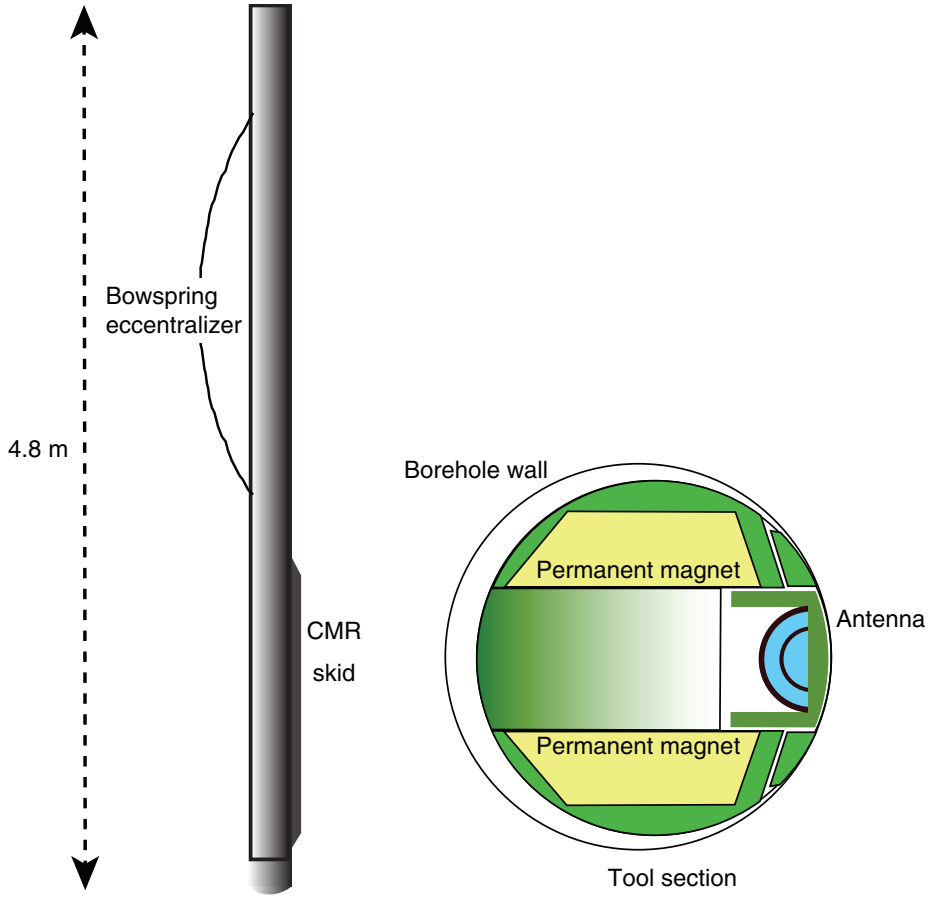

Figure F15. Diagram of shipboard data flow, Expedition 337. MAXIS = multitasking acquisition and imaging system. CDEX = Center for Deep Earth Exploration. VSP = vertical seismic profile. DLIS = digital log information standard, SEGY = Society of Exploration Geophysicists format "Y," LAS = log ASCII standard.

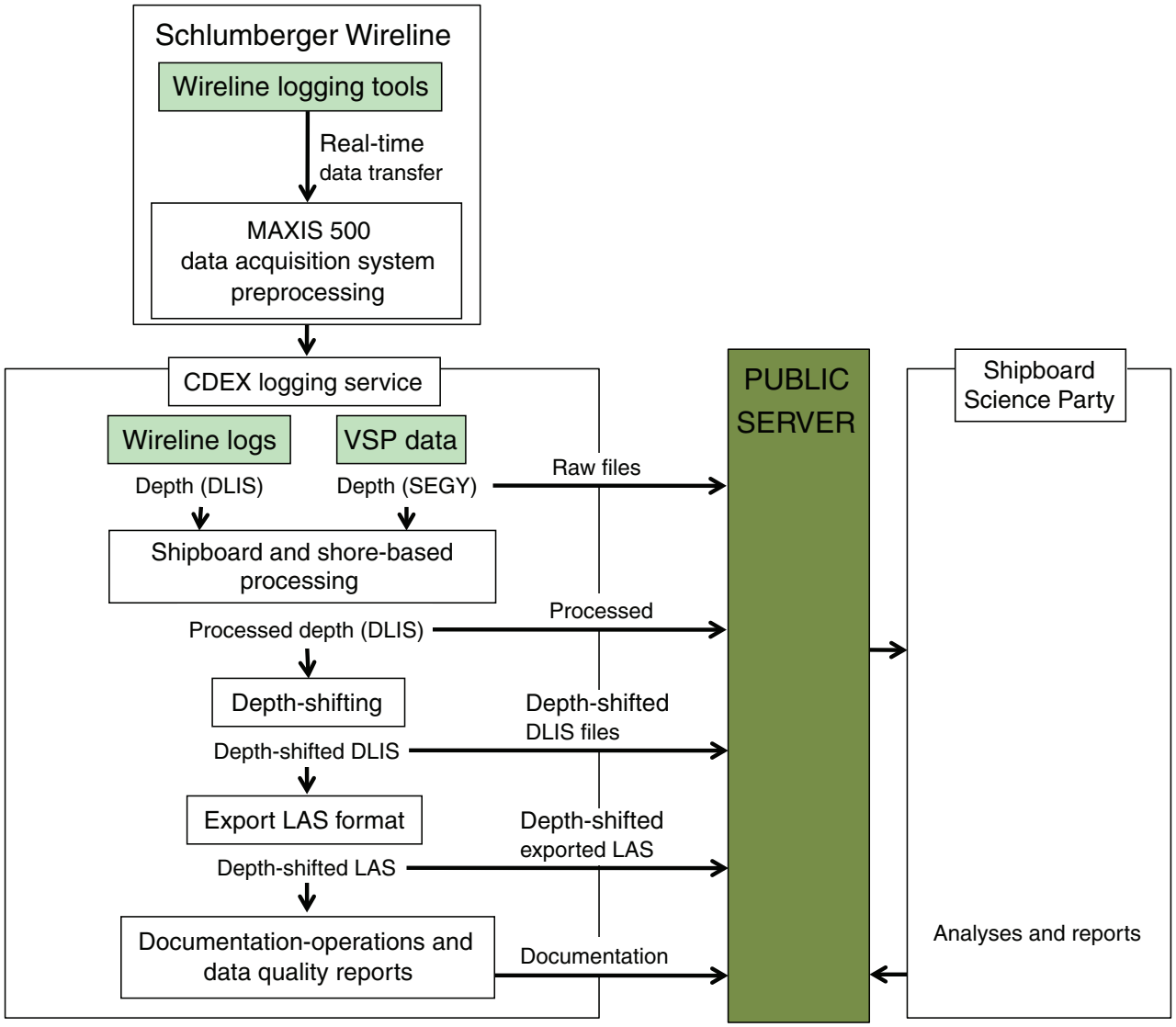

Figure F16. Schematic diagram of pressure measurement with the single probe, Expedition 337. CQG = crystal quartz gauge.

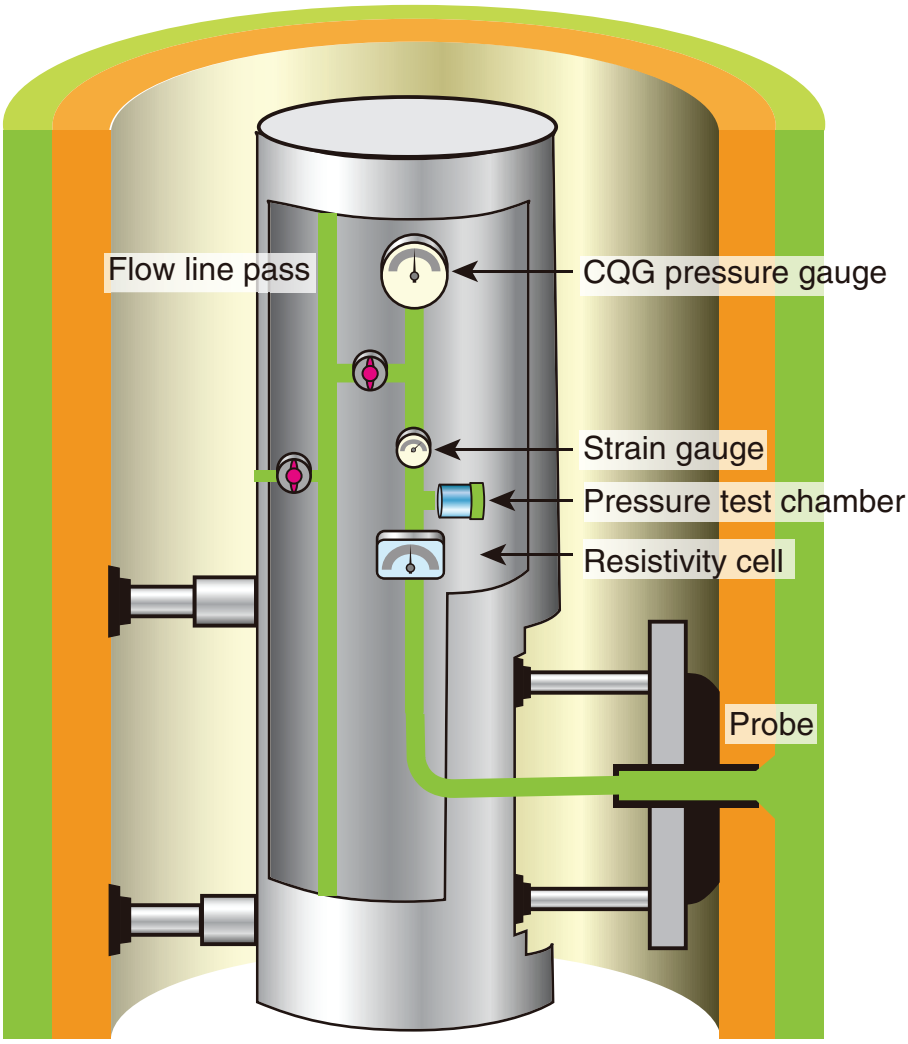

Figure F17. Simplified schematic diagram of fluid sampling module and the Quicksilver probe, Expedition 337. SPMC = single-phase multisample chamber.

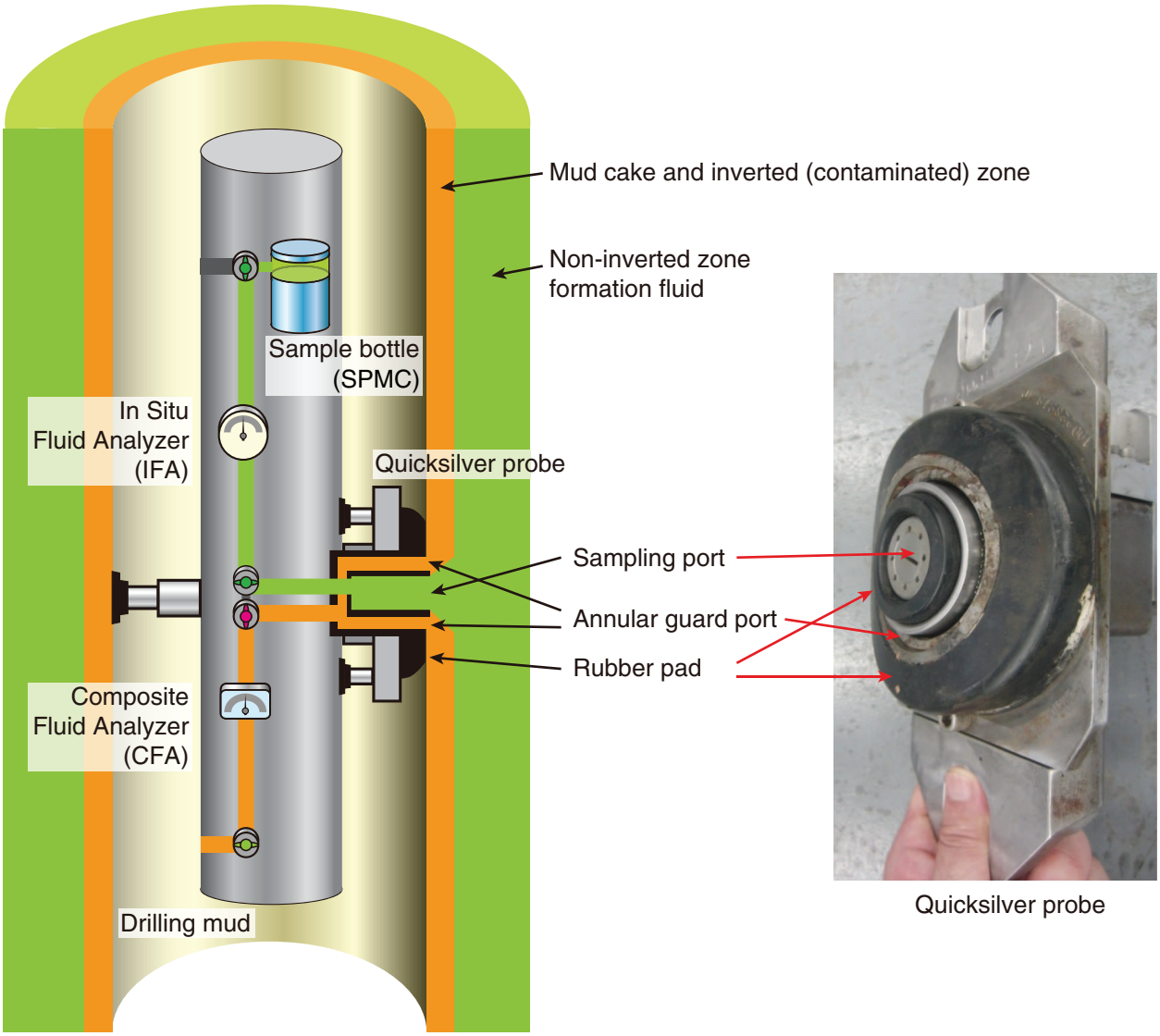

Figure F18. Schematic diagram of the single-phase multisample chamber, Expedition 337. Pressurized nitrogen gas keeps the sample liquid and gas pressurized.

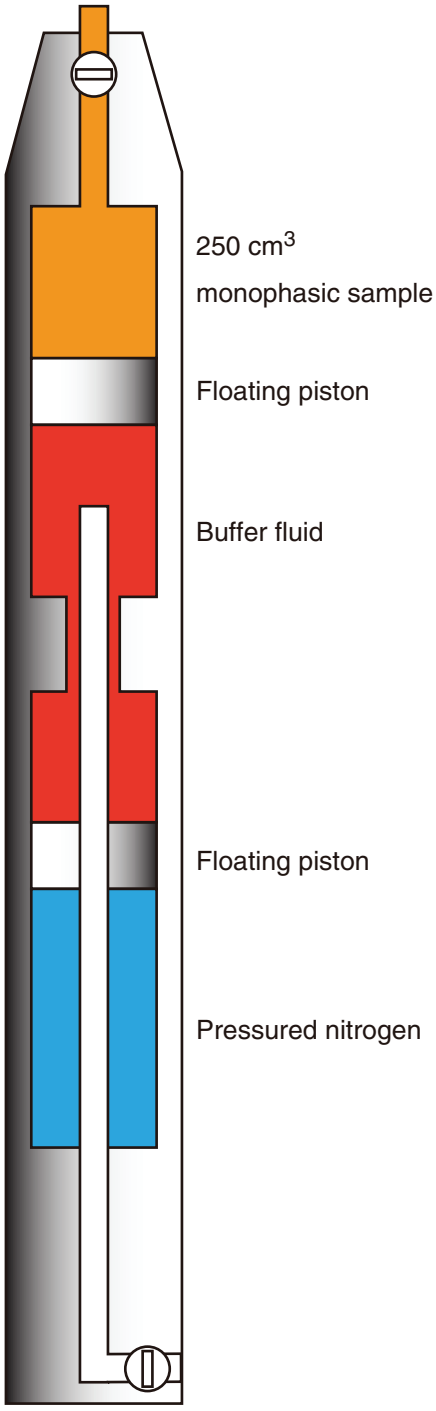

Figure F19. Photo image of 2-D measurement system for the elliptical section of whole-round cores, Expedition 337.

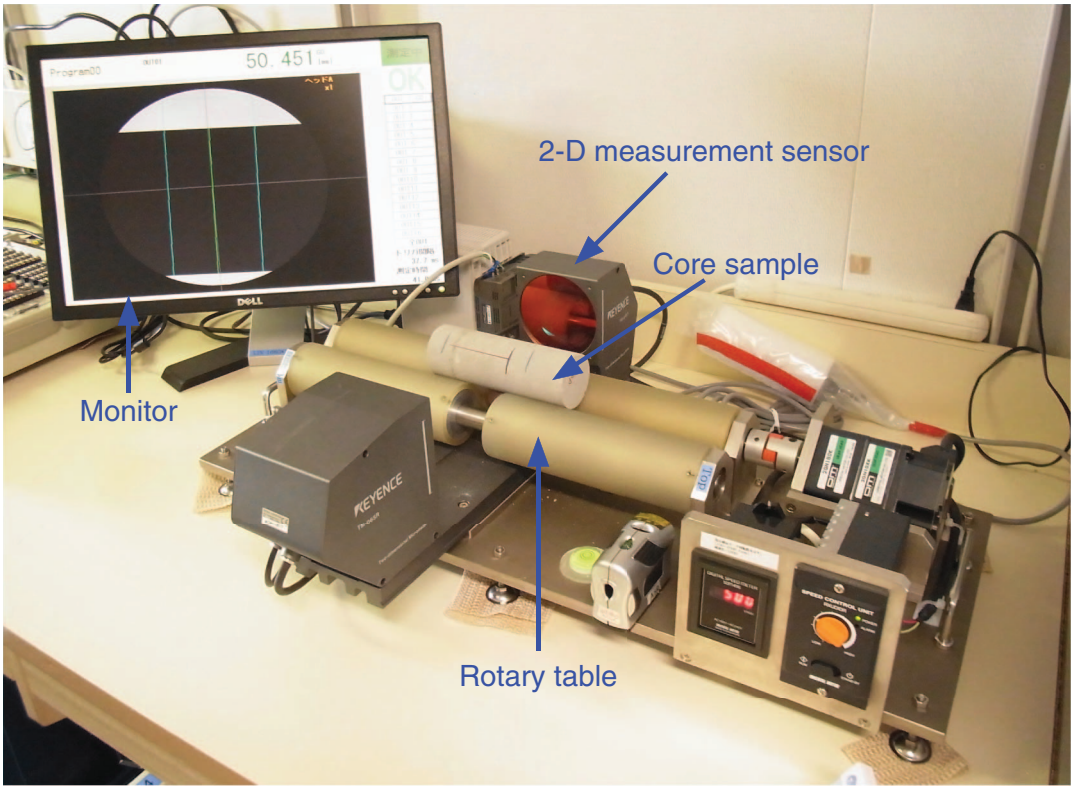

Figure F20. Overview of the setup showing the system for vitrinite reflectance analysis for small coal fragments. The spot analysis for small coal fragments down to 1.6 µm in diameter is achieved by using Köhler and critical illuminations.

Figure F21. Diagram of the mud extraction system and the setup in the mud-gas monitoring laboratory (modified from Saffer, McNeill, Byrne, Araki, Toczko, Eguchi, Takahashi, and the Expedition 319 Scientists, 2010). **A.** The degasser used to separate drilling mud and dissolved gas is installed at the point where drilling mud is first exposed to the air. Dissolved gas is extracted from the fluid phase by pumping from the laboratory. **B.** A fraction of the drilling mud passes the flow splitter and bypasses the Gumbo separator. **C.** A safety valve is installed to compensate the pressure difference between pumping in the laboratory and gas pressure in the degasser. It also prevents the overflow of drilling mud into the gas monitoring system. **D.** Gas is filtered and dried upon arrival at the laboratory. An Isotube sampling system can collect gas samples before or after the gas dryer. A gas chromatograph, quadrupole mass spectrometer, Rn detector, and methane carbon isotope analyzer are connected to the pipeline and perform real-time monitoring of gas composition and methane carbon isotope. FID = flame ionization detector.

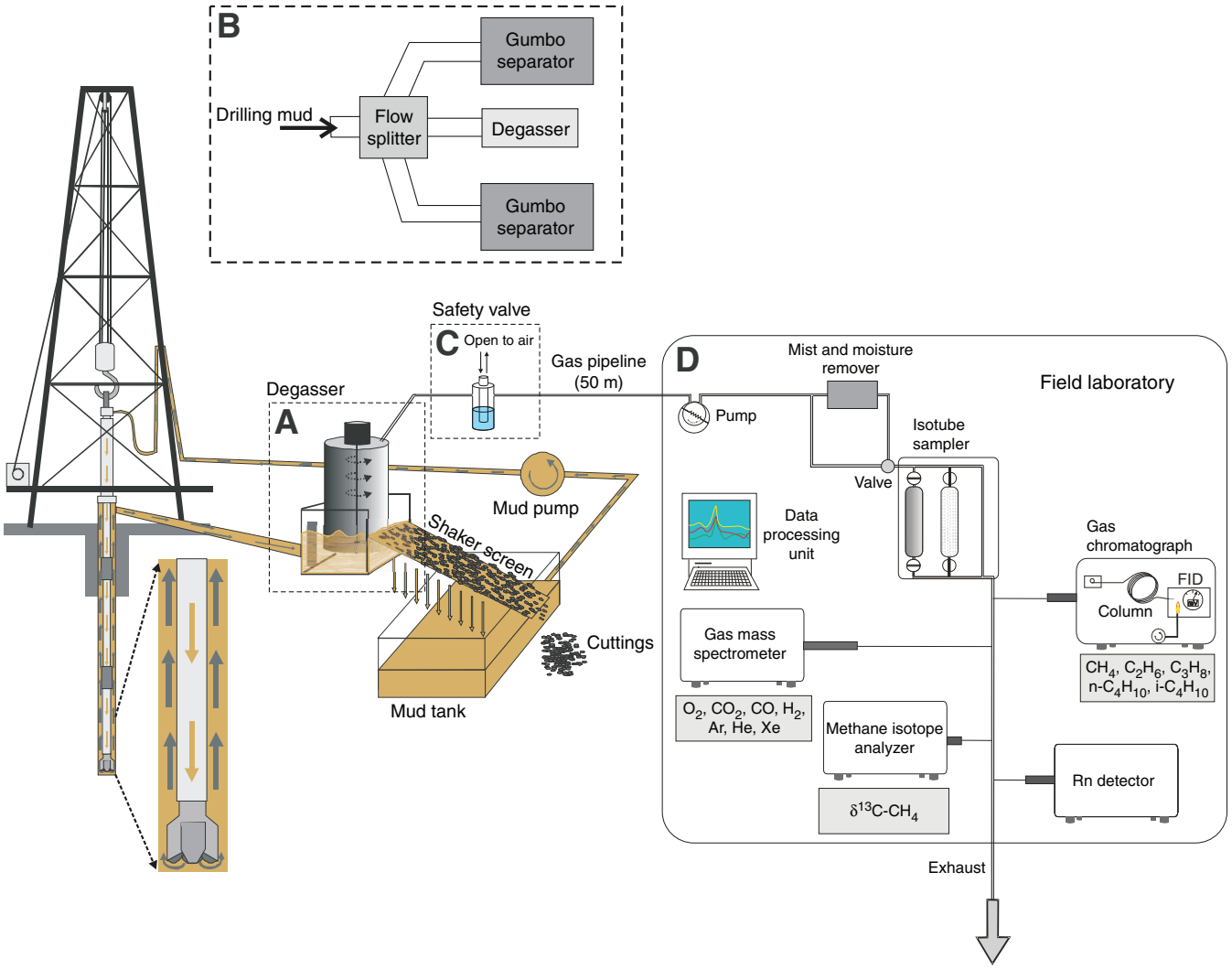

Figure F22. Schematic diagram for the analytical procedure for lipid analysis. ASE = accelerated solvent extraction, MeOH = methanol, DCM = dichloromethane, TLE = total lipid extract, PLFA = phospholipid fatty acid, IPL = intact polar lipid.

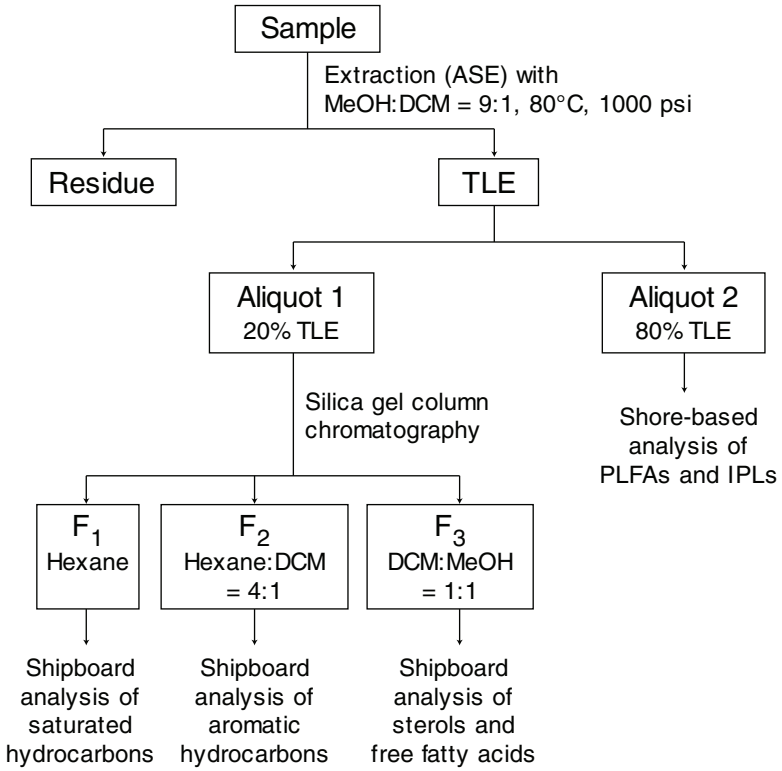

Figure F23. A. Side view of community WRC, Expedition 337. (a) A 2.5 cm interval for shipboard analyses of physical properties, total organic carbon (TOC), and lithology was taken adjacent to the (b) 12.5 cm interval used for microbiological and geochemical analyses. MAD = moisture and density, Mag = magnetic properties, smear = smear slides. **B.** Cross-sectional view of interval b sampling for microbiological and geochemical analyses. Note: Fe and S solid-phase analyses and fungal incubations were shore-based. Leftovers were used for shipboard lithologic analyses. X = exterior, H = halfway between liner and core center, IN = interior, PFC = perfluorocarbon, FISH = fluorescence in situ hybridization, DCC = direct cell counts.

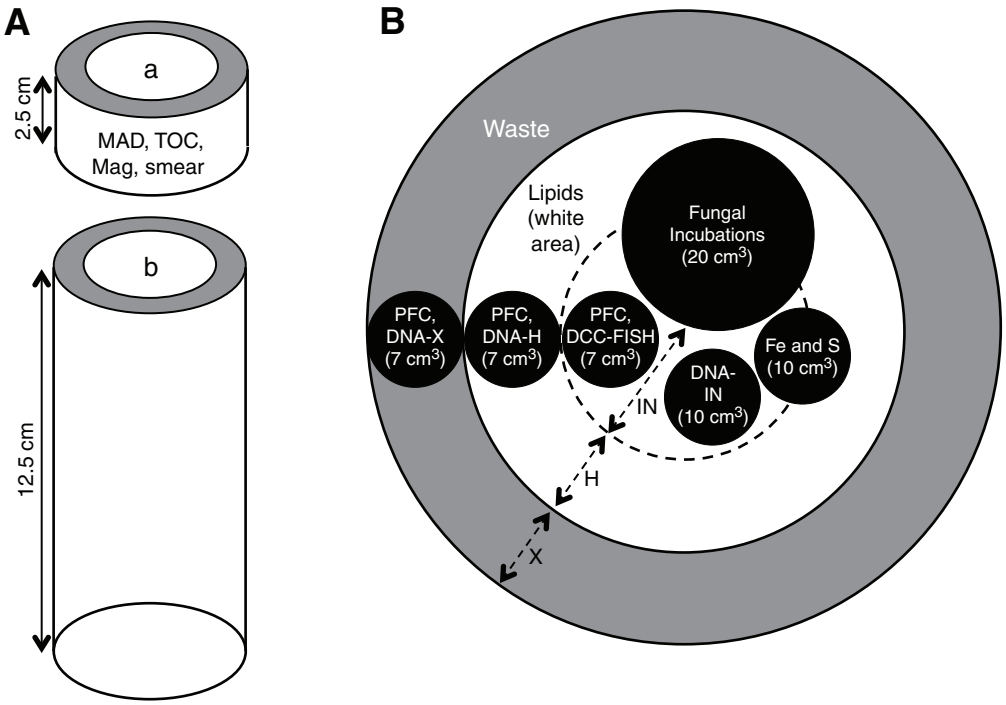

Figure F24. Perfluorocarbon (PFC) tracer concentrations in drilling mud determined by five different incubation treatments, Expedition 337. Treatment 1: 1 h preincubation with rotation in hybridization oven prior to 30 min incubation without motion in autosampler; Treatments 2–5: 30 min and 1, 2, and 5 h preincubation without motion in autosampler, respectively. For Treatment 2, two replicates were used (a and b).

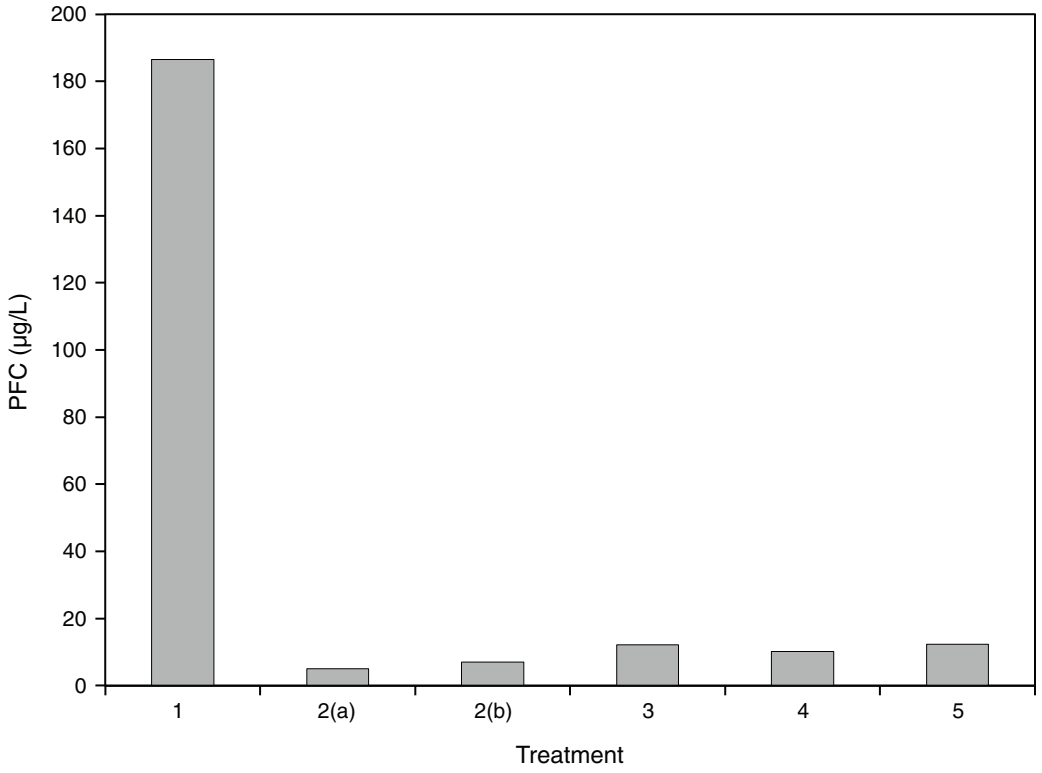

Figure F25. Photo of fluorescent image-based cell counting system used for cell counts, Expedition 337.

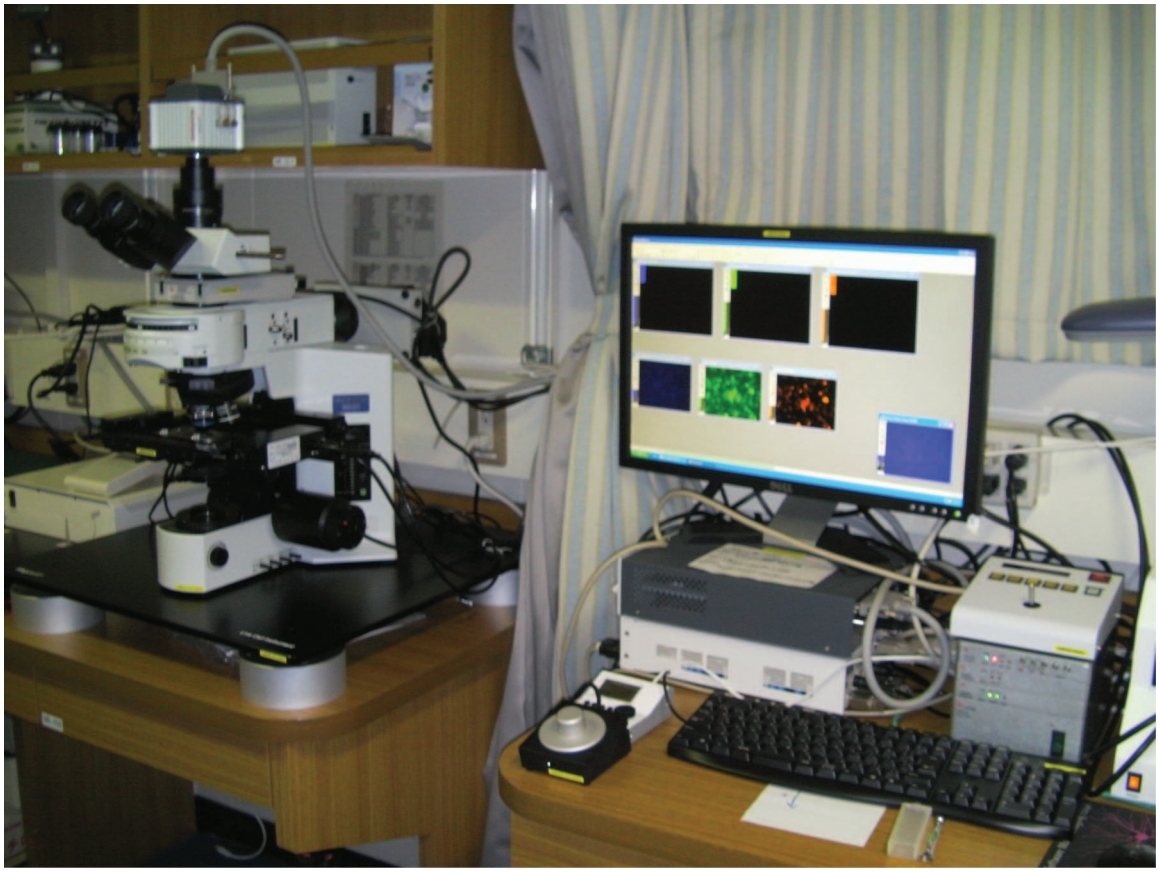

Figure F26. Photo of Gallios flow cytometer (Beckman Coulter) placed on the antivibration table in the core laboratory, Expedition 337.

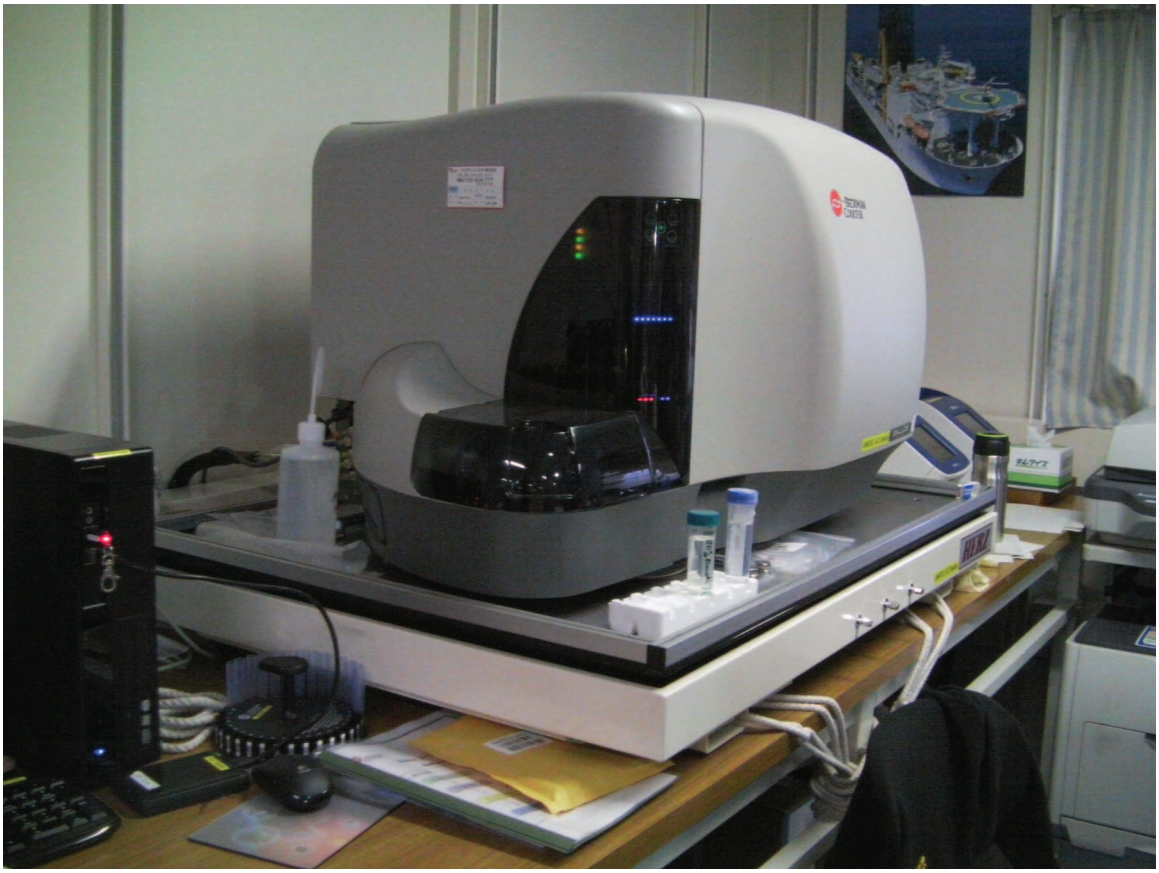

Figure F27. Photo of StepOnePlus real-time PCR system for gene quantification, Expedition 337.

Figure F28. Photo of DNA sequencer (ABI 3130 XL Genetic Analyzer) for T-RFLP analysis of microbial community structures, Expedition 337.

Table T1. IODP depth scales summary table.

	Depth scale name	Acronym	Datum	Description	Previous unit	Type depth
Drillers depth scales	Drilling depth below rig floor	DRF	Rig floor	The sum of lengths of all drill string components deployed beneath the rig floor. Includes length of all components and the portions thereof below rig floor.	mbrf	Measured
	Drilling depth below seafloor	DSF	Seafloor	The length of all drill string components between seafloor and target.	mbsf	Processed
LWD and MWD depth scales	LWD depth below rig floor	LRF	Rig floor	The sum of lengths of all drill string components deployed beneath the rig floor reference.	mbrf	Measured
	LWD depth below seafloor	LSF	Seafloor	The length of all drill string components between seafloor and target.	mbsf	Processed
Mud depth scales	Mud depth below rig floor	MRF	Rig floor	The length of all drill string components between where cuttings and gas originate and the rig floor based on lag time of arrival at rig floor and mud pump rate.	NA	Processed
	Mud depth below seafloor	MSF	Seafloor	MRF with seafloor depth below rig floor subtracted.	NA	Processed
Wireline depth scales	Wireline log depth below rig floor	WRF	Rig floor	Length of wireline and sensor offset between the rig floor and the target.	mbrf	Measured
	Wireline log depth below seafloor	WSF	Seafloor	WRF with seafloor depth below rig floor subtracted.	mbsf	Processed
	Wireline log speed-corrected depth below seafloor	WSSF	Seafloor	WSF corrected with accelerometer data.	mbsf	Processed
	Wireline log matched depth below seafloor	WMSF	Seafloor	Depth derived by correlation between reference run and another run to make a set of WSF runs internally consistent.	mbsf	Processed
Core depth scales	Core depth below seafloor	CSF-A	Seafloor	Distance from seafloor to target within recovered core. Combines DSF to top of cored interval with curated section length to target within cored material. This method allows overlap at cored interval and section boundaries.	mbsf	Processed
	Core depth below seafloor	CSF-B	Seafloor	Distance from seafloor to target within recovered core. Combines DSF to top of cored interval with curated length to target within cored material. This method applies compression algorithm (i.e., scaling) if recovery is >100%.		Processed
Composite depth scales	Core composite depth below seafloor	CCSF	Seafloor	Distance from seafloor to target within recovered core using a scale of adjusted depths constructed to resolve gaps in the core recovery and depth inconsistencies.	mcd	Composite
Seismic depth scales	Seismic depth below seafloor	SSF	Seafloor	Distance below seafloor and target derived from seismic traveltime, velocity, and water depth.	m	Processed
	Seismic depth below sea level	SSL	Sea level	Distance below sea level derived from seismic traveltime and velocity.	m	Processed

LWD = logging while drilling, MWD = measurement while drilling. NA = not applicable. See IODP Depth Scale Terminology at www.iodp.org/program-policies/.

Table T2. Data set included in the core scale images, Expedition 337.

Core description:
Depth CSF-B (m)
Core length scale (cm)
Piece number
Lithologic unit
Shipboard samples
Structural data:
Sedimentary structures
Bioturbation and fossils
Deformation structures
Drilling disturbance
Core imaging:
X-ray CT scan image
Section photograph
Munsell color data
MSCL-W data (PP):
Magnetic susceptibility
Bulk density
Natural gamma radiation

CT = computed tomography, MSCL-W = whole-round multisensor core logger, PP = physical properties.

Table T3. Scan settings for X-ray CT scanner.

Parameter	Setting
Scan type	Helical-full-0.5 s
Interval (mm)	0.625
Gantry tilt	S0.0
Scan field of view	Small
Voltage (kV)	120
Current (mA)	100
Detector rows	16
Helical thickness (mm)	0.625
Pitch	0.562:1
Speed (mm/rot)	5.62
Dual field of view (cm)	9.6
R/L center (mm)	R0.0
A/P center (mm)	A0.0
Recon type	Detail
Matrix size (pixel)	512 × 512
Recon option	Full
Direct vis	Off

Protocol name: 090624_Exp319 9.1 071210_Aluminum Piece. R/L center = distance right or left of the center line, A/P = distance anterior or posterior of the center line.

Table T4. IFA specifications, Expedition 337.

Measurement	Measurement range	Accuracy
Fluorescence	NA	NA
Resistivity (Ωm)	0.01–20	0.01
Density (g/cm^3)	0.05–1.2	0.012
Viscosity	NA	NA
Pressure (MPa)	to 172	10^{-4} FS (Typ), 2.5×10^{-4} FS (max)
Temperature (°C)	to 175	10^{-4} FS (Typ), 2.5×10^{-4} FS (max)

NA = not applicable.

Table T5. Overview of microbiological sampling performed during Expedition 337.

Sample test suite	Sample preparation	Methods text section
Shipboard community samples*		"Onboard incubation for shore-based microbiological cultivation experiments"
PFC	5 cm^3 sample in 20 cm^3 gas vial with silicon stopper; handed to technician.	"Chemical tracer"
DNA contamination	2 cm^3 sample from core exterior and halfway to core interior into 15 mL Falcon tubes; frozen at –20°C.	"DNA-based contamination tracers"
Cell counts + FISH	2 cm^3 sample into round-bottom (13 cm^3) tube, added 8 mL of 4% PFA, and shaken to slurry; stored at 4°C. Note: if too stiff to slurry by shaking, crushed in aluminum bag using hammer. If too hard to crush with hammer, inserted into round-bottom tube and without PFA addition.	"Cell separation and enumeration"
DNA for qPCR and T-RFLP	10 cm^3 into 15 mL Falcon tube; frozen at –20°C.	"DNA extraction and purification"
Sulfate reduction rates	5–10 cm WRC in gas-tight bag, flushed with N_2, and sealed; stored at 4°C. Processed within 24 h.	"Potential sulfate reduction rates"
Shore-based testing†		"Sampling for shore-based investigations"
Cultivation	10 cm WRC in gas-tight bag, flushed with N_2, vacuumed, and sealed; stored at 4°C.	"Cultivation experiments"
SIP/NanoSIMS	10 cm WRC in gas-tight bag, flushed with N_2, vacuumed, and sealed; stored at 4°C.	"Single-cell analyses of carbon and nitrogen assimilation rates of subseafloor microbes"
Extracellular DNA/functional genes/ amino acids and amino sugars	10 cm WRC in gas-tight bag, flushed with N_2, vacuumed, and sealed; stored at 4°C. Processed within 24 h.	"Shore-based DNA extraction, functional gene characterization, and organic acid analyses"
Sulfate reduction rates	5–10 cm WRC in gas-tight bag, flushed with N_2, and sealed.	"Shore-based ^{35}S incubations"
Fungi	20+ cm^3 sample in gas-tight bag, flushed with N_2, and sealed; stored at 4°. Processed within 24 h.	"Cultivation experiments"
Chemical degradation of coal/lignite and release of short-chain fatty acids	Sampled from split cores.	"Hydrogenase activity measurements"

* = underwent X-ray computed tomography. † = underwent X-ray computed tomography and whole-round multisensor core logging. Samples for shipboard community analyses were taken from 15 cm whole-round cores (WRCs) that were shared with other shipboard scientists for lipid biomarker, TOC = total organic carbon, iron and sulfur species, and sedimentology. PFC = perfluorocarbon, FISH = fluorescence in situ hybridization, PCR = polymerase chain reaction, T-RFLP = terminal restriction fragment length polymorphism, NanoSIMS = nanoscale secondary-ion mass spectrometry, PFA = paraformaldehyde.

Table T6. Overview of sampling plan for community analyses from shared WRCs, Expedition 337. (Continued on next page.)

		Microbiology*					Lithology†				Geochemistry*		
Core	Section	PFC (5 cm^3 each)	DNA contamination (2 cm^3 each)	DCC + FISH (cm^3)	qPCR (cm^3)	Fungi incubation (cm^3)	Sedimentology (cm^3)	MAD (cm^3)	Magnetic analyses (cm^3)	TOC (cm^3)	Fe and S species (cm^3)	Shipboard lipids (cm^3)	Shore-based lipids
337-C0020A-													
1R	2	X, H, IN	X, H	5	10		0.1	8	10	5	10	50	All leftovers from H and IN
	4	X, H, IN		5		20					10	50	All leftovers from H and IN
2R	2	X, H, IN	X, H	5	10		0.1	8	10	5	10	50	All leftovers from H and IN
	4	X, H, IN		5		20					10	50	All leftovers from H and IN
3R	2	X, H, IN	X, H	5	10		0.1	8	10	5	10	50	All leftovers from H and IN
	4	X, H, IN		5		20					10	50	All leftovers from H and IN
4R	2	X, H, IN	X, H	5	10		0.1	8	10	5	10	50	All leftovers from H and IN
	4	X, H, IN		5		20					10	50	All leftovers from H and IN
5R	2	X, H, IN	X, H	5	10		0.1	8	10	5	10	50	All leftovers from H and IN
	4	X, H, IN		5		20					10	50	All leftovers from H and IN
6R	2	X, H, IN	X, H	5	10		0.1	8	10	5	10	50	All leftovers from H and IN
	4	X, H, IN		5		20					10	50	All leftovers from H and IN
7R	2	X, H, IN	X, H	5	10		0.1	8	10	5	10	50	All leftovers from H and IN
	4	X, H, IN		5		20					10	50	All leftovers from H and IN
8L	2	X, H, IN	X, H	5	10		0.1	8	10	5	10	50	All leftovers from H and IN
	4	X, H, IN		5		20					10	50	All leftovers from H and IN
9R	2	X, H, IN	X, H	5	10		0.1	8	10	5	10	50	All leftovers from H and IN
	4	X, H, IN		5		20					10	50	All leftovers from H and IN
10R	2	X, H, IN	X, H	5	10		0.1	8	10	5	10	50	All leftovers from H and IN
	4	X, H, IN		5		20					10	50	All leftovers from H and IN
11R	2	X, H, IN	X, H	5	10		0.1	8	10	5	10	50	All leftovers from H and IN
	4	X, H, IN		5		20					10	50	All leftovers from H and IN
12R	2	X, H, IN	X, H	5	10		0.1	8	10	5	10	50	All leftovers from H and IN
	4	X, H, IN		5		20					10	50	All leftovers from H and IN
13R	2	X, H, IN	X, H	5	10		0.1	8	10	5	10	50	All leftovers from H and IN
	4	X, H, IN		5		20					10	50	All leftovers from H and IN
14R	2	X, H, IN	X, H	5	10		0.1	8	10	5	10	50	All leftovers from H and IN
	4	X, H, IN		5		20					10	50	All leftovers from H and IN
15R	2	X, H, IN	X, H	5	10		0.1	8	10	5	10	50	All leftovers from H and IN
	4	X, H, IN		5		20					10	50	All leftovers from H and IN
16R	2	X, H, IN	X, H	5	10		0.1	8	10	5	10	50	All leftovers from H and IN
	4	X, H, IN		5		20					10	50	All leftovers from H and IN
17R	2	X, H, IN	X, H	5	10		0.1	8	10	5	10	50	All leftovers from H and IN
	4	X, H, IN		5		20					10	50	All leftovers from H and IN
18R	2	X, H, IN	X, H	5	10		0.1	8	10	5	10	50	All leftovers from H and IN
	4	X, H, IN		5		20					10	50	All leftovers from H and IN
19R	2	X, H, IN	X, H	5	10		0.1	8	10	5	10	50	All leftovers from H and IN
	4	X, H, IN		5		20					10	50	All leftovers from H and IN
20R	2	X, H, IN	X, H	5	10		0.1	8	10	5	10	50	All leftovers from H and IN
	4	X, H, IN		5		20					10	50	All leftovers from H and IN
21R	2	X, H, IN	X, H	5	10		0.1	8	10	5	10	50	All leftovers from H and IN
	4	X, H, IN		5		20					10	50	All leftovers from H and IN
22R	2	X, H, IN	X, H	5	10		0.1	8	10	5	10	50	All leftovers from H and IN
	4	X, H, IN		5		20					10	50	All leftovers from H and IN
23R	2	X, H, IN	X, H	5	10		0.1	8	10	5	10	50	All leftovers from H and IN
	4	X, H, IN		5		20					10	50	All leftovers from H and IN
24R	2	X, H, IN	X, H	5	10		0.1	8	10	5	10	50	All leftovers from H and IN
	4	X, H, IN		5		20					10	50	All leftovers from H and IN

Table T6 (continued).

* = samples collected from Sections 2b and 4. † = samples collected from Section 2a. The combined volume of interior and halfway sections was greater than or equal to 220 cm^3. One to four 15 cm WRCs were typically taken per core. X = exterior, H = halfway, IN = interior (also see Fig. F23 for further clarification). PFC = perfluorocarbon, DCC = direct cell counts, FISH = florescence in situ hybridization, RT = real time, PCR = polymerase chain reaction, MAD = moisture and density, TOC = total organic carbon.

Table T7. Sampling for monitoring of contamination in drilling mud, Expedition 337.

Sample type	Sampling method	Sampling frequency	Analysis
Active tanks before drilling	Directly from active tank(s)	50 mL, every day, from both actively mixed tanks	PFC (every sample), DNA, cell counts (certain samples)
Active tanks during drilling	From mud fluid line, before drilling mud goes into borehole	50 mL, every day, from both actively mixed tanks	PFC (every sample), DNA, cell counts (certain samples)
Unwashed cuttings	Every 50 m except during coring	50 mL, every day, from both actively mixed tanks	PFC (every sample), DNA, cell counts (certain samples)
Circulating mud fluid from mud ditch	Every 50 m except during coring	50 mL, every day, from both actively mixed tanks	PFC (every sample), DNA, cell counts (certain samples)

PFC = perfluorocarbon.

Table T8. PCR primers used during Expedition 337.

Primer	Gene	Target	T_m (°C)	Sequence (5'–3')	Reference
General domain specific:					
8Fmod	16S	Bacteria	60	AGA GTT TGA TYM TGG CTC AG	Modified from Loy et al., 2002
27F	16S	Bacteria	55	AGA GTT TGA TCM TGG CTC AG	Lane, 1991
338Rabc	16S	Bacteria	60	ACW CCT ACG GGW GGC WGC	Daims et al., 1999
Bac806R	16S	Bacteria	60	GG ACT ACC AGG GTA TCT AAT CCT GTT	Nadkarni et al., 2002
Bac806F	16S	Bacteria	60	AAC AGG ATT AGA TAC CCT GGT AGT CC	Nadkarni et al., 2002
Bac908F	16S	Bacteria	60	AAC TCA AAK GAA TTG ACG GG	M. Lever, unpubl. data
Bac908R	16S	Bacteria	60	CCC GTC AAT TCM TTT GAG TT	M. Lever, unpubl. data
926R	16S	Bacteria	55	CCG TCA ATT CCT TTR AGT TT	Muyzer et al.,1993
Bac1075R	16S	Bacteria	60	CAC GAG CTG ACG ACA RCC	M. Lever, unpubl. data
21F	16S	Archaea	55	TTC CGG TTG ATC CYG CCG GA	DeLong, 1992
806F	16S	Archaea	55	ATTAGATACCCSBGTAGTCC	Takai and Horikoshi, 2000
915Rmod	16S	Archaea	55	GTG CTC CCC CGC CAA TT	Modified from Stahl and Amann, 1991
915Fmod	16S	Archaea	55	AAT TGG CGG GGG AGC AC	Modified from Stahl and Amann, 1991
958R	16S	Archaea	55	YCC GGC GTT GAM TCC AAT T	DeLong, 1992
1059R	16S	Archaea	55	GCC ATG CAC CWC CTC T	Yu et al., 2005
Medlin A	18S	Eukarya	60	AACCTGGTTGATCCTGCCAGT	Medlin et al., 1988
Medlin B	18S	Eukarya	60	GATCCTTCTGCAGGTTCACCTAC	Medlin et al., 1988
Euk 570R	18S	Eukarya	60	GCTATTGGAGCTGGAATTAC	Elwood et al., 1985
Group specific:					
Bif-16S-F*	16S	*Bifidobacterium*	55	CCA TCG CTT AAC GGT GGA T	M. Lever, unpubl. data
Bif-16S-R*	16S	*Bifidobacterium*	55	CCA CAT CCA GCA TCC ACC	M. Lever, unpubl. data
Blau-16S-F*	16S	*Blautia*	55	CGG TAT GTA AAC TTC TAT CAG CA	M. Lever, unpubl. data
Blau-16S-R*	16S	*Blautia*	55	CAG TTT CCA ATG CAG TCC	M. Lever, unpubl. data
Xanth-16S-F*	16S	*Xanthomonas*	TBD	GGA AAG AAA AGC AGT CGG TT	M. Lever, unpubl. data
Xanth-16S-R*	16S	*Xanthomonas*	TBD	AGT GAC CCA GTA TCC ACT GC	M. Lever, unpubl. data
Halo-16S-F*	16S	*Halomonas*	TBD	GAT AAG CCG GTT GTG AAA GC	M. Lever, unpubl. data
Halo-16S-R*	16S	*Halomonas*	TBD	TCA GTG TCA GTC CAG AAG GC	M. Lever, unpubl. data
SAR11-16S-F*	16S	SAR 11	55	AAG GTC CGG CTA ACT TCG T	M. Lever, unpubl. data
SAR11-16S-R*	16S	SAR 11	55	AAT CCT CTT CGC TAC CCA TG	M. Lever, unpubl. data
MGI-16S-F*	16S	Marine Group I Archaea	60	TAA AAC CAG CAC CTC AAG TGG	M. Lever, unpubl. data
MGI-16S-R*	16S	Marine Group I Archaea	60	TCG RAC GTG TTC TGG TAG ACC	M. Lever, unpubl. data
Mbb arb-mcrI-F*	*mcrA*	*Methanobrevibacter*	TBD	TTT GGA ATA TGT GAA GCT CCA AA	M. Lever, unpubl. data
Mbb arb-mcrI-R*	*mcrA*	*Methanobrevibacter*	TBD	AGT AGC GAA AGC TGT TGC ACA A	M. Lever, unpubl. data
mcrIRD F	*mcrA*	Methanogens and methanotrophs	55	TWYGACCARATMTGGYT	Lever, 2008
mcrIRD R	*mcrA*	Methanogens and methanotrophs	55	ACRTTCATBGCRTARTT	Lever, 2008
ANME-1-mcrI F	*mcrA*	ANME-1 Archaea	63	GACCAGTTGTGGTTCGGAAC	Lever, 2008
ANME-1-mcrI R	*mcrA*	ANME-1 Archaea	63	ATCTCGAATGGCATTCCCTC	Lever, 2008
fhs F	*fhs*	Acetogens and other C_1 metabolizers	60	GAT GAT CGA CAA CCA CRT CTA	Lever et al., 2010
fhs R	*fhs*	Acetogens and other C_1 metabolizers	60	GGC ACT TGA TGT CGA AGA A	Lever et al., 2010
dsrB F1a	*dsrB*	All *dsrB* except xenologous Firmicutes	56	CAC ACC CAG GGC TGG	Lever et al., 2013
dsrB F1b	*dsrB*	All *dsrB* except xenologous Firmicutes	56	CAT ACT CAG GGC TGG	Lever et al., 2013
dsrB F1c	*dsrB*	All *dsrB* except xenologous Firmicutes	56	CAT ACC CAG GGC TGG	Lever et al., 2013
dsrB F1d	*dsrB*	All *dsrB* except xenologous Firmicutes	56	CAC ACT CAA GGT TGG	Lever et al., 2013
dsrB F1e	*dsrB*	All *dsrB* except xenologous Firmicutes	56	CAC ACA CAG GGA TGG	Lever et al., 2013
dsrB F1f	*dsrB*	All *dsrB* except xenologous Firmicutes	56	CAC ACG CAG GGA TGG	Lever et al., 2013
dsrB F1g	*dsrB*	All *dsrB* except xenologous Firmicutes	56	CAC ACG CAG GGG TGG	Lever et al., 2013
dsrB F1h	*dsrB*	All *dsrB* except xenologous Firmicutes	56	CAT ACG CAA GGT TGG	Lever et al., 2013
dsrB F2a	*dsrB*	Xenologous Firmicutes	56	CGT CCA CAC CCA GGG	Lever et al., 2013
dsrB F2b	*dsrB*	Xenologous Firmicutes	56	TGT GCA TAC CCA GGG	Lever et al., 2013
dsrB F2c	*dsrB*	Xenologous Firmicutes	56	CAT TCA TAC CCA GGG	Lever et al., 2013
dsrB F2d	*dsrB*	Xenologous Firmicutes	56	TGT TCA CAC CCA GGG	Lever et al., 2013
dsrB F2e	*dsrB*	Xenologous Firmicutes	56	CGT GCA CAC GCA GGG	Lever et al., 2013
dsrB F2f	*dsrB*	Xenologous Firmicutes	56	CGT TCA TAC ACA GGG	Lever et al., 2013
dsrB F2g	*dsrB*	Xenologous Firmicutes	56	TGT CCA CAC TCA GGG	Lever et al., 2013
dsrB F2h	*dsrB*	Xenologous Firmicutes	56	CGT GCA TAC GCA GGG	Lever et al., 2013
dsrB F2i	*dsrB*	Xenologous Firmicutes	56	CAT CCA TAC TCA GGG	Lever et al., 2013
dsrB 4RSI1a	*dsrB*	All *dsrB* except xenologous Firmicutes	56	CAG TTA CCG CAG TAC AT	Lever et al., 2013
dsrB 4RSI1b	*dsrB*	All *dsrB*	56	CAG TTA CCG CAG AAC AT	Lever et al., 2013
dsrB 4RSI1c	*dsrB*	All *dsrB* except xenologous Firmicutes	56	CAG TTG CCG CAG TAC AT	Lever et al., 2013
dsrB 4RSI1d	*dsrB*	All *dsrB* except xenologous Firmicutes	56	CAG TTT CCG CAG TAC AT	Lever et al., 2013
dsrB 4RSI1e	*dsrB*	All *dsrB*	56	CAG TTG CCG CAG AAC AT	Lever et al., 2013
dsrB 4RSI1f	*dsrB*	All *dsrB* except xenologous Firmicutes	56	CAG TTT CCA CAG AAC AT	Lever et al., 2013

* = used for DNA contamination tests only. For dissimilatory sulfate-reducing microbesa mixture consisting of *dsrB* F1a–h and 4RSIa–f was used to target all sulfate reducers, except for xenologous Firmicutes. To target the latter, a different primer mixture, consisting of *dsrB* F2a–i and 4RSIb and e was used. TBD = to be determined.

Table T9. Sterile mineral solution, made up in deionized water.

Component	Concentration (g/L)	Amendment (mL)
Salt solution:		
KH_2PO	0.2	NA
NH_4Cl	0.25	NA
NaCl	25	NA
$MgCl_2·6H_2O$	5	NA
KCl	0.5	NA
$CaCl_2·2H_2O$	0.15	NA
Amendments (add to 1 L salt solution):		
Resazurin	0.1 (w/v)	1
$NaHCO_3$	84	30
$Na_2S·9H_2O$	12	3

NA = not applicable.

Table T10. Incubation for shore-based cultivation experiments, Expedition 337.

Target microbes	Sample type	Electron donor (mM)	Electron acceptor (mM)	Reducing reagents	BES (40 mM)	Incubation temperature (°C)
Methanogens						
Hydrogenotrophic	Cuttings/in situ fluid	H_2	CO_2	Na_2S and cystein	—	25–55
	Cuttings/in situ fluid	Formate (20)	CO_2	Na_2S and cystein	—	25–55
Aceticlastic	Cuttings/in situ fluid	Acetate (20)	CO_2	Na_2S and cystein	—	25–55
	Cuttings/in situ fluid	Methanol (20)	CO_2	Na_2S and cystein	—	25–55
Homoacetogens	Cuttings/in situ fluid	H_2	CO_2	Na_2S and cystein	+	25–55
	Cuttings/in situ fluid	Methanol (20)	CO_2	Na_2S and cystein	+	25–55
Iron reducers	Cuttings/in situ fluid	Acetate (20)	NTA-Fe(III) (10)	—	+	25–55
	Cuttings/in situ fluid	Acetate (10)	Ferric citrate (30)	—	+	25–55
	Cuttings/in situ fluid	Acetate (20)	Lepidocrocite (20)	—	+	25–55
	Cuttings/in situ fluid	Acetate (20)	Goethite (20)	—	+	25–55
	Cuttings/in situ fluid	Acetate (20)	Hematite (10)	—	+	25–55
	Cuttings/in situ fluid	Acetate (20)	Magnetite (10)	—	+	25–55
Syntrophic oxidizers	Cuttings/in situ fluid	Ethanol (20)	Proton	Na_2S and cystein	—	25–55
	Cuttings/in situ fluid	Propionate (20)	Proton	Na_2S and cystein	—	25–55
	Cuttings/in situ fluid	Butyrate (20)	Proton	Na_2S and cystein	—	25–55

BES = 2-bromoethane sulfonic acid, a methanogen-specific inhibitor, NTA = nitrilotriacetic acid. + = added, — = not added.

Table T11. Freshwater basal medium (pH 7) made up in deionized water, Expedition 337.

Component	Concentration (g/L)
Salt solution:	
NH_4Cl	0.535
KH_2PO_4	0.136
$MgCl_2·6H_2O$	0.204
$CaCl_2·2H_2O$	0.147
$NaHCO_3$	2.52
Vitamin solution (add 1 mL/L):	
Biotin	0.005
4-aminobenzoic acid	0.005
Pantothenate	0.005
Pyridoxine	0.01
Nicotinamide	0.005
Thiamine	0.005
Lipoic acid	0.005
Folic acid	0.005
Vitamin B12	0.005
Riboflavin	0.005
Trace element solution (add 1 mL/L):	
$FeCl_2$	1.27
$CoCl_2$	0.13
$MnCl_2·4H_2O$	0.198
$ZnCl_2$	0.136
B_3BO_3	0.0062
$NiCl_2$	0.013
$AlCl_3$	0.0133
$Na_2MoO_4·2H_2O$	0.0242
Na_2SeO_3	0.0033
$Na_2WO_4·H_2O$	0.0033
$CuCl_2$	0.0013

Table T12. Seawater basal medium (pH 7), Expedition 337.

Component	Concentration (g/L)
Salt solution:	
NaCl	20.45
NH_4Cl	0.535
KH_2PO_4	0.136
$MgC_{l2}·6H_2O$	0.204
$CaCl_2·2H_2O$	0.147
$NaHCO_3$	2.52
Vitamin solution (add 1 mL/L):	
Biotin	0.005
4-aminobenzoic acid	0.005
Pantothenate	0.005
Pyridoxine	0.01
Nicotinamide	0.005
Thiamine	0.005
Lipoic acid	0.005
Folic acid	0.005
Vitamin B12	0.005
Riboflavin	0.005
Trace element solution (add 1 mL/L):	
$FeCl_2$	1.27
$CoCl_2$	0.13
$MnCl_2·4H_2O$	0.198
$ZnCl_2$	0.136
B_3BO_3	0.0062
$NiCl_2$	0.013
$AlCl_3$	0.0133
$Na_2MoO_4·2H_2O$	0.0242
Na_2SeO_3	0.0033
$Na_2WO_4·H_2O$	0.0033
$CuCl_2$	0.0013

Table T13. Overview of WRCs obtained from the coal formation between 1950 and 2000 m CSF-B, including coal and sandstone layers that were used to prepare mixture, Expedition 337.

Core, section	Top depth CSF-B (m)	Bottom depth CSF-B (m)	Weight (g)
337-C0020A-			
19R-1	1951.061	1951.301	320
19R-5	1954.872	1954.965	310
19R-7	1957.65	1957.844	300
20R-3	1961.795	1961.695	260
23R-6	1987.463	1987.629	400
23R-8	1989.417	1989.563	230
24R-3	1993.865	1993.97	260
25R-1	1995.6	1995.75	230
25R-2	1996.41	1996.61	640
25R-2	1997.26	1997.46	410
25R-3	1998.85	1999.02	400

Table T14. Stable isotope tracer incubation experiments for single-cell metabolic assay using NanoSIMS and molecular ecological techniques, Expedition 337. (Continued on next page.)

No.	^{13}C source	^{12}C source	^{15}N source	D	Headspace	Target metabolic type	Sampling depth
1	$H^{13}CO_3^-$		$^{15}NH_4^+$	D_2O	Ar	Autotrophs	6 depths
2	$H^{13}CO_3^-$		$^{15}N_2$	D_2O	Ar, $^{15}N_2$*	Autotrophs	6 depths
3	$H^{13}CO_3^-$		$^{15}NH_4^+$	D_2O	H_2*	Hydrogenotrophic autotrophs	6 depths
4	$H^{13}CO_3^-$	Glucose	$^{15}NH_4^+$	D_2O	Ar	Mixotrophs	6 depths
5	$H^{13}CO_3^-$	Formate	$^{15}NH_4^+$	D_2O	Ar	Mixotrophs	6 depths
6	$H^{13}CO_3^-$	Acetate	$^{15}NH_4^+$	D_2O	Ar	Mixotrophs	6 depths
7	$H^{13}CO_3^-$	Amino acids	$^{15}NH_4^+$	D_2O	Ar	Mixo-oligotrophs	6 depths
8	$H^{13}CO_3^-$	(Glucose, amino acids)		D_2O	Ar	Autotrophs	Max. 10 depths
9	$H^{13}CO_3^-$				Ar	Autotrophs	6 depths
10	$^{13}C^{18}O$		$^{15}NH_4^+$	D_2O	Ar, $^{13}C^{18}O$*	Carboxydotrophs	6 depths
11	$^{13}C^{18}O$			D_2O	Ar, $^{13}C^{18}O$*	Carboxydotrophs	6 depths
12	$^{13}C^{18}O$	Glucose	$^{15}NH_4^+$	D_2O	Ar, $^{13}C^{18}O$*	Carboxydo-organotrophs	6 depths
13	$^{13}C^{18}O$	Glucose		D_2O	Ar, $^{13}C^{18}O$*	Carboxydo-organotrophs	6 depths
14	$^{13}C^{18}O$				Ar, $^{13}C^{18}O$*	Carboxydotrophs	6 depths
15	$^{13}CH_4$		$^{15}NH_4^+$	D_2O	Ar, $^{13}CH_4$†	Methanotrophs	6 depths
16	$^{13}CH_4$		$^{15}N_2$	D_2O	Ar, $^{13}CH_4$†, $^{15}N_2$†	Methanotrophs	6 depths
17	$^{13}CH_4$				Ar, $^{13}CH_4$†	Methanotrophs	6 depths
18	$H^{13}CO_3^-$	CH_4	$^{15}NH_4^+$	D_2O	Ar, CH_4*	Methanotrophs	6 depths
19	$H^{13}CO_3^-$	CH_4	$^{15}N_2$	D_2O	Ar, CH_4*, $^{15}N_2$†	Methanotrophs	6 depths
20	^{13}C-methylamine		^{14}N-methylamine	D_2O	H_2*	Hydrogenotrophic methylotrophs	6 depths
21	^{13}C-methylamine		^{14}N-methylamine	D_2O	Ar	Methylotrophs	6 depths
22	^{13}C-methylamine		$^{15}NH_4^+$	D_2O	Ar, H_2*	Hydrogenotrophic methylotrophs	6 depths
23	^{13}C-methylamine			D_2O	Ar	Methylotrophs	6 depths
24	^{13}C-methanol		$^{15}NH_4^+$	D_2O	Ar, H_2*	Hydrogenotrophic methylotrophs	6 depths
25	^{13}C-methanol			D_2O	Ar	Methylotrophs	6 depths
26	^{13}C-glucose		$^{15}NH_4^+$	D_2O	Ar	Heterotrophs	6 depths
27	^{13}C-glucose		$^{15}N_2$	D_2O	Ar, $^{15}N_2$†	Heterotrophs	6 depths
28	^{13}C-glucose				Ar	Heterotrophs	6 depths
29	^{13}C-formate		$^{15}NH_4^+$	D_2O	Ar	Heterotrophs	6 depths
30	^{13}C-formate		$^{15}N_2$	D_2O	Ar, $^{15}N_2$†	Heterotrophs	6 depths
31	^{13}C-formate				Ar	Heterotrophs	6 depths
32	^{13}C-acetate		$^{15}NH_4^+$	D_2O	Ar	Heterotrophs	6 depths
33	^{13}C-acetate		$^{15}N_2$	D_2O	Ar, $^{15}N_2$†	Heterotrophs	6 depths
34	^{13}C-acetate				Ar	Heterotrophs	6 depths
35	^{13}C-benzoic acid (carboxyl)		$^{15}NH_4^+$	D_2O	Ar	Hydrocarbon degraders	1 from a lignite layer
36	^{13}C-benzoic acid (ring, ^{13}C6)		$^{15}NH_4^+$	D_2O	Ar	Hydrocarbon degraders	1 from a lignite layer
37	^{13}C-toluene (methyl)		$^{15}NH_4^+$		Ar	Hydrocarbon degraders	1 from a lignite layer
38	^{13}C-toluene (ring, ^{13}C6)		$^{15}NH_4^+$		Ar	Hydrocarbon degraders	1 from a lignite layer
39	^{13}C-benzene (ring, ^{13}C6)		$^{15}NH_4^+$		Ar	Hydrocarbon degraders	1 from a lignite layer
40	^{13}C-naphtalene (ring, ^{13}C12)		$^{15}NH_4^+$		Ar	Hydrocarbon degraders	1 from a lignite layer
41	^{13}C-ferulic acid (^{13}C1,2,3)		$^{15}NH_4^+$	D_2O	Ar	Hydrocarbon degraders	1 from a lignite layer
42	^{13}C-p-coumaric acid (^{13}C1,2,3)		$^{15}NH_4^+$	D_2O	Ar	Hydrocarbon degraders	1 from a lignite layer
43	^{13}C-vanillin (^{13}C-methoxy and/or ^{13}C-carbonyl)		$^{15}NH_4^+$	D_2O	Ar	Hydrocarbon degraders	Max. 15 depths
44	^{13}C-lignin (from maize)		$^{15}NH_4^+$	D_2O	Ar	Hydrocarbon degraders	Max. 15 depths
45	^{13}C-n-hexadecane (^{13}C1,2)		$^{15}NH_4^+$	D_2O	Ar	Hydrocarbon degraders	Max. 15 depths
46	^{13}C,^{15}N-amino acids		^{13}C,^{15}N-amino acids	D_2O	Ar	Oligotrophs	6 depths
47			^{15}N-amino acids	D_2O	Ar	Oligotrophs	6 depths
48	^{13}C-dNTP		$^{15}NH_4^+$	D_2O	Ar	Oligotrophs	6 depths
49			$^{15}NH_4^+$	D_2O	Ar		
50			$^{15}N_2$	D_2O	Ar, $^{15}N_2$†		

Table 14 (continued).

No.	^{13}C source	^{12}C source	^{15}N source	D	Headspace	Target metabolic type	Sampling depth
51				D_2O	Ar		
52				$D_2{}^{18}O$	Ar		

* = 5 mL of gas substrate was added, † = 5mL of 50% ^{13}C or ^{15}N gas substrate was added.